FULL PAPER DOI: 10.1002/adsc.202001461

Advanced Synthesis & Catalysis

Gold-Catalyzed Synthesis of π-Extended Carbazole-Based Systems and their Application as Organic Semiconductors

Christoph M. Hendrich,[a] Valentin D. Hannibal,[a] Lukas Eberle,[a] Leif E. Hertwig,[a] Ute Zschieschang,[b] Frank Rominger,[+a] Matthias Rudolph,[a] Hagen Klauk,[b,*] and A. Stephen K. Hashmi[a,*]

[a] Organisch-Chemisches Institut
Heidelberg University
Im Neuenheimer Feld 270, 69120 Heidelberg (Germany)
(+49)-6221-54-4205
E-mail: hashmi@hashmi.de
Homepage: http://www.hashmi.de

[b] Max Planck Institute for Solid State Research
Heisenbergstr. 1, 70569 Stuttgart (Germany)
E-mail: h.klauk@fkf.mpg.de

[+] Crystallographic investigation

Manuscript received: November 23, 2020; Revised manuscript received: December 23, 2020;
Version of record online: Februar 1, 2021

Supporting information for this article is available on the WWW under https://doi.org/10.1002/adsc.202001461

Abstract: Herein we describe a gold-catalyzed bidirectional synthesis of *N*-heteropolycyclic compounds bearing carbazole moieties – namely π-extended benzodicarbazoles and π-extended indolocarbazoles. Overall, four previously unknown core structures were synthesized. This approach is convergent, modular and the gold-catalyzed key step comprises of a cascade reaction starting from stable di-azido compounds. The obtained molecules were fully characterized and their optical and electronic properties as well as their performance in organic thin-film transistors generated by vacuum deposition were studied. Charge-carrier mobilities of up to 0.3 cm^2/Vs were measured.

Keywords: Homogeneous gold catalysis; cascade cyclization, azides; organic semiconductors; thin-film transistors

Introduction

Since decades small semiconducting molecules bearing heteroatoms are of special interest for organic electronics. This rise was started by the first attempts for the replacement of the benchmark substance pentacene.[1] Acenes themselves show high charge carrier mobilities, but have some disadvantages like low solubility and sensitivity towards oxygen. In addition, higher acenes are intrinsically instable.[2] One solution is the replacement of carbon atoms by heteroatoms in the core structures, which for example lowers the HOMO-energy level of the molecule or, in the case of nitrogen, allows to further manipulate the chemical behavior.[3] Based on this principle, a huge variety of nitrogen-based small molecules were synthesized, investigated and successfully applied as organic semiconductors, donor-acceptor molecules and emitters in electronic devices like OFETs (organic field-effect transistors), OLEDs (organic light-emitting diodes) or OSCs (organic solar cells).[4] Carbazole/indole substructures are among the large number of molecular motifs that have been explored so far. Besides the already existing series of examples,

continuously publications with new carbazole-based structures, including new synthetic strategies and deeper investigations on their electronic structures, arise.[5] For example indolocarbazoles are widely used as p-type organic semiconductors in transistors.[6] Other structurally similar compounds such as benzodicarbazoles were successfully applied as emitters in organic light emitting diodes.[7]

We previously reported a gold-catalyzed approach to π-extended indolocarbazoles (Scheme 1, upper part, BBICZs, benzo[a]benzo[6,7]indolo[2,3-h] carbazoles).[8] These organic semiconductors were also studied with regard to their performance in thin-film transistors (TFTs), reaching charge transport mobilities of up to 1 cm^2/Vs for the unsubstituted BBICZ **1** (Scheme 2, upper part). The focus on this study was on a substituent-dependent structure-effect analysis. We now present an isomer-structure analysis of further π-extended and previously unknown structures (Scheme 2, lower part). Again, a gold-catalyzed[9] cascade cyclization is the key step of this synthesis, a powerful tool, which in our opinion is ideal for the synthesis of molecules for organic electronics.[10] This

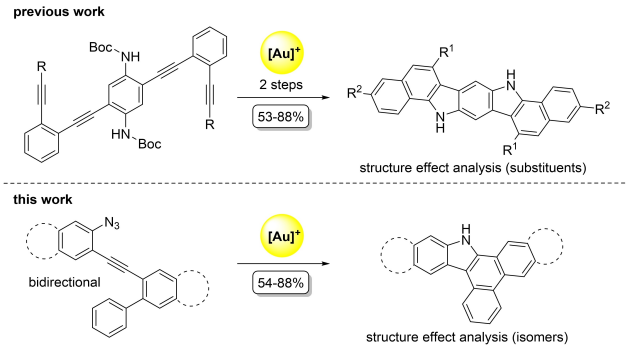

Scheme 1. Previous strategy for BBICZs and our new approach towards π-extended BBICZs and BDCs (Benzodicarbazoles).

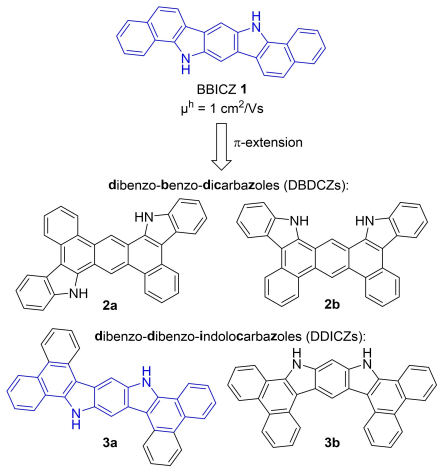

Scheme 2. Overview of the developed structures.

is underlined by various effective strategies that use the principle of cascade reactions for the construction of large molecules and large carbon skeletons.[11]

Results and Discussion

One of the key outcomes of our previous study to BBICZs was the observation that substituents in general had a negative impact on charge carrier mobilities – at least for the used vacuum deposition method. As a next evolution process, we turned our focus on a different approach, which instead of differently substituted scaffolds of the same motif now focused on the synthesis of regioisomeric heterocyclic scaffolds. Like in the previous study the effect on material properties of the compounds was analyzed but this time by comparing the data of isomers all consisting of the same sum formula. For this purpose, four new literature unknown unsubstituted carbazole skeletons were synthesized; the **d**ibenzo-**b**enzo-**dic**arba**z**oles (DBDCZ) **2a** and **2b** and the **d**ibenzo-**d**ibenzo-**i**ndolo**c**arba**z**oles (DDICZ) **3a** and **3b. 3a**, which is most closely related to the BBICZs of our previous study, constituted the "foundation stone" of our research. **3b** is the C_s-symmetrical isomer of the C_2-symmetrical **3a**. In addition, **2a** and **2b** were synthesized, both being π-extended variants of the benzodicarbazoles with nitrogen atoms showing a larger distance. As already mentioned, all of these compounds are constitutional isomers.

In contrast to our foregoing synthesis, the carbazole moiety was not built from an amine cascade cyclization, but instead from an azide cascade cyclization. Azide cyclizations like this already served as tool in homogenous gold catalysis,[12] and our approach is the bidirectional variant of a reaction reported from Qiu and Xu *et al.* in 2018.[13] By using the azide instead of the formerly used amines as nucleophiles, an intermediate gold carbene[14] is generated, which can be regarded as an Umpolung of the prior synthetic strategy. This paves an unprecedented way to new and large conjugated π-systems. In the first step of this known reaction,[13] a nucleophilic attack of the azide functionality at the gold(I)-activated[15] alkyne moiety, after extrusion of dinitrogen, in a 5-*endo-dig* cyclization generates a gold carbene intermediate, which after electrophilic attack at the tethered phenyl substituent and a final deprotonation/reprotonation furnishes the carbazole moiety.

The azide starting materials were prepared from the corresponding amines. Starting from 1,4-dibromo-2,5-diiodobenzene or 1,5-dibromo-2,4-diiodobenzene, **7a** and **7b** were accessible by a Sonogashira reaction followed by a Suzuki cross coupling (Scheme 3). **5** was used as alkyne for the Sonogashira reaction, for the Suzuki reaction phenylboronic acid was used. The yields for these bidirectional cross couplings were

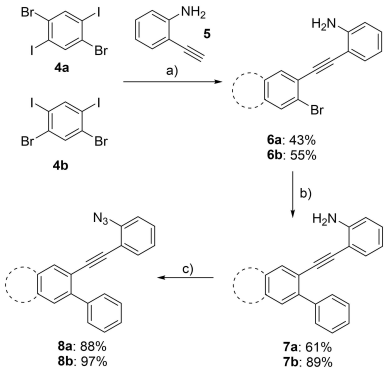

Scheme 3. Synthetic route to the di-azides **8a** and **8b**. a) 2.1 eq **5**, 2 mol% $PdCl_2(PPh_3)_2$, 2 mol% CuI, THF, NEt_3; b) 2.5 eq $PhB(OH)_2$, 4 eq K_2CO_3, 1 mol% $Pd_2(dba)_3$, 4 mol% P(*o*-tolyl)$_3$, H_2O, THF; c) 3 eq ^{t}BuONO, 3 eq $TMSN_3$, MeCN, DCM.

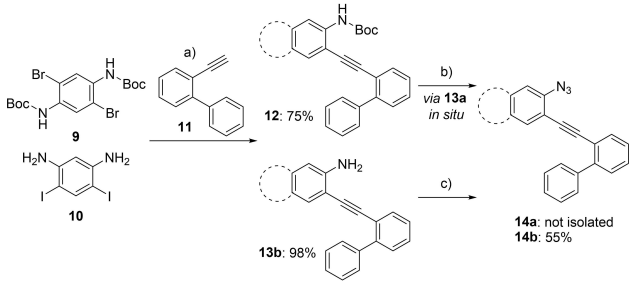

Scheme 4. Synthetic route to the di-azides **14a** and **14b**. a) 2.6 eq **11**, 4 mol% $PdCl_2(PPh_3)_2$, 4 mol% CuI, THF, NEt_3; b) i) HCl/dioxane; ii) 5 eq ^{t}BuONO, 5 eq $TMSN_3$, MeCN, DCM; c) 3 eq ^{t}BuONO, 3 eq $TMSN_3$, MeCN, DCM.

moderate to very good. The bidirectional azidation of these compounds, analogous to a procedure of Cooper *et al.*[16] delivered excellent yields for both substrates. Both di-azides **8a** and **8b** are stable at room temperature, and purification by flash column chromatography with silica gel was possible.[17]

For the DDICZs, a different synthetic strategy was used. Since the azide functionality has to be attached to the inner core, halogenated amines **9** and **10** were used as starting materials (Scheme 4). As *para*-diamines are just moderately stable, Boc-protected amines were applied for synthetic reasons. Again, the first step consisted of a Sonogashira cross coupling with alkyne **11**. In case of **13b**, an azidation analogous to the previously mentioned examples was possible. Because of the already mentioned instability of the *para*-substituted derivative, for **12** it was not possible to isolate the primary diamine after removal of the Boc protecting group with HCl in dioxane (4 M). Instead, the in situ-formed diamine was directly used for the azidation. Due to the significant formation of a side product during this transformation, azide **14a** could not be isolated in satisfactory purity and it was directly used for the next step (compare Table 1).

For the gold-catalyzed cyclization the azides were treated with 2.5–3 mol% of JohnPhosAu(MeCN)SbF_6 in DCE at 50–80 °C (the optimized conditions of Qiu and Xu *et al.*,[13] Scheme 5). The reaction times for complete conversion ranged between 2 h and stirring over night. Due to the large π-system which is formed in a single reaction step, the desired products precipitated during the reaction, which made the isolation very easy – a simple filtration and washing with ice cold DCM. For the application as organic semiconductor, multiple recrystallizations from THF further increased the purity.

The secondary amine moiety of the carbazole derivatives enabled a late stage functionalization by alkylation (Scheme 5). Based on a prior report of Ivaniuk *et al.*,[7a] who used benzodicarbazoles bearing a hexyl chain as organic emitter in OLEDs, **2a–b** and **3a–b** were deprotonated with KO^{t}Bu in anhydrous DMSO and then alkylated with 1-bromohexane in good to excellent yields. Again, the products were precipitated by the addition of methanol, just filtrated and washed to obtain the corresponding alkylated **15a–b** and **16a–b**. The rather low yield for **16a** can be explained by the significant smaller scale of the reaction for this compound in combination with the applied purification method.

Next, the optical properties of the obtained carbazoles **2a–b** and **3a–b** were analyzed (Figure 1 and Table 2; for the corresponding alkylated **15a–b** and **16a–b** see Supporting Information). All emission spectra have a similar shape showing three local emission maxima. Benzodicarbazole **2a** shows the most bathocromic shift, whereas the indolocarbazole **3b** has the most hypsochromic shift. The extinction

Table 1. Yields of the azidation, the gold-catalyzed cyclization and the final alkylation for all four substances.

Starting material	Yield of the azidation	Yield of the gold catalysis	Yield of the alkylation
7a	88% (**8a**)	76% (**2a**)	94% (**15a**)
7b	97% (**8b**)	76% (**2b**)	91% (**15b**)
12	Not isolated (**14a**)	54%[a,b] (**3a**)	57% (**16a**)
13b	55% (**14b**)	88% (**3b**)	78% (**16b**)

[a] Yield over three steps.
[b] 10 mol% catalyst was used.

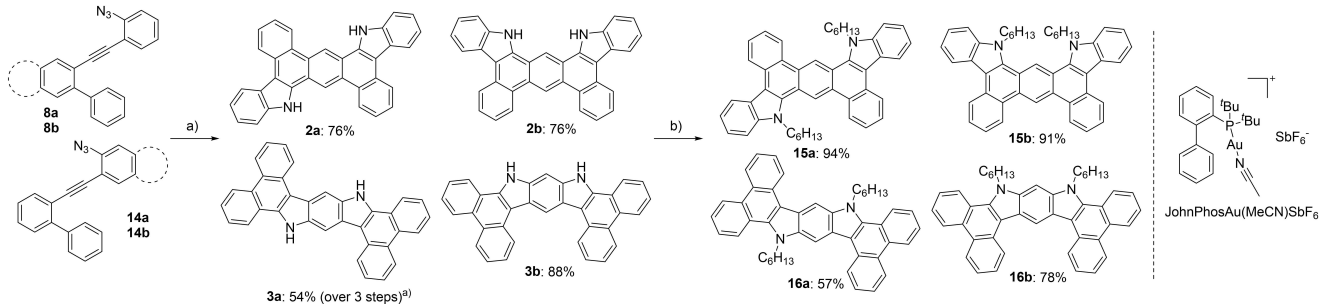

Scheme 5. Gold-catalyzed cyclization and following alkylation. a) 2.5–3 mol% JohnPhosAu(MeCN)SbF_6, DCE, 50–80 °C, o/n. b) 4 eq KO^{t}Bu, 20 eq $C_6H_{13}Br$, DMSO, 3 h, rt.[a)] 10 mol% catalyst was used.

coefficients are all in the same range, with absorption maxima between 387 nm for **3 b** and 426 nm for **2 a**. The calculated HOMO energy levels are in very good agreement with the results obtained from cyclic voltammetry (Table 2). This applies for the actual values as well as for the tendencies between the four substrates. For the estimated band gaps the values from the calculations show a deviation of around 0.3 eV compared to the CV measurements for each compound. Interestingly, the optical band gaps, which are estimated from the onset of the absorption maxima, are again around 0.3 eV less than the data from CV. The measured fluorescence quantum yields are between 28% and 52%.

High-quality X-ray structures of all carbazoles **2 a-b** and **3 a–b**, as well as the alkylated **15 b** could be obtained.[18] **2 a** packs with all-parallel π-systems in two-dimensional brick wall-like arrangements, separated from each other by interleaving layers of hydrogen-bound THF solvent (Figure 2, left). However, π-contacts occur only one-dimensional in declined stacks. **2 b** and **3 a** build one-dimensional declined columns, as well as alkylated **15 b**, where the stacks are built of laterally staggered molecules. In contrast, **3 b** with two hydrogen-bonded THF molecules, shows up π-contacts only in isolated molecule pairs (Figure 2, right).

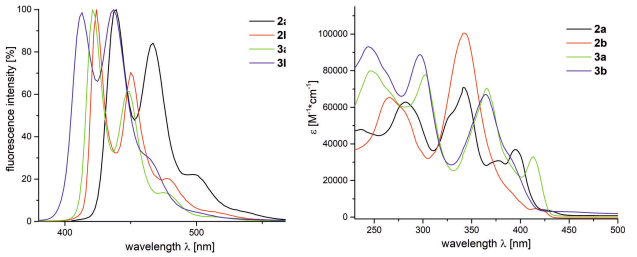

Figure 1. Emission (left) and absorption (right) spectra of carbazoles **2 a–b** and **3 a–b** (in THF).

The charge-transport properties of the benzodicarbazoles **2 a–b** and the indolocarbazoles **3 a–b** were investigated by characterizing organic TFTs fabricated in the inverted staggered (bottom-gate, top-contact) device architecture on heavily doped silicon[19,20] and flexible polyethylene naphthalate (PEN) substrates.[21] The semiconductors were deposited by thermal sublimation in vacuum; for more details see the Supporting Information. All TFTs show p-channel transistor behavior with effective charge-carrier mobilities up to 0.3 cm^2/Vs (Table 3). One finding is that the molecules in which the aromatic rings are fused in a predominantly *ortho*-anellated zigzag-like manner, namely **2 a** and **3 a**, perform substantially better than the compounds with a bent molecular shape, **2 b** and **3 b**. This indicates that the former lend themselves better to tight

Table 2. Overview of the optical and electronic properties. QY = quantum yield, CV = cyclic voltammetry.

Compound	$\lambda_{abs,max}$ [nm]	λ_{em} [nm]	$E_{g,opt}$ [eV][a]	QY	$E_{HOMO,CV}$ [eV][b]	$E_{LUMO,CV}$ [eV][b]	$E_{g,CV}$ [eV][b]	$E_{HOMO,cal}$ [eV][c]	$E_{LUMO,cal}$ [eV][c]	$E_{g,cal}$ [eV][c]
2 a	426	438	2.81	28%	−5.30	−2.15	3.15	−5.36	−1.88	3.48
2 b	415	424	2.88	30%	−5.32	−2.23	3.09	−5.44	−1.88	3.56
3 a	413	422	2.90	52%	−5.08	−1.94	3.14	−5.14	−1.68	3.46
3 b	387	412	3.00	37%	−5.26	−1.94	3.32	−5.17	−1.60	3.57

[a] From the onset of absorption maximum.
[b] Data obtained from CV measurements in DMSO.
[c] Structures were optimized using PBEH-3c/def2-mSVP. Canonical HOMO/LUMO-levels were calculated using B3LYP/6-311 + G**.

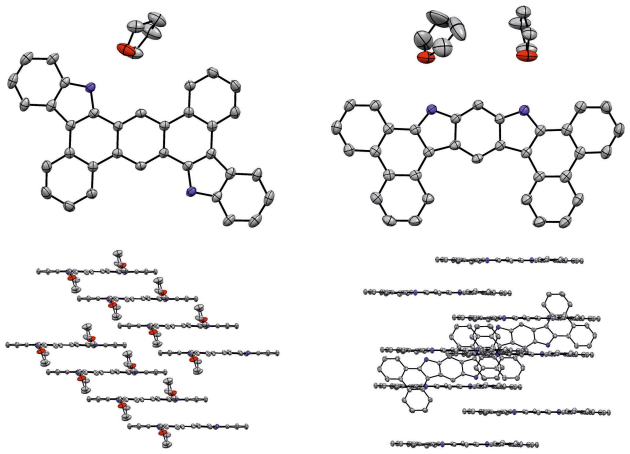

Figure 2. Left: X-ray structure (upper part) and brick wall-like packing (lower part) of **2 a**. Right: X-ray structure of **3 b** and packing of **3 a** in one-dimensional declined columns. The structures are shown in a probability level of 50% and hydrogens are omitted for clarity.

solid-state packing than the latter, at least when deposited in vacuum. With properly optimized solution-deposition methods, it may also be possible to achieve good solid-state packing for molecules with a bent shape. The other finding is that the carrier mobility in the DDICZ derivative **3 a**, which is closely related to the BBICZ **1**, is about an order of magnitude higher than the mobility in the DBDCZ derivative **2 a**.

Conclusion

We present a bidirectional, modular and convergent synthetic strategy to new π-extended *N*-heteropolycyclic compounds based on benzodicarbazole and indolocarbazole substructures using a gold-catalyzed cascade cyclization as key step. This method enables the access to yet unexplored carbazole-based molecules with interest for materials science. Overall, four different structures were synthesized in good overall yields and their optical and electronic properties as well as their solid state structures were studied. Based on our previous results on BBICZs, we analyzed a potentially useful structure/isomer-property relationship for the application in organic devices. Interestingly, the investigated C_2-symmetric compounds in general seem to be better semiconductors than their C_s-symmetric counterparts, sometimes orders of magnitude, resulting in a top charge carrier mobility of 0.3 cm^2/Vs for DDICZ **3 a**. It was also possible to modify the carbazoles in a late stage alkylation.

Experimental Section

General Procedure for the Gold Catalysis

1.00 eq of the corresponding azide was dissolved in DCE. 2.5–3 mol% JohnPhosAuMeCNSbF$_6$ were added and the mixture was stirred at given temperature for the given time until TLC showed full conversion. The precipitate was filtered, washed with ice-cold DCM and the residue was dried under vacuum.

Example DBDCZ 2 a

According to the General Procedure, 1.00 eq of the corresponding azide **8 a** (399 mg, 778 µmol) was dissolved in 50 mL DCE. 2.5 mol% JohnPhosAuMeCNSbF$_6$ (15.0 mg, 19.5 µmol) were added and the mixture was stirred at 80 °C overnight. The precipitate was filtered, washed with ice-cold DCM and the residue was dried under vacuum. A yellow solid was obtained (271 mg, 594 µmol, 76%).

Mp.: >410 °C; IR(ATR): $\tilde{\nu}$[cm^{-1}] = 3447, 3093, 3048, 1608, 1597, 1535, 1488, 1459, 1431, 1399, 1360, 1338, 1304, 1256, 1207, 1191, 1166, 1149, 1117, 1048, 1018, 970, 935, 860, 787, 757, 738, 681, 642, 613; ^{1}H NMR (DMSO-d$_6$, 600.2 MHz): δ[ppm] = 7.37–7.39 (m, 2H), 7.47–7.50 (m, 2H), 7.75–7.78 (m, 2H), 7.82 (d, $^3J_{H\text{-}H}$ = 8.0 Hz, 2H), 7.86–7.89 (m, 2H), 8.62 (d, $^3J_{H\text{-}H}$ = 8.0 Hz, 2H), 8.87 (d, $^3J_{H\text{-}H}$ = 7.8 Hz, 2H), 9.27 (d, $^3J_{H\text{-}H}$ = 8.2 Hz, 2H), 10.15 (s, 2H), 12.75 (s, 2H); ^{13}C NMR (DMSO-d^6, 150.9 MHz): δ[ppm] = 111.2 (s, 2C), 111.9 (d, 2C), 117.4 (d, 2C), 120.3 (d, 2C), 121.4 (s, 2C), 121.4 (d, 2C), 123.7 (d, 2C), 123.8 (d, 4C), 123.9 (s, 2C), 124.3 (d, 2C), 126.6 (s, 2C), 128.2 (d, 2C), 128.5 (s, 2C), 130.2 (s, 2C), 134.6 (s, 2C), 138.6 (s, 2C), HRMS (ESI+): $C_{34}H_{20}N_2^+$, calculated: 456.1621 [M+], observed: 456.1622 [M+]; UV/VIS (DCM, 4.40 µg/mL): λ[nm] (log ε) = 281 (4.79), 327 (4.74), 342 (4.85), 377 (4.49), 395 (4.57), 425 (3.58); Fluorescence (THF): λ_{ex} = 425 nm, λ_{max} = 438 nm, 467 nm, 497 nm; Quantum yield: Φ = 28.4%.

Table 3. Summary of the effective charge-carrier mobilities measured in organic TFTs based on vacuum-deposited films of **2 a**–**b** and **3 a**–**b** fabricated on three types of substrate.

Compound	$\mu^h_{Si\text{-}substrate}$ [cm^2/Vs][a]	$\mu^h_{Si\text{-}substrate}$ [cm^2/Vs][b]	$\mu^h_{PEN\text{-}substrate}$ [cm^2/Vs][b]
2 a	0.02	0.02	0.004
2 b	1×10^{-4}	1×10^{-4}	2×10^{-5}
3 a	0.1	0.3	0.2
3 b	3×10^{-5}	5×10^{-5}	No field effect

[a] Thick gate dielectric.
[b] Thin gate dielectric.

Acknowledgements

The authors are grateful to funding by the DFG (SFB 1249 -N-Heteropolyzyklen als Funktionsmaterialien). Open access funding enabled and organized by Projekt DEAL.

References

[1] J. E. Anthony, *Chem. Rev.* **2006**, *106*, 5028–5048.
[2] J. E. Anthony, *Angew. Chem. Int. Ed.* **2008**, *47*, 452–483; *Angew. Chem.* **2008**, *120*, 460–492.
[3] U. H. F. Bunz, *Acc. Chem. Res.* **2015**, *6*, 1676–1686.
[4] a) W. Jiang, Y. Li, Z. Wang, *Chem. Soc. Rev.* **2013**, *42*, 6113–6127; b) W. Zhang, Y. Liu, G. Yu, *Adv. Mater.* **2014**, *26*, 6898–6904; c) V. Lami, D. Leibold, P. Fassl, Y. Hofstetter, D. Becker-Koch, P. Biegger, F. Paulus, P. Hopkinson, M. Adams, U. H. F. Bunz, S. Huettner, I. Howard, A. Bakulin, Y. Vaynzof, *RRL Solar* **2017**, *1*, 1700053; d) M. Ganschow, S. Koser, S. Hahn, F. Rominger, J. Freudenberg, U. H. F. Bunz, *Chem. Eur. J.* **2017**, *23*, 4415–4421; e) L. Hahn, A. Hermannsdorfer, B. Günther, T. Wesp, B. Bühler, U. Zschieschang, H. Wadepohl, H. Klauk, L. H. Gade, *J. Org. Chem.* **2017**, *82*, 12492; f) P. Reiser, F. S. Benneckendorf, M.-M. Barf, L. Müller, R. Bäuerle, S. Hillebrandt, S. Beck, R. Lovrincic, E. Mankel, J. Freudenberg, D. Jänsch, W. Kowalsky, A. Pucci, W. Jaegermann, U. H. F. Bunz, K. Müllen, *Chem. Mater.* **2019**, *31*, 4213–4221; g) M. Hauschild, M. Borkowski, P. Dral, T. Marszalek, F. Hampel, G. Xie, J. Freudenberg, U. H. F. Bunz, M. Kivala, *Organic Materials* **2020**, *2*, 204–213.
[5] a) H. Srour, T.-H. Doan, E. Da Silva, R. J. Whitby, B. Witulski, *J. Mater. Chem. C* **2016**, *4*, 6270–6279; b) G. V. Baryshnikov, P. Gawrys, K. Ivaniuk, B. Witulski, R. J. Whitby, A. Al-Muhammad, B. Minaev, V. Cherpak, P. Stakhira, D. Volyniuk, G. Wiosna-Salyg, B. Luszczynsk, A. Lazauskas, S. Tamuleviciush, J. V. Grazulevicius, *J. Mater. Chem. C* **2016**, *4*, 5795–5805; c) G. V. Baryshnikov, D. A. Sunchugashev, R. R. Valiev, B. F. Minaev, H. Ågrenad, *Chem. Phys.* **2018**, *513*, 105–111; d) P. Gong, P. Xue, C. Qian, Z. Zhang, R. Lu, *Org. Biomol. Chem.* **2014**, *12*, 6134–6144; e) H. Jiang, P. Hu, J. Ye, A. Chaturvedi, K. K. Zhang, Y. Li, Y. Long, D. Fichou, C. Kloc, W. Hu, *Angew. Chem. Int. Ed.* **2018**, *57*, 8875–8880; *Angew. Chem.* **2018**, *130*, 9013–9018; f) M. Más-Montoya, S. Georgakopoulos, J. P. Cerón-Carrasco, J. Pérez, A. Tárraga, D. Curiel, *J. Phys. Chem. C* **2018**, *22*, 11736–11746; g) S. Georgakopoulos, M. Más-Montoya, J. Pérez, G. Ortuño, A. Tárraga, D. Curiel, *Synth. Met.* **2020**, *261*, 116308.
[6] a) S. Wakim, J. Bouchard, M. Simard, N. Drolet, Y. Tao, M. Leclerc, *Chem. Mater.* **2004**, *16*, 4386–4388; b) Y. Li, Y. Wu, S. Gardner, B. S. Ong, *Adv. Mater.* **2005**, *17*, 849–853; Y. Wu, Y. Li, S. Gardner, B. S. Ong, *J. Am. Chem. Soc.* **2005**, *127*, 614–618; c) P.-L. T. Boudreault, S. Wakim, M. L. Tang, Y. Tao, Z. Bao, M. Leclerc, *J. Mater. Chem.* **2009**, *19*, 2921–2928; d) G. Zhao, H. Dong, H. Zhao, L. Jiang, X. Zhang, J. Tan, Q. Meng, W. Hu, *J. Mater. Chem.* **2012**, *22*, 4409–4417; e) K. S. Park, S. M. Salunkhe, I. Lim, C. G. Cho, S. H. Han, M. M. Sung, *Adv. Mater.* **2013**, *25*, 3351–3356.
[7] a) K. Ivaniuk, V. Cherpak, P. Stakhira, Z. Hotra, B. Minaev, G. Baryshnikov, E. Stromylo, D. Volyniuk, J. V. Grazulevicius, A. Lazauskas, S. Tamulevicius, B. Witulski, M. E. Light, P. Gawrys, R. J. Whitby, G. Wiosna-Salyga, B. Luszczynska, *J. Phys. Chem. C* **2016**, *120*, 6206–6217; for a review on carbazole based molecules for light emitting diodes, see: b) P. Ledwon, *Org. Electron.* **2019**, *75*, 105422.
[8] a) C. M. Hendrich, L. M. Bongartz, M. T. Hoffmann, U. Zschieschang, J. W. Borchert, D. Sauter, P. Krämer, F. Rominger, F. F. Mulks, M. Rudolph, A. Dreuw, H. Klauk, A. S. K. Hashmi, *Adv. Synth. Catal.* **2021**, *363*, 549–557; b) for a review on gold catalysis for materials science, see: C. M. Hendrich, K. Sekine, T. Koshikawa, K. Tanaka, A. S. K. Hashmi, *Chem. Rev.* 10.1021/acs.chemrev.0c00824.
[9] a) A. S. K. Hashmi, *Chem. Rev.* **2007**, *107*, 3180–3211; b) J. Xie, H. Jin, A. S. K. Hashmi, *Chem. Soc. Rev.* **2017**, *46*, 5193–5203; c) X. Zhao, M. Rudolph, A. S. K. Hashmi, *Chem. Commun.* **2019**, *55*, 12127–12135; d) X. Tian, L. Song, A. S. K. Hashmi, *Chem. Eur. J.* **2020**, *26*, 3197–3204.
[10] a) K. Sekine, J. Schulmeister, F. Paulus, K. P. Goetz, F. Rominger, M. Rudolph, J. Zaumseil, A. S. K. Hashmi, *Chem. Eur. J.* **2019**, *25*, 216–220; b) K. P. Goetz, K. Sekine, F. Paulus, Y. Zhong, D. Roth, D. Becker-Koch, Y. J. Hofstetter, E. Michel, L. Reichert, F. Rominger, M. Rudolph, S. Huettner, Y. Vaynzof, E. M. Herzig, A. S. K. Hashmi, J. Zaumseil, *J. Mater. Chem. C* **2019**, *7*, 13493–13501.
[11] For general reviews about cascade reactions see: a) K. C. Nicolaou, D. J. Edmonds, P. G. Bulger, *Angew. Chem. Int. Ed.* **2006**, *45*, 7134; b) S. F. Kirsch, *Synthesis* **2008**, *20*, 3183–3204; c) K. Sugimoto, Y. Matsuya, *Tetrahedron Lett.* **2017**, *58*, 4420–4426.
[12] a) D. J. Gorin, N. R. Davis, F. D. Toste, *J. Am. Chem. Soc.* **2005**, *127*, 11260–11261; b) A. Wetzel, F. Gagosz, *Angew. Chem. Int. Ed.* **2011**, *50*, 7354–7358; *Angew. Chem.* **2011**, *123*, 7492–7496; c) B. Lu, Y. Luo, L. Liu, L. Ye, Y. Wang, L. Zhang, *Angew. Chem. Int. Ed.* **2011**, *50*, 8358–8362; *Angew. Chem.* **2011**, *123*, 8508–8512; d) C. Gronnier, G. Boissonnat, F. Gagosz, *Org. Lett.* **2013**, *15*, 4234–4237; e) N. Li, X.-L. Lian, Y.-H. Li, T.-Y. Wang, Z.-Y. Han, L. Zhang, L.-Z. Gong, *Org. Lett.* **2016**, *18*, 4178–4181; f) W.-B. Shen, Q. Sun, L. Li, X. Liu, B. Zhou, J.-Z. Yan, X. Lu, L.-W. Ye, *Nat. Commun.* **2017**, *8*, 1748; g) G. H. Lonca, C. Tejo, H. L. Chan, S. Chiba, F. Gagosz, *Chem. Commun.* **2017**, *53*, 736–739; h) J. Matsuoka, Y. Matsuda, Y. Kawada, S. Oishi, H. Ohno, *Angew. Chem. Int. Ed.* **2017**, *56*, 7444–7448; *Angew. Chem.* **2017**, *129*, 7552–7556.
[13] J. Cai, B. Wu, G. Rong, C. Zhang, L. Qiu, X. Xu, *Org. Lett.* **2018**, *20*, 2733–2736.
[14] a) L. N. dos Santos Comprido, J. E. M. N. Klein, G. Knizia, J. Kästner, A. S. K. Hashmi, *Angew. Chem. Int.*

Ed. **2015**, *54*, 10336–10340; *Angew. Chem.* **2015**, *127*, 10477–10481; b) D. Sorbelli, L. N. dos Santos Comprido, G. Knizia, A. S. K. Hashmi, L. Belpassi, P. Belanzoni, J. E. M. N. Klein, *ChemPhysChem* **2019**, *20*, 1671–1679; c) J. E. M. N. Klein, G. Knizia, L. N. dos Santos Comprido, J. Kästner, A. S. K. Hashmi, *Chem. Eur. J.* **2017**, *23*, 16097–16103.

[15] a) M. Pernpointner, A. S. K. Hashmi, *J. Chem. Theory Comput.* **2009**, *5*, 2717–2725; b) M. Lein, M. Rudolph, A. S. K. Hashmi, P. Schwerdtfeger, *Organometallics* **2010**, *29*, 2206–2210.

[16] S. K. Mamidyala, M. A. Cooper, *Chem. Commun.* **2013**, *49*, 8407–8409.

[17] It must be noted that – although we didn't have any problems – azides are intrinsic explosive and therefore all relevant precautions should be taken.

[18] CCDC 2043834 (**2a**), 2043835 (**2b**), 2043836 (**15b**), 2043837 (**3b**) and 2043838 (**3a**) contain the supplementary crystallographic data for this paper. These data can be obtained free of charge from The Cambrigde Cristallographic Data Centre via www.ccdc.cam.ac.uk/data request/cif.

[19] M. Aghamohammadi, R. Rödel, U. Zschieschang, C. Ocal, H. Boschker, R. T. Weitz, E. Barrena, H. Klauk, *ACS Appl. Mater. Interfaces* **2015**, *7*, 22775–22785.

[20] U. Kraft, J. E. Anthony, E. Ripaud, M. A. Loth, E. Weber, H. Klauk, *Chem. Mater.* **2015**, *27*, 998–1004.

[21] J. Milvich, T. Zaki, M. Aghamohammadi, R. Rödel, U. Kraft, H. Klauk, J. N. Burghartz, *Org. Electron.* **2015**, *20*, 63–68.

Supporting Information

Gold-Catalyzed Synthesis of π-Extended Carbazole-Based Systems and their Application as Organic Semiconductors

Christoph M. Hendrich,[a] Valentin D. Hannibal,[a] Lukas Eberle,[a] Leif E. Hertwig,[a] Ute Zschieschang,[b] Frank Rominger[+],[a] Matthias Rudolph,[a] Hagen Klauk,[b]* A. Stephen K. Hashmi[a]*

[a] Organisch-Chemisches Institut, Heidelberg University, Im Neuenheimer Feld 270, 69120 Heidelberg (Germany)
Fax: (+49)-6221-54-4205; e-mail: hashmi@hashmi.de (homepage: http://www.hashmi.de)
[b] Max Planck Institute for Solid State Research, Heisenbergstr. 1, 70569 Stuttgart (Germany)
[+] Crystallographic investigation

Table of Contents

1. General Information

All employed chemicals were bought from commercial suppliers (ABCR, TCI, Carbolution, Acros, Alfa Aesar, Chempur, Merck and Sigma Aldrich). Dry solvents were used from the solvent purification system MB SPS 800. Solvents for Sonogashira cross couplings, namely THF and NEt_3, were degassed using freeze pump techniques. Water and toluene for the Suzuki cross couplings were freshly degassed by bubbling nitrogen through a canula. Deuterated solvents were purchased from Euriso Top or Sigma Aldrich. Melting points were measured in open glass capillaries on a Stuart SMP10 melting point apparatus and have not been corrected. R_f-values were determined using aluminium sheets coated with silica gel produced by Merck (TLC Silica gel 60 F254). Visualization of substances proceeded either by employing a coloring reagent (vanillin, ninhydrin) or by exposing the TLC-plate to ultraviolet light (254 and 366 nm). Infrared spectra were recorded on a FT IR spectrometer (Bruker LUMOS) with a Germanium ATR-crystal. For the most significant bands the wave number (cm^{-1}) is given. NMR spectra were, if not mentioned otherwise, recorded at room temperature at the chemistry department of Heidelberg University under the direction of Dr. J. Graf on the following spectrometers: Bruker Avance III 300 (300 MHz), Bruker Avance DRX 300 (300 MHz), Bruker Avance III 400 (400 MHz), Bruker Avance III 500 (500 MHz) and Bruker Avance III 600 (600 MHz). Chemical shifts are given in ppm and coupling constants in Hz. ^1H and ^{13}C NMR spectra were calibrated in relation to deuterated solvents according to Fulmer *et al.*[1] The following abbreviations were used to describe the observed multiplicities: for ^1H NMR spectra: s = singlet, bs = broad singlet, d = doublet, t = triplet, q = quartet, quint = quintet, m = multiplet, dd = doublet of a doublet, dt = doublet of triplet; for ^{13}C NMR spectra: s = quaternary carbon, d = CH carbon, t = CH_2 carbon and q = CH_3 carbon. ^{13}C NMR spectra are proton decoupled (as well as ^{31}P NMR spectra) and interpreted with help of DEPT and 2D spectra. All spectra were integrated and processed using the TopSpin 3.5 software. Mass spectra and high-resolution mass spectra (HRMS) were recorded at the chemical department of Heidelberg University under the direction of Dr. J. Gross. EI spectra were measured on a JEOL JMS 700 spectrometer, ESI spectra on a Bruker ApexQe hybrid 9.4 T FT-ICR (also for MALDI spectra) or a Finnigan LCQ spectrometer. GC/MS spectra were measured on an Agilent 7890A gas chromatograph, coupled with an Agilent 5975C mass selective detector. An OPTIMA 5 cross-linked methyl silicone capillary column (30 Mesh, 0.25 mm, 0.25 µm) was employed. Nitrogen served as carrier gas. UV/Vis spectra were recorded on a Jasco UV-VIS V-670. Fluorescence spectra were recorded on a Jasco FT6500. X-Ray structures were measured on a Stoe Stadivari or Bruker Smart APEX II instrument. All data were processed using the Mercury 3.8 software. CV-spectra were measured on a VERSASTAT3-200 potentiostat using a glassy carbon working electrode, a silver reference electrode and a platinum/titanium counter electrode. Measurements were carried out in a 0.1 M tetrabutyl-ammonium hexafluorophosphate solution in anhydrous and degassed DMSO with a scan rate of 0.5 s^{-1}. Ferrocene/ferrocenium was used as internal standard. For flash column chromatography silica gel of Sigma-Aldrich (silica gel, pore size 60 Å, 230-400 mesh particle size, particle size 40-63 µm) was used as stationary phase. As eluents different mixtures of petroleum ether (PE) and ethyl acetate (EA) or DCM were used.

If not mentioned differently, all reactions were carried out at normal laboratory conditions.

CAUTION: Please note, that azides are potentially explosive and – although we didn't observe any indications of explosive nature – all relevant precautions should be taken.

2. General Procedures

GP1: Sonogashira cross coupling

A Schlenk flask was evacuated and backfilled with nitrogen for three times. 1.00 eq of the aryl halide was dissolved in a degassed 1:1 solution of THF and NEt_3 and 0.5-2 mol% (2-4 mol% for bidirectional Sonogashira) of $PdCl_2(PPh_3)_2$ were added. After stirring for 10 min at room temperature, 1.10-1.50 eq (2.10-2.60 eq) of the corresponding alkyne and 0.5-2 mol% (2-4 mol%) copper(I)-iodide were added. The mixture was stirred at the given temperature for the given time until full conversion. The progress of the reaction was controlled by GC/MS and/or TLC. After the reaction was finished, solvents were removed under reduced pressure and the residue was adsorbed onto Celite®. The crude product was purified using flash column chromatography (silica gel).

GP2: Azidation

According to a slightly modified procedure from Mamidyala and Cooper[2], 1.00 eq of the corresponding amine was dissolved in anhydrous acetonitrile and anhydrous DCM in a flame dried Schlenk flask. The solution was cooled to 0 °C and successively 3.00 eq *tert*-butyl nitrite and 3.00 eq trimethylsilyl azide were added dropwise. After stirring for 30 minutes at 0 °C the reaction mixture was stirred at room temperature for give time until TLC showed full conversion. The reaction mixture was concentrated under reduced pressure and adsorbed onto Celite®. The crude product was purified by flash column chromatography (silica gel).

GP3: Gold catalysis

1.00 eq of the corresponding azide was dissolved in DCE. 2.5-3 mol% JohnPhosAuMeCNSbF_6 were added and the mixture was stirred at given temperature for the given time until TLC showed full conversion. The precipitate was filtered, washed with ice-cold DCM and the residue was dried under vacuum.

GP4: General procedure for alkylation of DBDCZs **2a-b** and DDICZs **3a-b**

In a baked-out Schlenk flask, 1.00 eq of the corresponding carbazole was dissolved in anhydrous DMSO under nitrogen atmosphere. After adding 4.00 eq KO^tBu the solution was stirred for 20 min. Then 20.0 eq 1-bromohexane were added and the mixture was stirred at room temperature for the given time until TLC showed full conversion. The mixture was poured into a beaker of methanol. The precipitate was filtered off and washed successively with water and methanol. The residue was dried under vacuum.

3. Experimental Section

2-((Trimethylsilyl)ethynyl)aniline

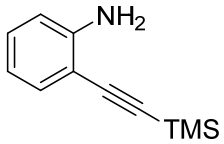

According to GP1, 1.10 eq trimethylsilylacetylene (7.40 g, 10.4 mL, 75.3 mmol) and 0.5 mol% copper(I) iodide (65.2 mg, 342 µmol) were added to a solution of 1.00 eq 2-iodoaniline (15.0 g, 68.5 mmol) and 0.5 mol% $PdCl_2(PPh_3)_2$ (240 mg, 342 µmol) in 100 mL solvent. The solution was stirred for 3 h at room temperature and treated according to GP1 (silica gel, PE:EA = 100:1). A red liquid was obtained (12.2 g, 64.4 mmol, 94%).

R_f: 0.33 (silica gel, PE:EA = 20:1); **^{1}H NMR** ($CDCl_3$, 300.5 MHz): δ[ppm] = 0.26 (s, 9H), 4.22 (bs, 2H), 6.63-6.69 (m, 2H), 7.08-7.14 (m, 1H), 7.29 (dd, $^3J_{H-H}$ = 7.6 Hz, $^4J_{H-H}$ = 1.4 Hz, 1H).

This spectroscopic data confirms to previously reported data.[3]

2-Ethynylaniline, 5

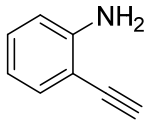

In a 100 mL one necked flask, 1.50 eq potassium carbonate (4.36 g, 31.6 mmol) were added to a solution of 1.00 eq 2-((trimethylsilyl)-ethinyl)-aniline (3.77 g, 19.9 mmol) in 60 mL of methanol. The reaction was stirred for 2 h at room temperature. Then the mixture was concentrated under reduced pressure, quenched with water and extracted with DCM. After drying over magnesium sulphate and evaporation of the solvents, the crude product was adsorbed onto Celite® and purified by flash column chromatography (silica gel, PE to PE:EA = 20:1). A light yellow oil was obtained (2.33 g, 19.9 mmol, 90%).

R_f: 0.47 (silica gel, PE:EA = 5:1); **^{1}H NMR** ($CDCl_3$, 300.5 MHz): δ [ppm] = 3.38 (s, 1H), 4.24 (bs, 2H), 6.65-6.71 (m, 2H), 7.15 (dt, $^3J_{H-H}$ = 7.4 Hz, $^4J_{H-H}$ = 1.5 Hz, 1H), 7.31 (dd, $^3J_{H-H}$ = 7.5 Hz, $^4J_{H-H}$ = 1.1 Hz, 1H).

This spectroscopic data confirms to previously reported data.[3]

1,4-Dibromo-2,5-diiodobenzene, 4a

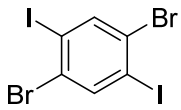

In a 250 mL single necked flask, 4.00 eq iodine (64.6 g, 254 mmol) were added portion wise to a solution of 1.00 eq 1,4-dibromobenzene (15.0 g, 63.6 mmol) in 150 mL of concentrated sulphuric acid. After refluxing for two days, the mixture was poured in a beaker of ice water and extracted with DCM. The crude product was recrystalized from DCM and methanol. The precipitate was filtrated and washed with ice-cold methanol. A colorless solid was obtained (22.6 g, 46.3 mmol, 73%).

R_f: 0.79 (silica gel, PE:EA = 20:1); **^{1}H NMR** ($CDCl_3$, 300.5 MHz): δ[ppm] = 8.05 (s, 2H).

This spectroscopic data confirms to previously reported data.[4]

1,5-Dibromo-2,4-diiodobenzene, 4b

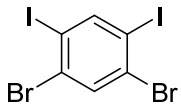

In a 100 mL single necked flask, 0.50 eq periodic acid (4.85 g, 21.2 mmol) were added to 50 mL of concentrated sulphuric acid. The reaction mixture was cooled down to 0°C and 1.00 eq 1,3-dibromobenzene (10.0 g, 42.4 mmol) were dissolved. Then 1.50 eq potassium iodide (10.7 g, 63.6 mmol) were added carefully in portions. Another 20 mL of concentrated sulphuric acid were added subsequently, since the solution started to solidify. After 30 min the solution was quenched with ice and filtrated. The crude product was recrystallized from toluene. The product was filtrated and washed with ice-cold hexane. A light pink powder was obtained (6.12 g, 12.5 mmol, 30%).

R_f: 0.82 (silica gel, PE:EA = 5:1); **^{1}H NMR** ($CDCl_3$, 300.5 MHz): δ[ppm] = 7.83 (s, 1H), 8.28 (s, 1H).

This spectroscopic data confirms to previously reported data.[5]

4,6-Diiodobenzene-1,3-diamine, 10

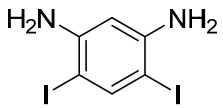

According to a slightly modified procedure of Zupan *et al.*[6], 1.00 eq *m*-phenylendiamine (2.00 g, 18.5 mmol) and 2.00 eq potassium iodide (6.14 g, 37.0 mmol) were added to a mixture of 1.50 eq of concentrated sulphuric acid (2.72 g, 1.49 mL, 27.7 mmol) and 100 mL methanol. The solution was cooled down to 0 °C. 4.00 eq H_2O_2 (35 wt%, 7.19 g, 6.33 mL, 74.0 mmol) were added over the course of 1 h under continuous cooling. After that, the reaction mixture was stirred further for 1.5 h at the same temperature. The reaction mixture was neutralized with 2 M NaOH, extracted with DCM and dried over sodium sulphate. The solution was concentrated under vacuum and the product precipitated at -20 °C to obtain a colorless solid (1.72 g, 4.78 mmol, 26%).

R_f: 0.30 (silica gel, PE:EA = 1:1); **^{1}H NMR** (DMSO-d_6, 300.5 MHz): δ[ppm] = 5.03 (bs, 4H), 6.23 (s, 1H), 7.52 (s, 1H).

This spectroscopic data confirms to previously reported data.[6]

([1,1'-Biphenyl]-2-ylethynyl)trimethylsilane

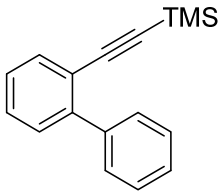

According to GP1, 1.50 eq trimethylsilylacetylene (2.42 g, 3.41 mL, 42.6 mmol) and 2 mol% copper(I) iodide (62.6 mg, 328 µmol) were added to a solution of 1.00 eq 2-iodo-1,1'-biphenyl (4.60 g, 16.4 mmol) and 2 mol% $PdCl_2(PPh_3)_2$ (231 mg, 328 µmol) in 70 mL solvent. The solution was stirred overnight at room temperature and treated according to GP1 (silica gel, PE to PE:EA = 10:1). A yellow liquid was obtained (4.04 g, 16.1 mmol, 98%).

R_f: 0.60 (silica gel, PE:EA = 10:1); **^{1}H NMR** ($CDCl_3$, 300.5 MHz): δ[ppm] = 0.13 (s, 9H), 7.26-7.35 (m, 1H), 7.35-7.44 (m, 5H), 7.57-7.63 (m, 3H).

This spectroscopic data confirms to previously reported data.[7]

2-Ethynyl-1,1'-biphenyl, 11

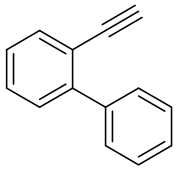

In a 100 mL one necked flask, 2.00 eq potassium carbonate (4.42 g, 32.0 mmol) were added to a solution of 1.00 eq ([1,1'-biphenyl]-2-ylethynyl)trimethylsilane (4.00 g, 16.0 mmol) in 75 mL of methanol. The reaction was stirred for 3 h at room temperature. Then the mixture was concentrated under reduced pressure, quenched with water and extracted with DCM. After drying with sodium sulphate and evaporation of the solvents, the crude product was adsorbed onto Celite® and purified by flash column chromatography (silica gel, PE to PE:EA = 10:1). A colorless oil was obtained (2.70 g, 15.2 mmol, 95%).

R_f: 0.55 (silica gel, PE:EA = 10:1); **^{1}H NMR** ($CDCl_3$, 300.5 MHz): δ[ppm] = 3.04 (s, 1H), 7.34-7.40 (m, 1H), 7.40-7.44 (m, 5H), 7.58-7.61 (m, 3H).

This spectroscopic data confirms to previously reported data.[8]

Di-*tert*-butyl (2,5-dibromo-1,4-phenylene)dicarbamate, 9

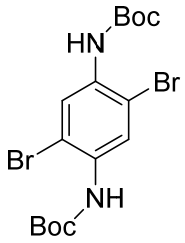

Compound **9** was synthesized in a three step synthesis from *p*-phenylenediamine according to a previously reported procedure.[9]

R_f: 0.69 (silica gel, PE:EA = 5:1); **^{1}H NMR** ($CDCl_3$, 300.5 MHz): δ[ppm] = 1.53 (s, 18H), 6.87 (s, 2H), 8.38 (s, 2H).

This spectroscopic data confirms to previously reported data.[9]

2,2'-((2,5-Dibromo-1,4-phenylene)bis(ethyne-2,1-diyl))dianiline, 6a

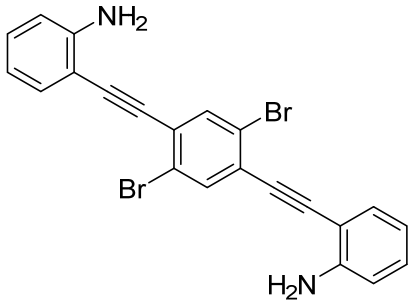

According to GP1, 2.10 eq 2-ethynylaniline (1.26 g, 10.8 mmol) and later 2 mol% copper(I) iodide (19.5 mg, 103 µmol) were added to a mixture of 1.00 eq 1,4-dibromo-2,5-diiodobenzene (2.50 g, 5.13 mmol) and 2 mol% $PdCl_2(PPh_3)_2$ (80.0 mg, 103 µmol) in 70 mL solvent. The solution was stirred overnight at room temperature and treated according to GP1 (silica gel, PE:EA = 2:1 to 1:2+DCM). The residue was precipitated from EE and PE. An orange-yellow solid was obtained (1.02 g, 2.19 mmol, 43%).

Mp.: 230 °C (decomposition); **R_f:** 0.55 (silica gel, PE:EA = 2:1); **IR**(ATR): $\tilde{\nu}$[cm^{-1}] = 3405, 3302, 3192, 3082, 2208, 2189, 1784, 1734, 1624, 1598, 1567, 1498, 1469, 1449, 1363, 1312, 1271, 1252, 1155, 1057, 934, 898, 854, 800, 747; **^{1}H NMR** ($CDCl_3$, 400.3 MHz): δ[ppm] = 4.47 (bs, 4H), 6.71-6.75 (m, 4H), 7.16-7.21 (m, 2H), 7.37-7.39 (m, 2H), 7.79 (s, 2H); **^{13}C NMR** ($CDCl_3$, 100.7 MHz): δ[ppm] = 92.4 (s, 2C), 94.2 (s, 2C), 106.8 (s, 2C), 114.6 (d, 2C), 118.1 (d, 2C); 123.3 (s, 2C), 126.4 (s, 2C), 130.9 (d, 2C), 132.4 (d, 2C), 135.7 (d, 2C), 148.8 (s, 2C); **HRMS** (DART+): $C_{22}H_{15}N_2{}^{79}Br^{81}Br^+$, calculated: 466.9571 [$M^+$+H], observed: 466.9574 [M^++H].

2,2'-((4,6-Dibromo-1,3-phenylene)bis(ethyne-2,1-diyl))dianiline, 6b

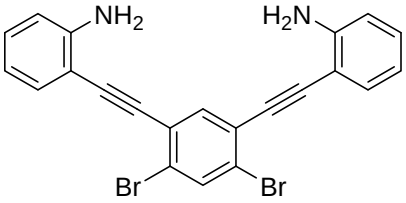

According to GP1, 2.10 eq 2-ethynylaniline (504 mg, 4.31 mmol) and later 2 mol% copper(I) iodide (7.81 mg, 41.0 mmol) were added to a mixture of 1.00 eq 1,5-dibromo-2,4-diiodobenzene (1.00 g, 2.05 mmol) and 2 mol% $PdCl_2(PPh_3)_2$ (28.8 mg, 41.0 mmol) in 30 mL solvent. The solution was stirred over three days at 60°C and treated according to GP1 (silica gel, PE:EA = 10:1 to DCM). The product was recrystalized in EA and filtered. A yellow to beige solid was obtained (526 mg, 1.13 mmol, 55%).

Mp.: 185-187 °C; **R_f:** 0.24 (silica gel, PE: EA = 5:1); **IR**(ATR): $\tilde{\nu}$[cm^{-1}] = 3406, 3304, 3188, 3058, 2913, 2200, 1914, 1886, 1743, 1614, 1572, 1520, 1490, 1454, 1371, 1318, 1308, 1253, 1155, 1132, 1053, 963, 935, 897, 863, 851, 752, 731, 666, 606; **^{1}H NMR** ($CDCl_3$, 600.2 MHz): δ [ppm] = 4.45 (bs, 4H), 6.71-6.74 (m, 4H), 7.17-7.20 (m, 2H), 7.38 (dd, $^3J_{H-H}$ = 8.3, 1.6 Hz, 2H), 7.74 (s, 1H), 7.90 (s, 1H); **^{13}C NMR** (150.9 MHz, $CDCl_3$) δ = 92.1 (s, 2C), 92.8 (s, 2C), 106.9 (s, 2C), 114.6 (d, 2C), 118.1 (d, 2C), 124.4 (s, 2C), 125.3 (s, 2C), 130.8 (d, 2C), 132.4 (d, 2C), 135.7 (d, 1C), 136.0 (s, 2C), 148.7 (d, 1C); **HRMS** (DART+): $C_{22}H_{15}N_2Br^{79}Br^{81+}$, calculated: 466.9576 [$M^+$+H], observed: 466.9582 [M^++H].

2,2'-([1,1':4',1''-Terphenyl]-2',5'-diylbis(ethyne-2,1-diyl))dianiline, 7a

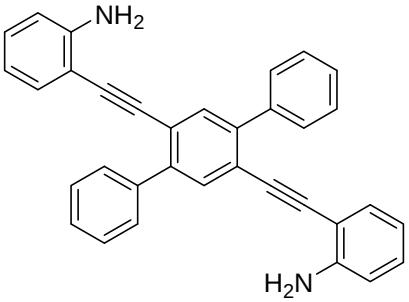

Under nitrogen atmosphere, 1.00 eq 2,2'-((2,5-dibromo-1,4-phenylene)bis(ethyne-2,1-diyl))dianiline (1.00 g, 2.15 mmol), 2.50 eq phenylboronic acid (654 mg, 5.36 mmol), 4.00 eq potassium carbonate (2.83 g, 20.5 mmol), 1 mol% $Pd_2(dba)_3$ (46.9 mg, 51.3 µmol) and 4 mol% P(*o*-tolyl)$_3$ (31.2 mg, 205 µmol) were successively added to 20 mL of a freshly degassed 4:1 mixture of toluene and water. Additional 10 mL anhydrous, degassed THF were added for solubility reasons. The reaction mixture was stirred at 90 °C overnight. The completion was determined via TLC. The reaction mixture was allowed to cool down to room temperature, diluted with water, extracted with DCM and dried over magnesium sulphate The crude product was concentrated under reduced pressure and purified via recrystallization in ethanol which furnished a brown solid (600 mg, 1.30 mmol, 61%).

Mp.: 217 °C (decomposition); **R_f:** 0.51 (silica gel, PE:EA 2:1); **IR**(ATR): $\tilde{\nu}$[cm^{-1}] = 3465, 3373, 3031, 2972, 2195, 1614, 1563, 1510, 1494, 1475, 1449, 1393, 1312, 1254, 1159, 1076, 1050, 1028, 967, 937, 899, 766, 749, 704; **^{1}H NMR** ($CDCl_3$, 400.3 MHz): δ[ppm] = 3.82 (bs, 4H), 6.58-6.60 (m, 2H), 6.64 (dt, $^3J_{H-H}$ = 7.6 Hz, $^4J_{H-H}$ = 1.0 Hz, 2H), 7.05-7.10 (m, 2H), 7.21 (dd, $^3J_{H-H}$ = 7.7 Hz, $^4J_{H-H}$ = 1.4 Hz, 2H), 7.40-

7.44 (m, 2H), 7.46-7.51 (m, 4H), 7.67 (s, 2H), 7.68-7.70 (m, 4H); **^{13}C NMR** ($CDCl_3$, 100.7 MHz): δ[ppm] = 91.1 (s, 2C), 94.4 (s, 2C), 107.8 (s, 2C), 114.3 (s, 2C), 117.9 (s, 2C), 122.0 (s, 2C), 128.0 (d, 4C), 128.5 (d, 4C), 129.3 (d, 2C); 130.0 (d, 2C), 132.2 (d, 2C), 133.4 (s, 2C), 140.3 (s, 2C), 142.4 (s, 2C), 148.2 (s, 2C); **HRMS** (ESI+): $C_{34}H_{24}N_2Na^+$, calculated: 483.1832 [M^++Na], observed 483.1842 [M^++Na]; **UV/VIS** (DCM, 4.60 µg/mL): λ[nm] (log ε) = 250 (4.50), 281 (4.51) 313 (4.24) 382 (4.53); **Fluorescence** (DCM): λ_{ex} = 380 nm, λ_{max} = 444 nm; **Quantum yield:** Φ = 79.8%.

2,2'-([1,1':3',1''-Terphenyl]-4',6'-diylbis(ethyne-2,1-diyl))dianiline, 7b

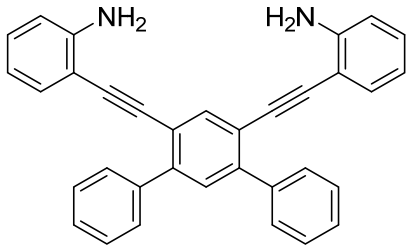

Under nitrogen atmosphere, 1.00 eq 2,2'-((4,6-dibromo-1,3-phenylene)bis(ethyne-2,1-diyl))dianiline (483 mg, 1.04 mmol), 2.50 eq phenylboronic acid (316 mg, 2.59 mmol), 4.00 eq potassium carbonate (573 mg, 4.14 mmol), 1 mol% $Pd_2(dba)_3$ (9.49 mg, 10.4 µmol) and 4 mol% P(*o*-tolyl)$_3$ (12.6 mg, 41.4 µmol) were successively added to 11 mL of a freshly degassed 10:1 mixture of THF and water. The reaction mixture was stirred at 70 °C overnight. The completion was determined via TLC. The reaction mixture was allowed to cool down to room temperature, diluted with water, extracted with DCM and dried over magnesium sulphate. The crude product was concentrated under reduced pressure and purified via flash column chromatography (silica gel, PE:EA = 10:1). A yellowish solid was obtained (424 mg, 921 µmol, 89%).

Mp.: 87 °C; **R_f:** 0.21 (silica gel, PE:EA = 5:1); **IR**(ATR): $\tilde{\nu}$[cm^{-1}] = 3473, 3376, 3056, 3028, 2199, 1738, 1612, 1571, 1508, 1490, 1475, 1455, 1442, 1386, 1314, 1253, 1157, 1075, 1029, 1010, 900, 850, 784, 767, 744, 698; **^{1}H NMR** ($CDCl_3$, 400.3 MHz): δ[ppm] = 3.87 (bs, 4H), 6.61 (d, $^3J_{H-H}$ = 8.1 Hz, 2H),), 6.67 (dt, $^3J_{H-H}$ = 7.6 Hz, $^4J_{H-H}$ = 0.9 Hz, 2H), 7.07-7.11 (m, 2H), 7.26 (dd, $^3J_{H-H}$ = 7.7 Hz, $^4J_{H-H}$ = 1.4 Hz, 2H), 7.38-7.48 m, 7H), 7.67-7.70 (m, 4H), 7.93 (s, 1H); **^{13}C NMR** ($CDCl_3$, 100.7 MHz): δ[ppm] = 90.1 (s, 2C), 93.7 (s, 2C), 107.8 (s, 2C), 114.3 (d, 2C), 117.9 (d, 2C), 121.4 (s, 2C), 128.0 (d, 2C), 128.5 (d, 4C), 129.2 (d, 4C), 130.0 (d, 2C), 130.7 (d, 1C), 132.2 (d, 2C), 136.5 (d, 1C), 140.5 (s, 2C), 143.1 (s, 2C), 148.2 (s, 2C); **HRMS** (ESI+): $C_{34}H_{25}N_2^+$, calculated: 461.2012 [M^++H], observed: 461.2018 [M^++H]; **UV/VIS** (DCM, 3.52 µg/mL): λ[nm] (log ε) = 254 (4.56), 285 (4.68), 350 (4.56); **Fluorescence** (DCM): λ_{ex} = 350 nm, λ_{max} = 444 nm; **Quantum yield:** Φ = 91.9%.

Di-*tert*-butyl (2,5-bis([1,1'-biphenyl]-2-ylethynyl)-1,4-phenylene)dicarbamate, 12

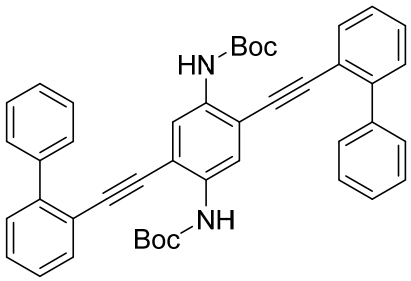

According to GP1, 2.60 eq 2-ethynyl-1,1'-biphenyl (994 mg, 5.58 mmol) and 4 mol% copper(I) iodide (16.3 mg, 85.8 µmol) were added to a solution of 1.00 eq di-*tert*-butyl(2,5-dibromo-1,4-phenylene)dicarbamate (1.00 g, 2.15 mmol) and 4 mol% $PdCl_2(PPh_3)_2$ (60.2 mg, 85.8 µmol) in 80 mL solvent. After stirring for 10 minutes, the reaction mixture turned black. The solution was stirred for 72 h at 60 °C and treated according to GP1 (silica gel, PE:EA = 10:1 to EE to DCM). The residue was precipitated from EE and PE). A colorless solid was obtained (1.06 g, 1.60 mmol, 75%).

Mp.: 203-205 °C; **R_f:** 0.43 (silica gel, PE:EA = 10:1); **IR** (ATR): $\tilde{\nu}$ [cm^{-1}] = 3406, 3336, 3058, 2966, 1708, 1532, 1500, 1487, 1435, 1415, 1390, 1366, 1285, 1241, 1153, 1053, 1028, 894, 860, 772, 750, 731, 700; **^{1}H NMR** ($CDCl_3$, 500.2 MHz): δ[ppm] = 1.51 (s, 18H), 6.79 (s, 2H), 7.36-7.39 (m, 4H), 7.43-7.48 (m, 8H), 7.60-7.66 (m, 6H), 8.12 (s, 2H); **^{13}C NMR** ($CDCl_3$, 125.8 MHz): δ[ppm] = 28.5 (d, 2C), 80.8 (s, 2C), 87.6 (s, 2C), 97.0 (s, 2C), 112.7 (s, 2C), 120.9 (s, 2C), 121.0 (d, 2C), 127.3 (d, 2C), 127.9 (s, 2C), 128.4 (d, 4C), 129.2 (d, 4C), 129.3 (d, 2C), 129.7 (d, 2C), 133.2 (d, 2C), 134.0 (s, 2C), 140.4 (s, 2C), 144.0 (s, 2C), 152. 6 (s, 2C); **HRMS** (ESI+): $C_{44}H_{40}N_2NaO_4^+$, calculated: 683.2880 [M^++Na], observed: 683.2885 [M^++Na]; **UV/VIS** (DCM, 6.60 µg/mL): λ[nm] (logε) = 264 (4.62), 324 (4.46), 371 (4.33); **Fluorescence** (DCM): λ_{Anr} = 320 nm, λ_{max} = 260 nm, 324 nm, 370 nm; **Quantum yield**: Φ = 69.1%.

2,5-Bis([1,1'-biphenyl]-2-ylethynyl)benzene-1,4-diamine, 13a

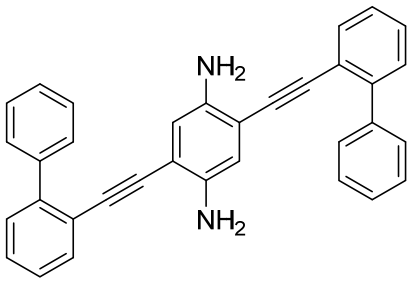

1.00 eq of di-*tert*-butyl(2,5-bis([1,1'-biphenyl]-2-ylethynyl)-1,4-phenylene)dicarbamate (500 mg, 757 µmol) was dissolved and treated with 28.4 mL HCl in dioxane (4M, 150 eq). After stirring for 1 h at room temperature, the formed colorless precipitate was filtered, washed with diethylether and again dissolved in DCM and water. The mixture was neutralized with saturated sodium hydrogen carbonate solution and the organic phase dried with sodium sulphate. After evaporation of the solvents, the crude was directly used for the next step without further purification.

4,6-Bis([1,1'-biphenyl]-2-ylethynyl)benzene-1,3-diamine, 13b

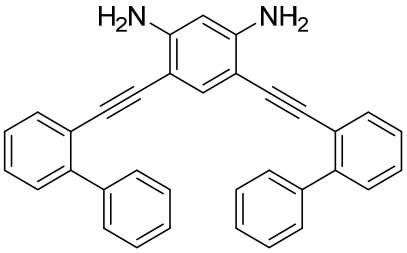

According to GP1, 2.60 eq 2-ethynyl-1,1'-biphenyl (1.29 g, 75.3 mmol) and 4 mol% copper(I) iodide (21.2 mg, 111 µmol) were added to a solution of 1.00 eq 4,6-diiodobenzene-1,3-diamine (1.00 g, 2.78 mmol) and 4 mol% $PdCl_2(PPh_3)_2$ (78.0 mg, 111 µmol) in 40 mL solvent. The solution was stirred overnight at room temperature and treated according to GP1 (silica gel, PE:EA = 1:1 to EE to DCM). The residue was precipitated from EE and PE. A yellow, brownish powder was obtained (1.25 g, 2.71 mmol, 98%).

R_f: 0.68 (silica gel, PE:EA = 1:1); **Mp.:** 131 °C; **IR** (ATR): $\tilde{\nu}$ [cm^{-1}] = 3464, 3365, 3196, 3058, 2185, 1953, 1890, 1812, 1622, 1542, 1508, 1476, 1444, 1354, 1331, 1263, 1157, 1076, 1045, 1007, 948, 905, 836, 773, 749, 734, 699, 625; **^{1}H NMR** ($CDCl_3$, 300.5 MHz): δ[ppm] = 3.78 (bs, 4H), 5.75 (s, 1H), 7.17 (s, 1H), 7.32-7.46 (m, 12H), 7.56-7.67 (m, 6H); **^{13}C NMR** ($CDCl_3$, 125.8 MHz): δ[ppm] = 89.3 (s, 2C), 92.8 (s, 2C), 97.9 (d, 1C), 98.8 (s, 2C), 122.6 (s, 2C), 127.3 (d, 2C), 127.5 (d, 2C), 127.7 (d, 2C), 128.3 (d, 4C), 129.3 (d, 4C), 129.5 (d, 2C), 132.1 (d, 2C), 136.0 (d, 1C), 141.5 (s, 2C), 143.1 (s, 2C), 149.6 (s, 2C); **HRMS** (ESI+): $C_{34}H_{24}N_2^+$, calculated: 460.1934 [M^+], observed: 460.1937 [M^+].

2',5'-Bis((2-azidophenyl)ethynyl)-1,1':4',1''-terphenyl, 8a

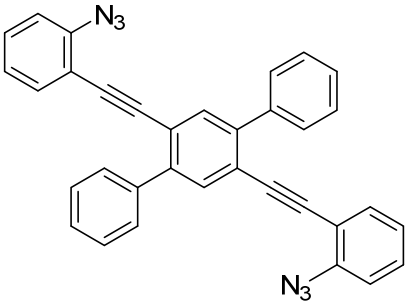

According to GP2, 1.00 eq 2,2'-([1,1':4',1''-terphenyl]-2',5'-diylbis(ethyne-2,1-diyl))dianiline (500 mg, 1.09 mmol) was dissolved in 15 mL anhydrous MeCN and 20 mL anhydrous DCM in a baked-out Schlenk flask. The solution was cooled down to 0 °C and successively 3.00 eq *tert*-butyl nitrite (90%, 373 mg, 430 µL, 3.26 mmol) and 3.00 eq trimethylsilyl azide (375 mg, 432 µL, 3.26 mmol) were added dropwise. After stirring for 30 minutes at 0 °C the reaction mixture was stirred 30 minutes at room temperature and treated according to GP2 (silica gel, PE:EA = 20:1 to 1:1+DCM) to give a dark red solid (487 mg, 950 µmol, 88%).

Mp.: 185 °C (decomposition); **R_f:** 0.47 (silica gel, PE:EA = 10:1); **IR**(ATR): $\tilde{\nu}$[cm^{-1}] = 2128, 2096, 1568, 1509, 1491, 1439, 1387, 1303, 1265, 1161, 1091, 1021, 941, 911, 863, 766, 752, 702, 666, 631; **^{1}H NMR** ($CDCl_3$, 400.3 MHz): δ[ppm] = 7.03-7.10 (m, 4H), 7.27-7.33 (m, 4H), 7.40-7.44 (m, 2H), 7.47-7.51 (m, 4H), 7.75-7.77 (m, 6H); **^{13}C NMR** ($CDCl_3$, 100.7 MHz): δ[ppm] = 89.7 (s, 2C), 94.9 (s, 2C), 115.6 (s,

2C), 118.9 (d, 2C), 21.9 (s, 2C), 124.7 (d, 2C), 127.9 (d, 2C), 128.2 (d, 4C), 129.6 (d, 4C), 129.7 (d, 2C), 133.6 (d, 2C), 134.1 (d, 2C), 139.4 (s, 2C), 141.2 (s, 2C), 142.6 (s, 2C); **HRMS** (EI+): $C_{34}H_{24}N_6^+$, calculated: 512.1771 [M^+], observed: 512.1752 [M^+]; **UV/VIS** (DCM, 11.6 µg/mL): λ[nm] (log ε) = 240 (4.20), 266 (4.55), 278 (4.53), 346 (4.52), 364 (4.44).

4',6'-Bis((2-azidophenyl)ethynyl)-1,1':3',1''-terphenyl, 8b

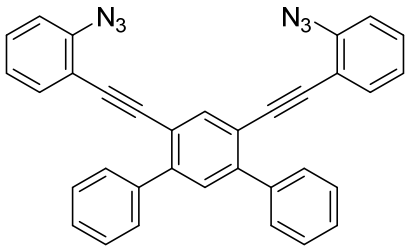

According to GP2, 1.00 eq 2,2'-([1,1':3',1''-terphenyl]-4',6'-diylbis(ethyne-2,1-diyl))dianiline (250 mg, 543 µmol) was dissolved in 8 mL anhydrous MeCN and 7 mL anhydrous DCM in a baked-out Schlenk flask. The solution was cooled down to 0 °C and successively 3.00 eq *tert*-butyl nitrite (90%, 187 mg, 215 µl, 1.63 mmol) and 3.00 eq trimethylsilyl azide (188 mg, 216 µl, 1.63 mmol) were added dropwise. After stirring for 30 minutes at 0 °C the reaction mixture was stirred 30 minutes at room temperature and treated according to GP2 (silica gel, PE:EA = 20:1) to give an orange-yellow solid (270 mg, 527 µmol, 97%).

Mp.: 116 °C; **R_f:** 0.44 (silica gel, PE:EA = 10:1); **IR**(ATR): $\tilde{\nu}$[cm^{-1}] = 3047, 3021, 2114, 2085, 1738, 1598, 1567, 1487, 1474, 1444, 1384, 1306, 1255, 1182, 1159, 1087, 1076, 1031, 1009, 933, 903, 888, 770, 742, 734, 711, 697, 671, 648; **^{1}H NMR** ($CDCl_3$, 400.3 MHz): δ[ppm] = 7.05-7.12 (m, 4H), 7.30-7.34 (m, 4H), 7.40-7.50 (m, 6H), 7.54 (s, 1H), 7.75-7.78 (m, 4H), 8.02 (s, 1H); **^{13}C NMR** ($CDCl_3$, 100.7 MHz): δ[ppm] = 88.8 (s, 2C), 94.2 (s, 2C), 115.6 (s, 2C), 118.9 (d, 2C), 120.5 (s, 2C), 124.7 (d, 2C), 128.0 (d, 2C), 128.1 (d, 4C), 129.6 (d, 4C), 129.7 (d, 2C), 130.9 (d, 1C), 133.6 (d, 2C), 137.7 (d, 1C), 139.7 (s, 2C), 141.2 (s, 2C), 144.0 (s, 2C); **HRMS** (EI+): $C_{34}H_{20}N_6^+$, calculated: 512.1744 [M^+], observed: 512.1730 [M^+] ; **UV/VIS** (DCM, 4.36 µg/mL): λ[nm] (log ε) = 264 (4.79), 307 (4.77).

2,2''-((4,6-Diazido-1,3-phenylene)bis(ethyne-2,1-diyl))di-1,1'-biphenyl, 14b

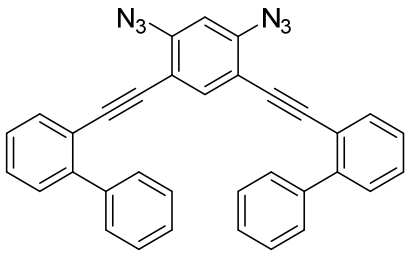

According to GP2, 1.00 eq 4,6-bis([1,1'-biphenyl]-2-ylethynyl)benzene-1,3-diamine (625 mg, 1.36 mmol) were dissolved in 18 mL anhydrous acetonitrile and 24 mL anhydrous DCM in a baked out Schlenk flask. The solution was cooled to 0 °C and successively 4.00 eq *tert*-butyl nitrite (90%, 806 mg, 1.03 mL, 7.82 mmol) and 4.00 eq trimethylsilyl azide (901 mg, 1.02 mL, 7.82 mmol) were added dropwise. After stirring for 30 minutes at 0 °C the reaction mixture was stirred 30 minutes at

room temperature and treated according to GP2 (silica gel, PE:EA = 20:1 to 10:1) to give a light yellow solid (550 mg, 1.07 mmol, 55%).

Mp.: 128-130 °C; **R_f:** 0.40 (silica gel, PE:EA = 10:1); **IR** (ATR): $\tilde{\nu}$ [cm^{-1}] = 3056, 3026, 2168, 2103, 1547, 1509, 1489, 1475, 1449, 1432, 1398, 1347, 1277, 1159, 1075, 1008, 948, 918, 891, 831, 777, 754, 738, 701, 663, 610; **^{1}H NMR** ($CDCl_3$, 400.3 MHz): δ[ppm] =6.68 (s, 1H), 7.16 (s, 1H), 7.33-7.46 (m, 12H), 7.64-7.67 (m, 6H); **^{13}C NMR** ($CDCl_3$, 100.7 MHz): δ[ppm] = 86.6 (s, 2C), 95.9 (s, 2C), 109.5 (d, 1C), 112.8 (s, 2C), 121.2 (s, 2C), 127.2 (d, 2C), 127.7 (d, 2C), 128.1 (d, 4C), 129.1 (d,2C), 129.6 (d, 4C), 129.7 (d, 2C), 133.1 (d, 2C), 137.9 (d, 1H), 140.4 (s, 2C), 141.6 (s, 2C), 144.1 (s, 2C); **HRMS** (EI+): $C_{34}H_{20}N_6^+$, calculated: 512.17440 [M^+], observed: 512.17109 [M^+]; **UV/VIS** (DCM, 7.20 µg/mL): λ[nm] (log ε) = 262 (4.66), 309 (4.73), 351 (4.46).

2,2''-((2,5-Diazido-1,4-phenylene)bis(ethyne-2,1-diyl))di-1,1'-biphenyl, 14a

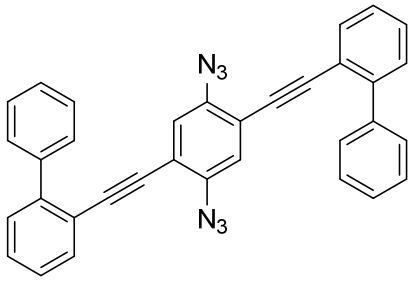

According to GP2, the crude 2,5-bis([1,1'-biphenyl]-2-ylethynyl)benzene-1,4-diamine **13a** (corresponding 757 µmol) was dissolved in 20 mL anhydrous acetonitrile and 20 mL anhydrous DCM in a baked out Schlenk flask. The solution was cooled down to 0 °C and successively 5.00 eq *tert*-butyl nitrite (90%, 433 mg, 499 µL, 3.78 mmol) and 5.00 eq trimethylsilyl azide (435 mg, 501 µL, 3.78 mmol) were added dropwise. After stirring for 30 minutes at 0 °C the reaction mixture was stirred 1 h at room temperature. The solvents were evaporated and due to a side product, which was observed via TLC, directly used for the next step without further purification.

DBDCZ 2a

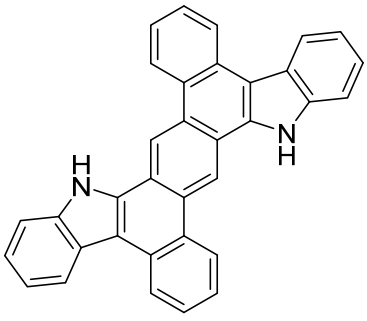

According to GP3, 1.00 eq of the corresponding azide **8a** (399 mg, 778 µmol) was dissolved in 50 mL DCE. 2.5 mol% JohnPhosAuMeCNSbF_6 (15.0 mg, 19.5 µmol) were added and the mixture was stirred at 80 °C overnight. The precipitate was filtered, washed with ice-cold DCM and the residue was dried under vacuum. A yellow solid was obtained (271 mg, 594 µmol, 76%).

Mp.: >410 °C; **IR**(ATR): $\tilde{\nu}$[cm^{-1}] = 3447, 3093, 3048, 1608, 1597, 1535, 1488, 1459, 1431, 1399, 1360, 1338, 1304, 1256, 1207, 1191, 1166, 1149, 1117, 1048, 1018, 970, 935, 860, 787, 757, 738, 681, 642, 613; **^{1}H NMR** (DMSO-d_6, 600.2 MHz): δ[ppm] = 7.37-7.39 (m, 2H), 7.47-7.50 (m, 2H), 7.75-7.78 (m, 2H), 7.82 (d, $^3J_{H-H}$ = 8.0 Hz, 2H), 7.86-7.89 (m, 2H), 8.62 (d, $^3J_{H-H}$ = 8.0 Hz, 2H), 8.87 (d, $^3J_{H-H}$ = 7.8 Hz, 2H), 9.27 (d, $^3J_{H-H}$ = 8.2 Hz, 2H), 10.15 (s, 2H), 12.75 (s, 2H); **^{13}C NMR** (DMSO-d_6, 150.9 MHz): δ[ppm] = 111.2 (s, 2C), 111.9 (d, 2C), 117.4 (d, 2C), 120.3 (d, 2C), 121.4 (s, 2C), 121.4 (d, 2C), 123.7 (d, 2C), 123.8 (d, 4C), 123.9 (s, 2C), 124.3 (d, 2C), 126.6 (s, 2C), 128.2 (d, 2C), 128.5 (s, 2C), 130.2 (s, 2C), 134.6 (s, 2C), 138.6 (s, 2C), **HRMS** (ESI+): $C_{34}H_{20}N_2^+$, calculated: 456.1621 [M$^+$], observed: 456.1622 [M$^+$]; **UV/VIS** (DCM, 4.40 µg/mL): λ[nm] (log ε) = 281 (4.79), 327 (4.74), 342 (4.85), 377 (4.49), 395 (4.57), 425 (3.58); **Fluorescence** (THF): λ_{ex} = 425 nm, λ_{max} = 438 nm, 467 nm, 497 nm; **Quantum yield:** Φ = 28.4%.

DBDCZ 2b

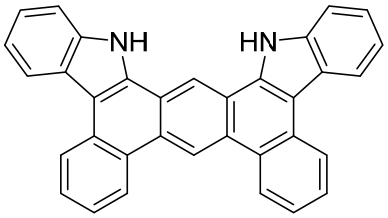

According to GP3, 1.00 eq of the corresponding azide **8b** (200 mg, 390 µmol) was dissolved in 50 mL DCE. 3 mol% JohnPhosAuMeCNSbF$_6$ (9.04 mg, 11.7 µmol) were added and the mixture was stirred was at 80 °C for 2 h. The precipitate was filtered, washed with ice-cold DCM and the residue was dried under vacuum. A greenish solid was obtained (136 mg, 298 µmol, 76%).

Mp.: 390 °C (decomposition); **IR**(ATR): $\tilde{\nu}$[cm^{-1}] = 3438, 3046, 3025, 1609, 1561, 1536, 1476, 1457, 1443, 1356, 1338, 1316, 1276, 1262, 1191, 1166, 1150, 1116, 1046, 1018, 960, 937, 975, 960, 937, 875, 844, 773, 758, 741, 720, 676, 611; **^{1}H NMR** (DMSO- d_6, 400.3 MHz): δ[ppm] = 7.37-7.41 (m, 2H), 7.47-7.51 (m, 2H), 7.70-7.74 (m, 2H), 7.83-7.87 (m, 4H), 8.62 (d, $^3J_{H-H}$ = 8.1 Hz, 2H), 8.86 (d, $^3J_{H-H}$ = 8.0 Hz, 2H), 9.49 (d, $^3J_{H-H}$ = 8.2 Hz, 2H), 9.59 (s, 1H), 10.39 (s, 1H), 12.13 (s, 2H); **^{13}C NMR** (DMSO- d_6, 100.7 MHz): δ[ppm] = 112.0 (s, 2C), 112.3 (d, 2C), 115.2 (d, 1C), 119.1 (d, 1C), 120.5 (d, 2C), 121.4 (d, 2C), 121.8 (s, 2C), 123.6 (d, 2C), 123.9 (d, 2C), 124.0 (d, 2C), 124.1 (s, 2C), 124.8 (d, 2C), 127.0 (s, 2C), 127.9 (s, 2C), 128.0 (d, 2C), 129.9 (s, 2C), 134.1 (s, 2C), 139.1 (s, 2C); **HRMS** (DART+): $C_{34}H_{21}N_2^+$, calculated: 457.1699 [M$^+$+H], observed: 457.1969 [M$^+$+H]; **UV/VIS** (THF, 4.05 µg/mL): λ[nm] (log ε) = 265 (4.81), 342 (5.00), 415 (3.66); **Fluorescence** (THF): λ_{ex} = 340 nm, λ_{max} = 424 nm, 450 nm, 478 nm; **Quantum yield:** Φ = 29.9%.

9,11-Dihydrodibenzo[*a,c*]dibenzo[4,5:6,7]indolo[3,2-*h*]carbazole, DDICZ 3b

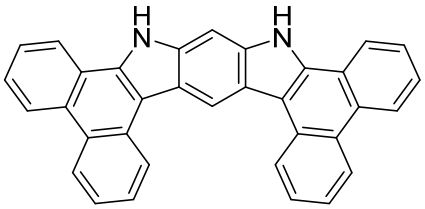

According to GP3, 1.00 eq of the corresponding azide **14a** (550 mg, 1.07 mmol) was dissolved in 2.50 mL DCE. 3.00 mol% JohnPhosAuMeCNSbF$_6$ were added and the mixture was stirred at 80 °C overnight. The precipitate was filtered, washed with ice-cold DCM and the residue was dried under vacuum to give a slightly off white solid (430 mg, 942 µmol, 88%).

Mp.: >300 °C; **IR** (ATR): $\tilde{\nu}$ [cm^{-1}] = 3426, 3092, 1635, 1611, 1572, 1519, 1462, 1435, 1372, 1329, 1304, 1286, 1273, 1230, 1157, 1069, 1042, 845, 909, 825, 751, 740, 716, 668, 650, 620; **^{1}H NMR** (DMSO-d_6, 400.3 MHz): δ[ppm] = 7.64-7.85 (m, 6H), 7.94 (s, 1H), 7.97-8.02 (m, 2H), 8.60 (d, $^3J_{H-H}$ = 8.0 Hz, 2H), 8.97 (d, $^3J_{H-H}$ = 8.1 Hz, 4H), 9.16 (d, $^3J_{H-H}$ = 7.8 Hz, 2H), 9.56 (s, 1H), 12.30 (s, 2H); **^{13}C NMR** (DMSO-d_6, 100.7 MHz): δ[ppm] = 92.6 (d, 1C), 111.3 (s, 2C), 112.6 (d, 1C), 120.3 (s, 2C), 122.0 (d, 2C), 122.5 (s, 2C), 123.3 (d, 2C), 123.5 (d, 2C), 129.9 (d, 4C), 126.0 (d, 2C), 126.1 (d, 2C), 126.9 (d, 2C), 127.9 (d, 2C), 129.0 (s, 2C), 129.7 (s, 2C), 134.8 (s, 2C), 137.8 (s, 2C); **HRMS** (ESI+): $C_{34}H_{20}N_2^+$, calculated: 456.1621 [M$^+$], observed: 456.1622 [M$^+$]; **UV/VIS** (THF, 3.60 µg/mL): λ[nm] (logε) = 244 (4.96), 265 (5.32), 297 (4.28), 364 (4.24), 394 (4.34); **Fluorescence** (THF): λ_{Anr} = 365 nm, λ_{max} = 412 nm, 437 nm, 462 nm; **Quantum yield**: Φ = 37.5%.

9,19-Dihydrodibenzo[*a,c*]dibenzo[4,5:6,7]indolo[2,3-*h*]carbazole, DDICZ 3a

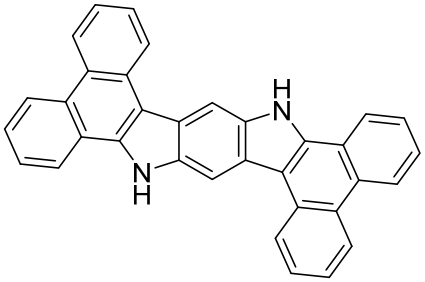

According to GP3, the crude of the corresponding azide **14b** (corresponding 755 µmol) was dissolved in 5 mL DCE. 5 mol% JohnPhosAuMeCNSbF$_6$ (29.2 mg, 37.8 µmol) were added and the mixture was stirred at 60 °C for 3 h. Again 5 mol% of the gold catalyst (29.2 mg, 37.8 µmol) were added and the mixture was stirred at 60 °C for another 3 h. The precipitate was filtered, washed with ice-cold DCM and the residue was dried under vacuum to give a yellowish solid (185 mg, 405 µmol, 54% over three steps).

Mp.: >300 °C; **IR** (ATR): $\tilde{\nu}$[cm^{-1}] = 3438, 3085, 2975, 2869, 1936, 1899, 1869, 1613, 1576, 1524, 1459, 1439, 1376, 1351, 1328, 1289, 1276, 1249, 1211, 1167, 1121, 1084, 1043, 954, 934, 915, 847, 815, 781, 751, 715, 676, 617; **^{1}H NMR** (DMSO-d_6, 600.2 MHz): δ[ppm] = 7.67-7.70 (m, 2H9, 7.80-7.82 (m, 2H), 7.88-7.90 (m, 2H), 7.95-7.98 (m, 2H), 8.69-8.71 (m, 2H), 8.81 (s, 2H), 8.92 (d, $^3J_{H-H}$ = 7.8 Hz, 2H), 9.01-9.03 (m, 4H), 12.40 (s, 2H); **^{13}C NMR** (DMSO-d_6, 150.9 MHz): δ[ppm] = 102.2 (d, 2C), 110.6 (s,

2C), 122.3 (s, 2C), 122.4 (d, 2C), 122.6 (s, 2C), 122.8 (d, 2C), 123.2 (d, 2C), 124.0 (d, 2C), 124.2 (d, 2C), 126.0 (s, 2C),126.5 (d, 2C), 127.1 (d, 2C), 127.7 (d, 2C), 129.4 (s, 2C), 129.8 (s, 2C), 135.5 (s, 2C), 135.7 (s, 2C); **HRMS** (EI+): $C_{34}H_{20}N_2^+$, calculated: 456.16210 [M^+], observed: 456.16298 [M^+]; **UV/VIS** (THF, 7.80 µg/mL): λ[nm] (logε) = 246 (4.72), 266 (4.70), 302 (4.55), 365 (4.68), 413 (4.24); **Fluorescence** (THF): λ_{Anr} = 365 nm, λ_{max} = 422 nm, 448 nm, 476 nm; **Quantum yield**: Φ = 52.1%.

DBDCZ 15a

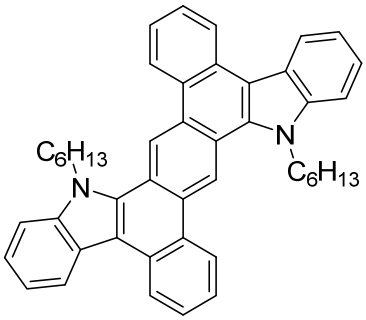

According to GP4, 1.00 eq of the corresponding carbazole **2a** (100 mg, 219 µmol) was dissolved in 8 mL anhydrous DMSO under nitrogen atmosphere. After adding 4.00 eq KO^{t}Bu (98.3 mg, 876 µmol) the solution was stirred for 20 min. Then 20.0 eq 1-bromohexane (723 mg, 614 µL, 4.38 mmol) were added and the mixture was stirred at room temperature for 2 h and treated according to GP4. A yellow solid was obtained (128 mg, 204 µmol, 94%).

Mp.: 268 °C; **IR**(ATR): $\tilde{\nu}$[cm^{-1}] = 3049, 2864, 2930, 2859, 1606, 1520, 1468, 1457, 1422, 1356, 1342, 1309, 1268, 1249, 1214, 1154, 1101, 1050, 1026, 939, 861, 786, 755, 742, 731, 642, 614; **^{1}H NMR** ($C_2D_2Cl_4$, 600.2 MHz): δ[ppm] = 1.01 (t, $^3J_{H-H}$ = 7.3 Hz, 6H), 1.46-1.52 (m, 4H), 1.55-1.60 (m, 4H), 1.80-1.85 (m, 4H), 2.38-2.43 (m, 4H), 4.96 (t, $^3J_{H-H}$ = 8.1 Hz, 4H), 7.48 (t, $^3J_{H-H}$ = 7.4 Hz, 2H), 7.58 (t, $^3J_{H-H}$ = 7.6 Hz, 2H), 7.68 (t, $^3J_{H-H}$ = 7.5 Hz, 2H), 7.73 (d, $^3J_{H-H}$ = 8.3 Hz, 2H), 7.85 (t, $^3J_{H-H}$ = 7.4 Hz, 2H), 8.67 (d, $^3J_{H-H}$ = 8.1 Hz, 2H), 8.87 (d, $^3J_{H-H}$ = 8.3 Hz, 2H), 8.94 (d, $^3J_{H-H}$ = 8.1 Hz, 2H), 9.90 (s, 2H); **^{13}C NMR** ($C_2D_2Cl_4$, 150.9 MHz): δ[ppm] = 15.1 (q, 2C), 23.8 (t, 2C), 28.0 (t, 2C), 31.3 (t, 2C), 32.7 (t, 2C), 47.9 (t, 2C), 110.9 (d, 2C), 114.3 (s, 2C), 118.7 (d, 2C), 121.7 (d, 2C), 122.4 (s, 2C), 122.7 (d, 2C), 124.0 (d, 2C), 124.3 (s, 2C), 124.9 (d, 2C), 125.0 (d, 4C), 127.9 (s, 2C), 128.8 (d, 2C), 130.1 (s, 2C), 131.4 (s, 2C), 134.6 (s, 2C), 141.4 (s, 2C); **HRMS** (DART+): $C_{46}H_{45}N_2^+$, calculated: 625.3577 [M^++H], observed: 625.2571 [M^++H]; **UV/VIS** (DCM, 3.20 µg/mL): λ[nm] (log ε) = 243 (4.78), 264 (4.82), 284 (4.96), 297 (4.97), 335 (4.98), 351 (5.08), 386 (4.65), 407 (4.71), 428 (4.14); **Fluoreszenz** (DCM): λ_{ex} = 410 nm, λ_{max} = 444 nm; **Quantum yield:** Φ = 30.0%.

DBDCZ 15b

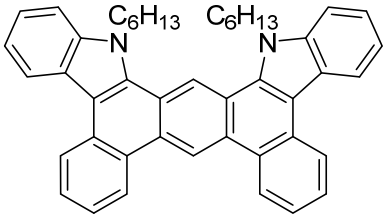

According to GP4, 1.00 eq of the corresponding carbazole **2b** (60.0 mg, 131 µmol) was dissolved in 6 mL anhydrous DMSO under nitrogen atmosphere. After adding 4.00 eq KO^{t}Bu (59.0 mg, 526 µmol) the solution was stirred for 20 min. Then 20.0 eq 1-bromohexane (434 mg, 368 µl, 2.63 mmol) were added and the mixture was stirred at room temperature for 2 h and treated according to GP4. A yellow solid was obtained (75.0 mg, 120 µmol, 91%).

Mp.: 187 °C; **R$_f$:** 0.47 (silica gel, PE:EA 10:1); **IR**(ATR): $\tilde{\nu}$[cm^{-1}] = 3071, 3049, 2949, 2925, 2855, 1607, 1547, 1518, 1478, 1462, 1435, 1343, 1318, 1268, 1237, 1160, 1101, 1051, 1027, 1004, 916, 875, 846, 788, 772, 756, 740, 729, 676, 630; **^{1}H NMR** ($CDCl_3$, 400.3 MHz): δ[ppm] = 0.76 (t, $^3J_{H-H}$ = 7.1 Hz, 6H), 1.15-1.26 (m, 8H), 1.28-1.36 (m, 4H), 1.99-2.03 (m, 4H), 4.98 (t, $^3J_{H-H}$ = 7.3 Hz, 4H), 7.43-7.47 (m, 2H), 7.52-7.56 (m, 2H), 7.66-7.70 (m, 4H), 7.78-7.82 (m, 2H), 8.67 (d, $^3J_{H-H}$ = 8.0 Hz, 2H), 8.92 (d, $^3J_{H-H}$ = 7.7 Hz, 2H), 9.06 (d, $^3J_{H-H}$ = 8.1 Hz, 2H), 9.56 (s, 1H), 10.28 (s, 1H); **^{13}C NMR** ($CDCl_3$, 100.7 MHz): δ[ppm] = 14.0 (q, 2C), 22.6 (t. 2C), 26.7 (t, 2C), 30.2 (t, 2C), 31.7 (t, 2C), 46.4 (t, 2C), 110.4 (s, 2C), 115.0 (s, 2C), 115.7 (d, 1C), 119.7 (d, 1C), 120.9 (d, 2C), 122.2 (d, 2C), 122.8 (s, 2C), 123.7 (d, 2C), 123.9 (d, 2C), 124.0 (d, 2C), 124.2 (s, 2C), 124.3 (d, 2C), 127.7 (s, 2C), 127.8 (d, 2C), 128.6 (s, 2C), 130.5 (s, 2C), 133.8 (s, 2C), 141.2 (s, 2C); **HRMS** (DART+): $C_{46}H_{45}N_2^+$, calculated: 625.3577 [M$^+$+H], observed: 625.3569 [M$^+$+H]; **UV/VIS** (DCM, 5.40 µg/mL): λ[nm] (log ε) = 269 (4.48), 281 (4.48), 313 (4.28), 346 (4.73), 371 (4.30), 400 (3.82), 428 (3.76); **Fluorescence** (DCM): λ_{ex} = 400 nm, λ_{max} = 434 nm; **Quantum yield:** Φ = 42.6%.

9,19-Dihexyl-9,19-dihydrodibenzo[*a,c*]dibenzo[4,5:6,7]indolo[2,3-*h*]carbazole, DDICZ 16a

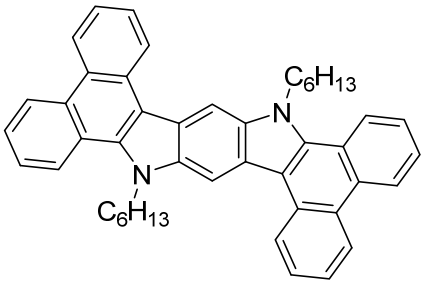

According to GP4, 1.00 eq of the corresponding carbazole **3a** (17.4 mg, 38.1 µmol) was dissolved in 4 mL anhydrous DMSO under nitrogen atmosphere. After adding 4.00 eq KO^{t}Bu (17.1 mg, 152 µmol) the solution was stirred for 20 min. Then 20.0 eq 1-bromohexane (126 mg, 107 µL, 762 µmol) were added and the mixture was stirred at room temperature for 2 h and treated according to GP4. A yellow solid was obtained (13.5 mg, 21.6 µmol, 57%).

Mp.: 282-283 °C; **IR** (ATR): $\tilde{\nu}$ [cm^{-1}] = 2956, 2921, 2852, 1607, 1566, 1520, 1491, 1466, 1434, 1370, 1348, 1326, 1303, 1251, 1160, 1125, 1101, 1044, 935, 901, 843, 807, 748, 714, 663, 625; **^{1}H NMR**

($CDCl_3$, 400.3 MHz, 323 K): δ[ppm] = 0.89 (t, $^3J_{H-H}$ = 7.2 Hz, 6H), 1.31-1.36 (m, 4H), 1.42-1.49 (m, 4H), 1.56-1.63 (m, 4H), 2.13-2.20 (m, 4H), 4.82-4.86 (m, 4H), 7.52-7.56 (m, 2H), 7.59-7.65 (m, 4H), 7.74-7.78 (m, 2H), 8.49-8.51 (m, 2H), 8.58 (s, 2H), 8.75 (d, $^3J_{H-H}$ = 8.2 Hz, 2H), 8.82-8.84 (m, 2H), 8.92 (d, $^3J_{H-H}$ = 8.2 Hz, 2H); **^{13}C NMR** ($CDCl_3$, 100.7 MHz, 323 K): δ[ppm] = 14.1 (q, 2C), 22.8 (t, 2C), 27.0 (t, 2C), 30.0 (t, 2C), 31.7 (t, 2C), 47.1 (t, 2C), 101.0 (d, 2C), 113.4 (s, 2C), 122.5 (s, 2C), 123.0 (d, 2C), 123.3 (d, 2C), 123.4 (d, 2C), 123.8 (d, 2C), 124.1 (s, 2C), 124.4 (d, 2C), 125.7 (d, 2C), 126.5 (d, 2C), 127.1 (s, 2C), 127.5 (d, 2C), 130.6 (s, 2C), 131.3 (s, 2C), 135.8 (s, 2C), 138.2 (s, 2C); **HRMS** (EI+): $C_{46}H_{44}N_2^+$, calculated: 624.34990 [M^+], observed: 625.35093 [M^+]; **UV/VIS** (DCM, 9.00 µg/mL): λ[nm] (logε) = 251 (4.79), 307 (4.77), 357 (4.62), 372 (4.75), 430 (4.32), 463 (3.32); **Fluorescence** (DCM): λ_{Anr} = 430 nm, λ_{max} = 441 nm, 469 nm, 502 nm; **Quantum yield**: Φ = 32.0%.

9,11-Dihexyl-9,11-dihydrodibenzo[*a,c*]dibenzo[4,5:6,7]indolo[3,2-*h*]carbazole, DDICZ 16b

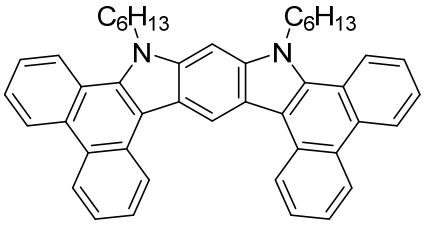

According to GP4, 1.00 eq of 9,11-dihydrodibenzo[*a,c*]dibenzo[4,5:6,7]indolo[3,2-*h*]carbazole (**3b**) (80.0 mg, 175 µmol) was dissolved in anhydrous DMSO in a baked out Schlenk flask under nitrogen atmosphere. After adding 4.00 eq KO^{t}Bu (78.7 mg, 701 µmol) the solution was stirred for 20 min. Then 20.0 eq 1-bromohexane (579 mg, 491 µL, 3.50 mmol) were added and the mixture was stirred at room temperature for 2 h until TLC showed full conversion. The mixture was poured into a beaker of methanol. The precipitate was filtered off and washed successively with water and methanol. The residue was dried under vacuum to afford a yellow solid (85.0 mg, 136 µmol, 78 %).

Mp.: 283 °C; **IR** (ATR): $\tilde{\nu}$ [cm^{-1}] = 3085, 3057, 2954, 2921, 2854, 1936, 1625, 1607, 1565, 1518, 1467, 1427, 1404, 1366, 1324, 1246, 1177, 1146, 1128, 1075, 1048, 1001, 867, 822, 780, 745, 711, 667, 639, 624; **^{1}H NMR** ($CDCl_3$, 600.2 MHz, 323 K): δ[ppm] = 0.93 (t, $^3J_{H-H}$ = 7.1 Hz, 6H), 1.34-1.43 (m, 8H), 1.50-1.54 (m, 4H), 2.04-2.09 (m, 4H), 4.53-4.55 (m, 4H), 7.56-7.64 (m, 6H), 7.28 (s, 1H), 7.58,7.64 (m, 6H), 7.91-7.93 (m, , 2H), 8.32 (d, $^3J_{H-H}$ = 7.7 Hz, 2H), 8.81 (d, $^3J_{H-H}$ = 8.2 Hz, 2H), 8.85 (d, $^3J_{H-H}$ = 7.8 Hz, 2H), 9.14 (d, $^3J_{H-H}$ = 8.0 Hz, 2H), 9.67 (s, 1H); **^{13}C NMR** ($CDCl_3$, 150.9 MHz, 323 K): δ[ppm] = 14.1 (q, 2C); 22.8 (t, 2C), 26.9 (t, 2C), 29.8 (t, 2C), 31.7 (t, 2C), 46.9 (t, 2C), 88.7 (d, 1C), 114.0 (s, 2C), 114.2 (d, 1C), 120.3 (s, 2C), 122.5 (d, 2C), 123.5 (d, 2C), 123.6 (d, 2C), 123.7 (d, 2C), 123.8 (s, 2C), 124.3 (d, 2C), 125.2 (d, 2C), 126.3 (d, 2C), 127.1 (s, 2C), 127.6 (d, 2C), 130.3 (s, 2C), 130.8 (s, 2C), 134.7 (s, 2C), 140.3 (s, 2C); **HRMS** (DART+): $C_{46}H_{45}N_2^+$, calculated: 625.3577 [M^++H], observed: 625.3556 [M^++H]; **UV/VIS** (DCM, 2.70 µg/mL): λ[nm] (logε) = 253 (5.10), 305 (5.10), 368 (5.01), 400 (4.56); **Fluorescence** (DCM): λ_{Anr} = 400 nm, λ_{max} = 427 nm, 453 nm, 483 nm; **Quantum yield**: Φ = 41.0 %.

---

4. NMR Spectra

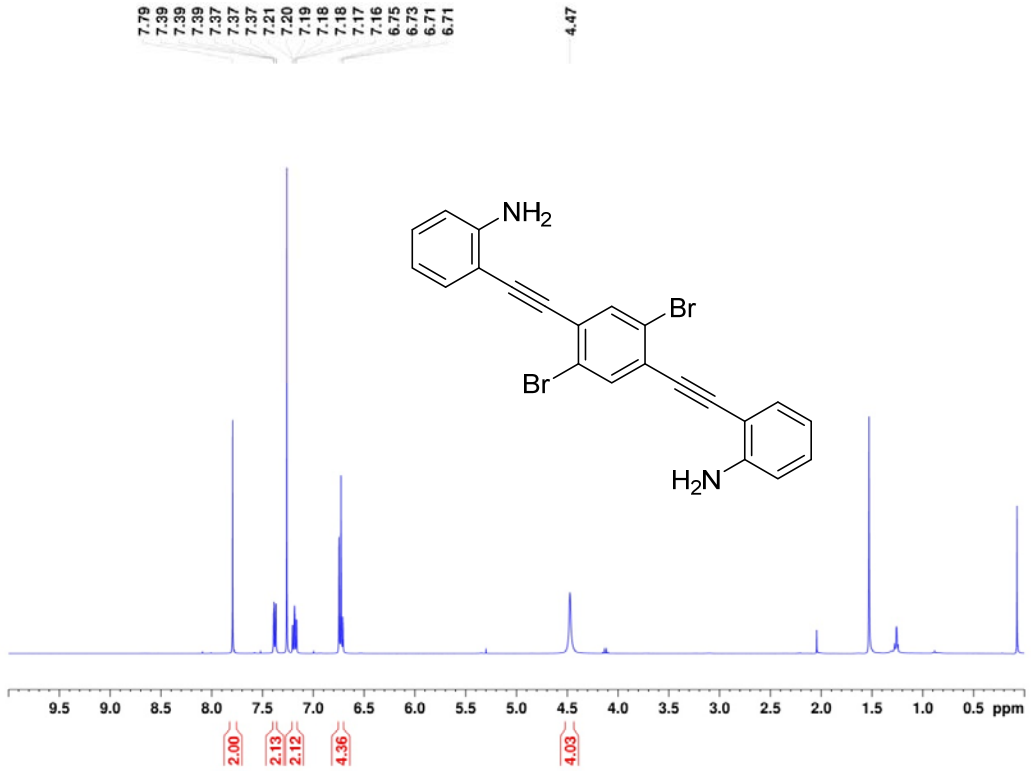

^{1}H NMR spectrum of **6a** in $CDCl_3$ at 400.3 MHz.

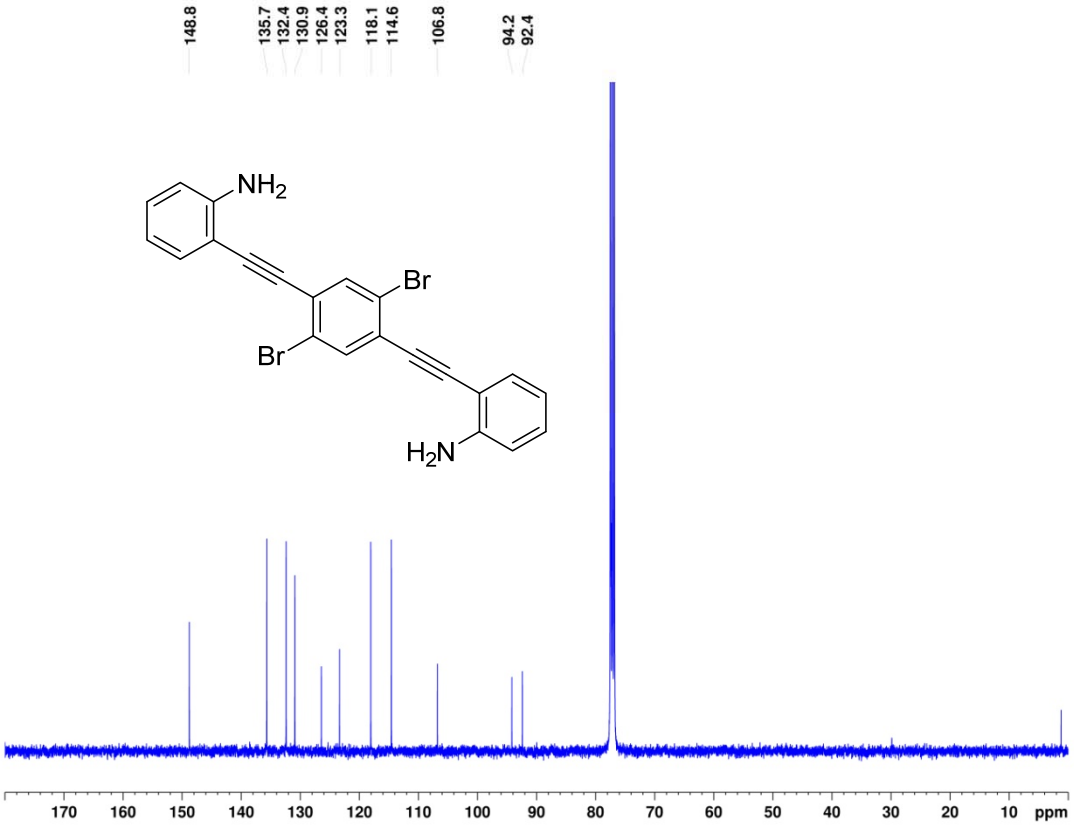

^{13}C NMR spectrum of **6a** in $CDCl_3$ at 100.7 MHz.

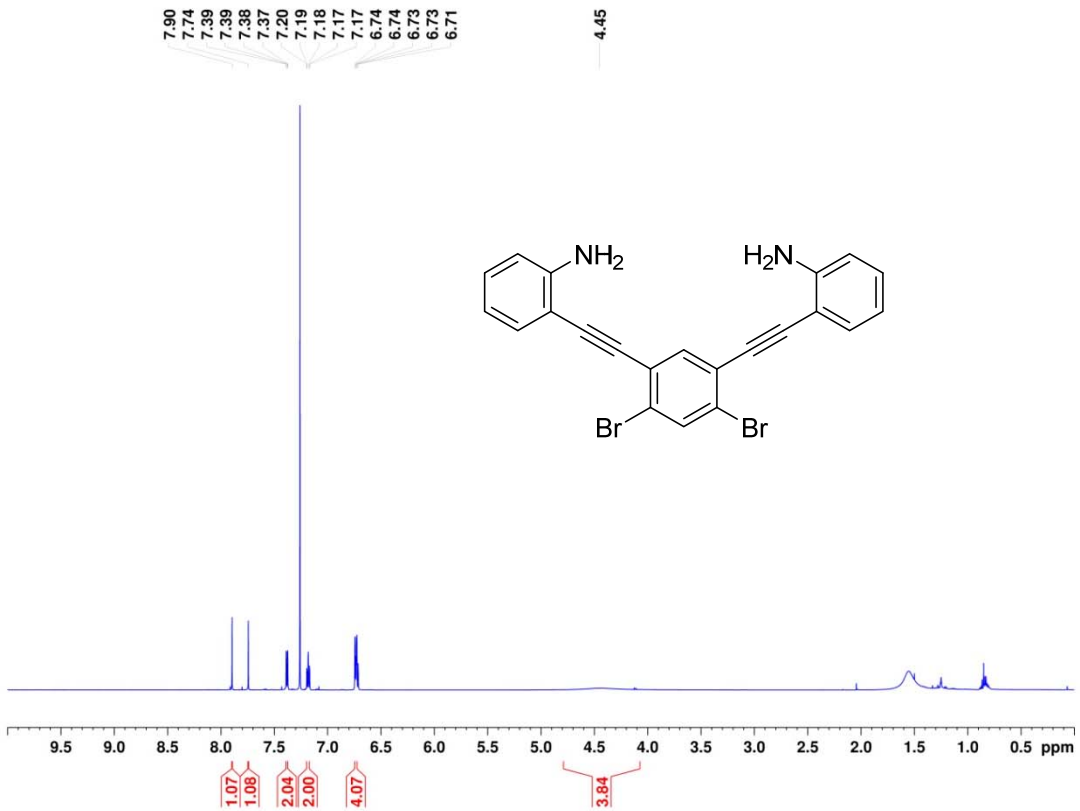

^{1}H NMR spectrum of **6b** in $CDCl_3$ at 600.2 MHz.

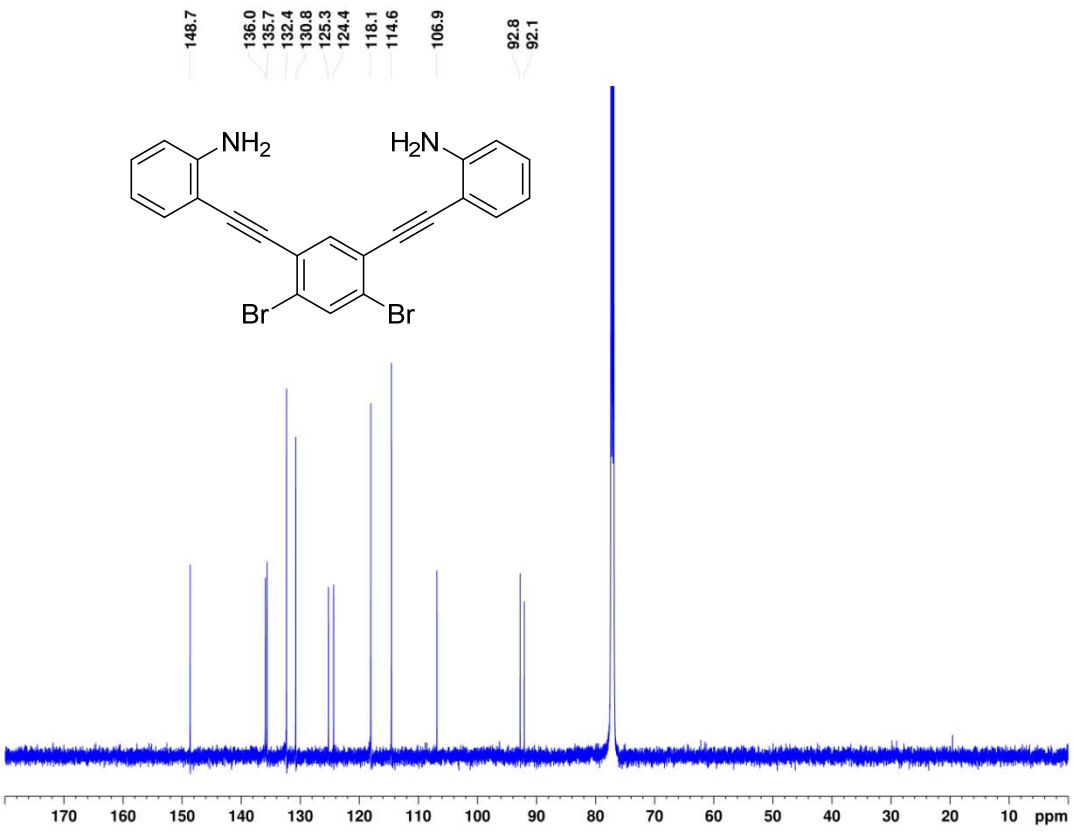

^{13}C NMR spectrum of **6b** in $CDCl_3$ at 150.9 MHz.

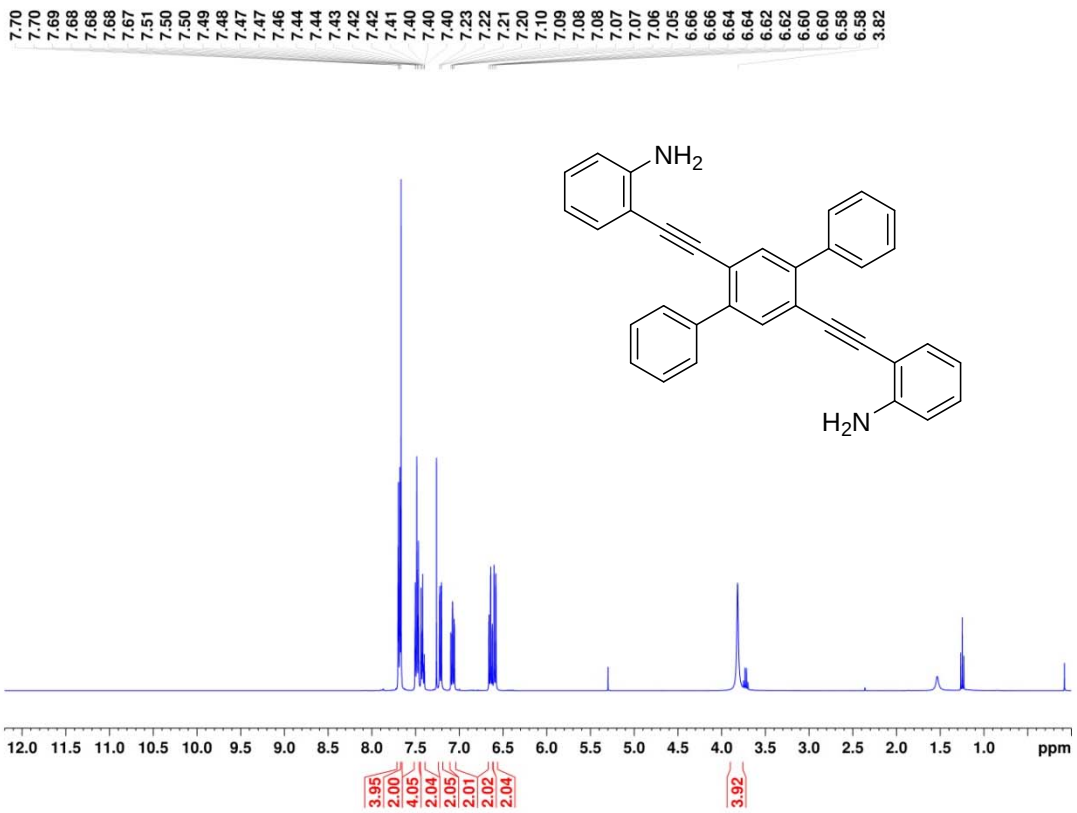

^{1}H NMR spectrum of **7a** in $CDCl_3$ at 400.3 MHz.

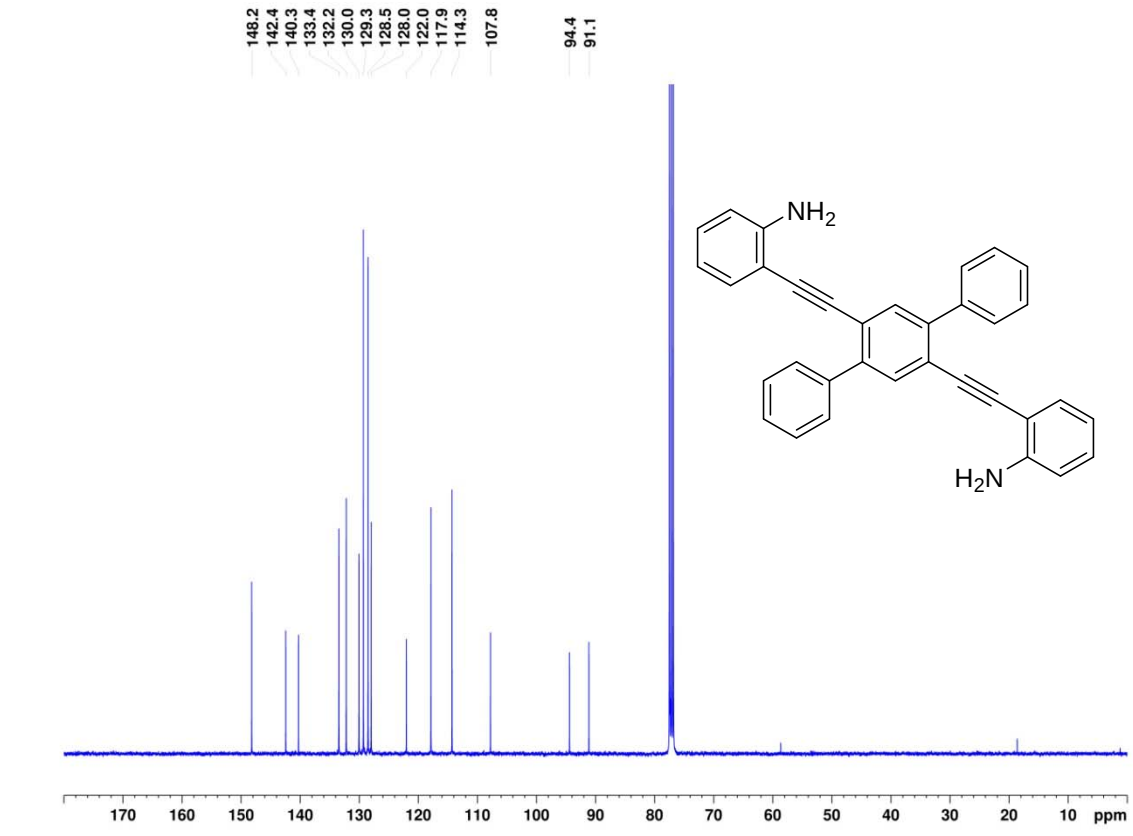

^{13}C NMR spectrum of **7a** in $CDCl_3$ at 100.7 MHz.

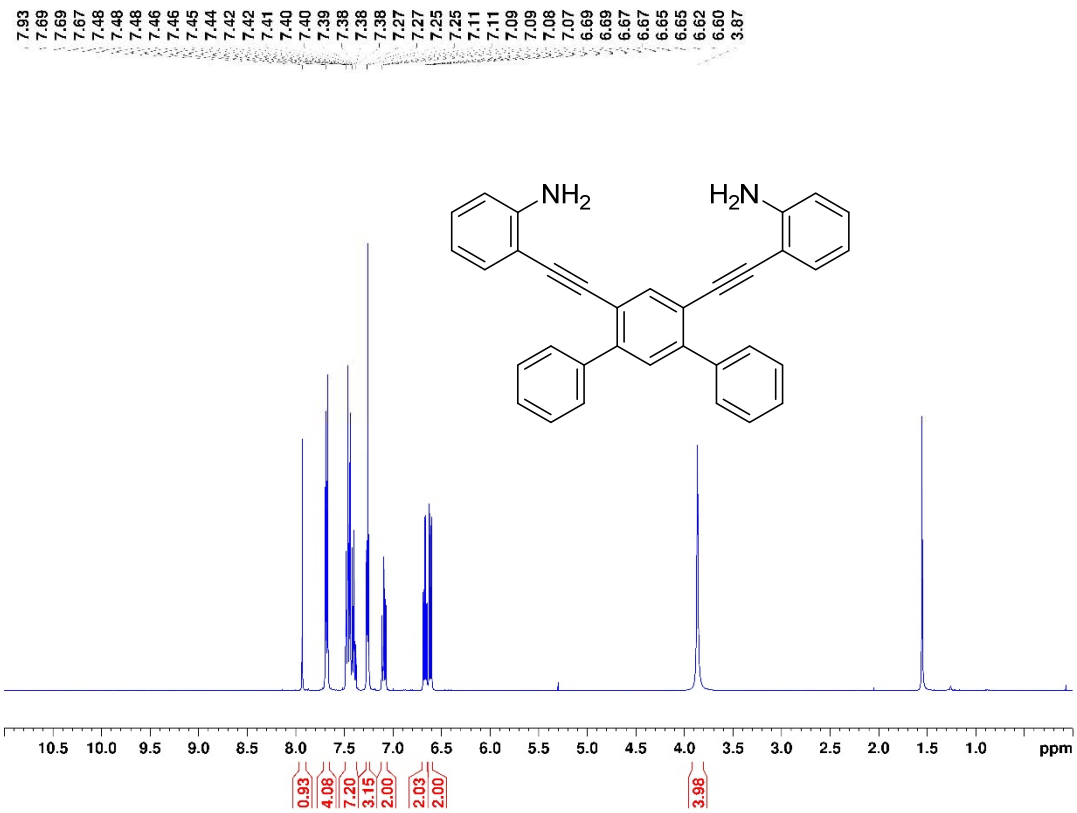

^{1}H NMR spectrum of **7b** in $CDCl_3$ at 400.3 MHz.

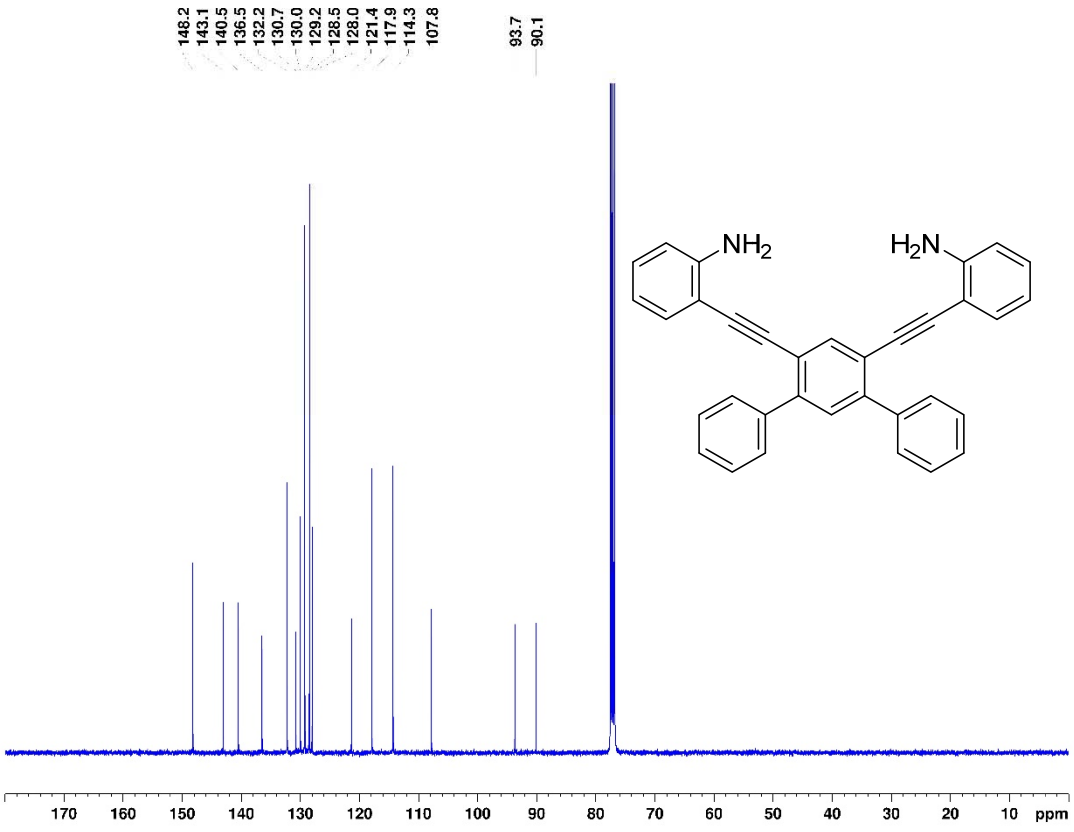

^{13}C NMR spectrum of **7b** in $CDCl_3$ at 100.7 MHz.

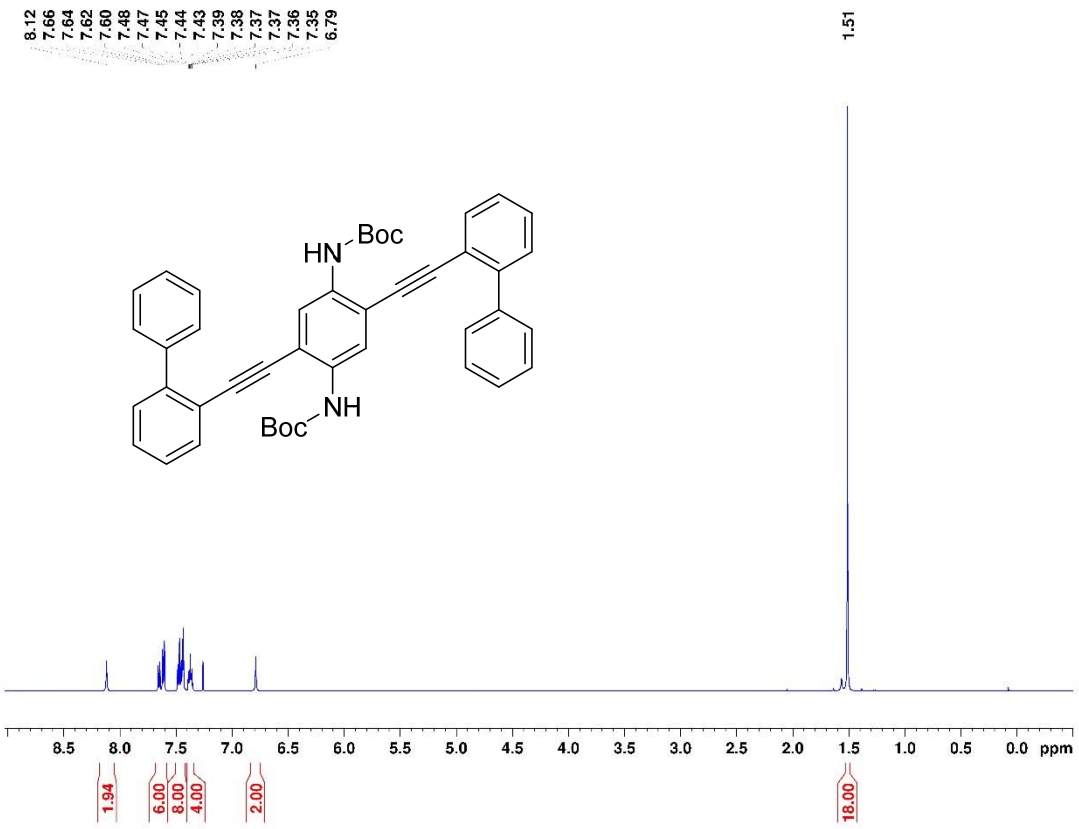

^{1}H NMR spectrum of **12** in $CDCl_3$ at 500.2 MHz.

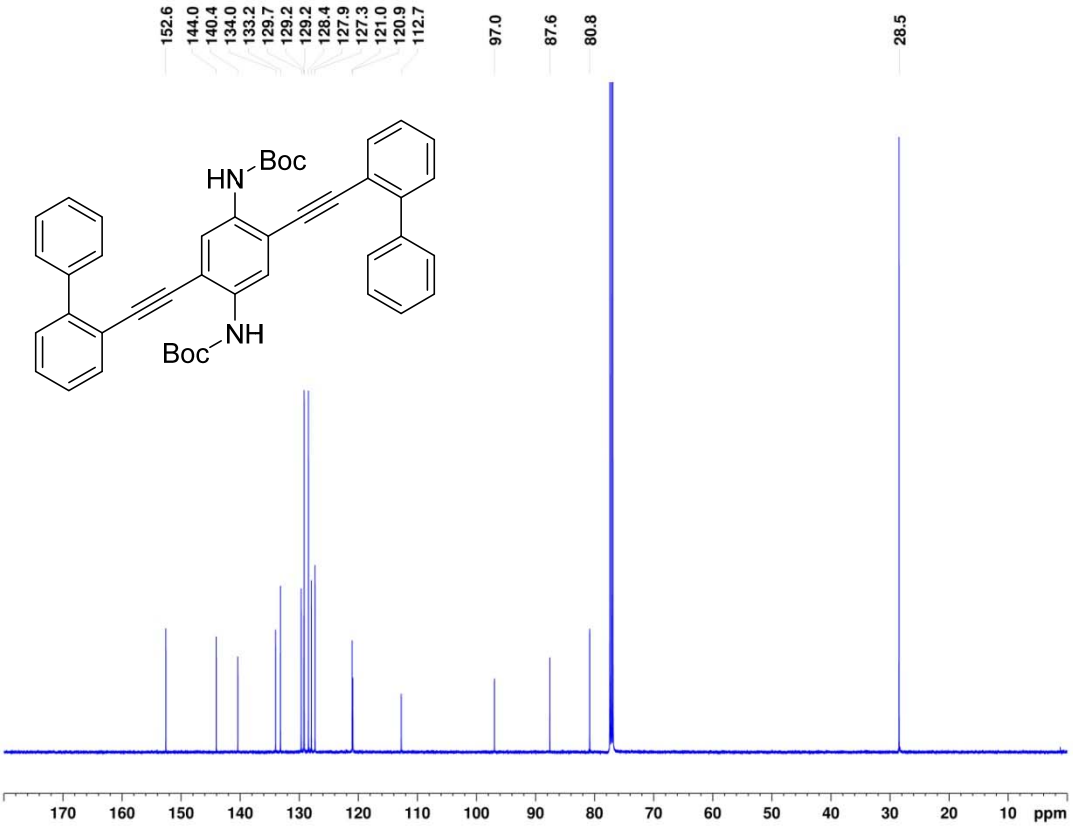

^{13}C NMR spectrum of **12** in $CDCl_3$ at 100.7 MHz.

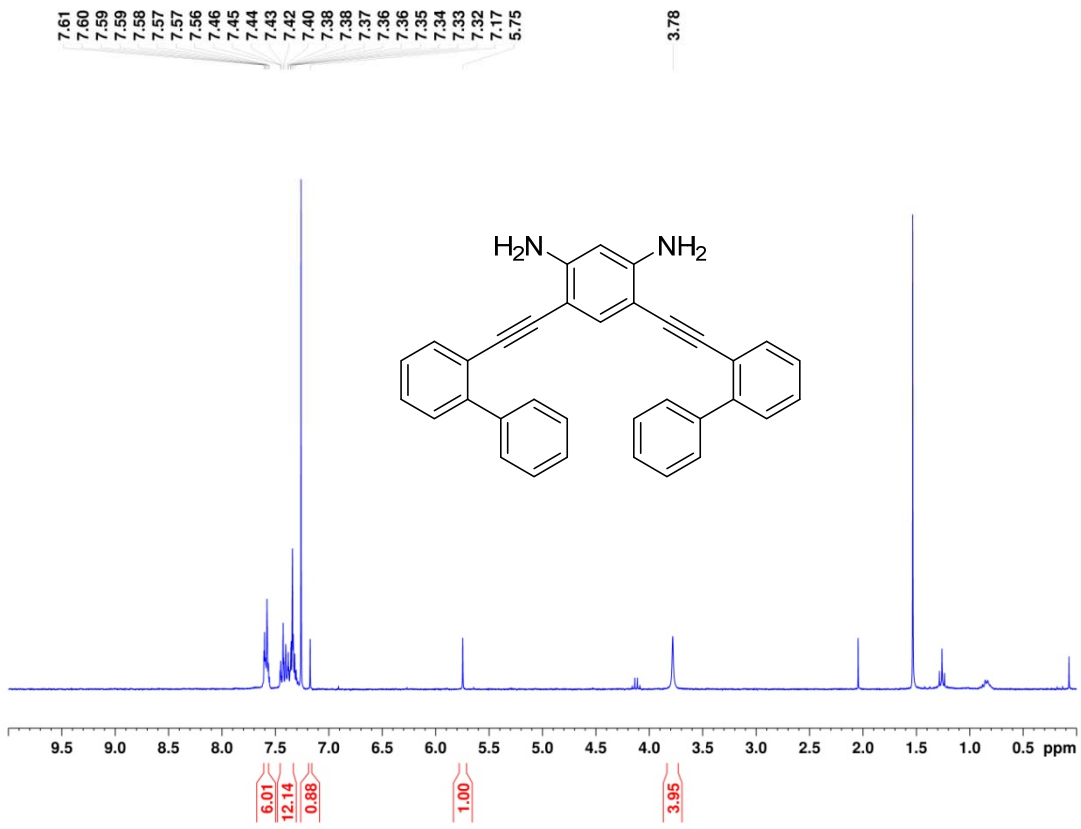

^{1}H NMR spectrum of **13b** in $CDCl_3$ at 300.5 MHz with slightly residues of ethyl acetate.

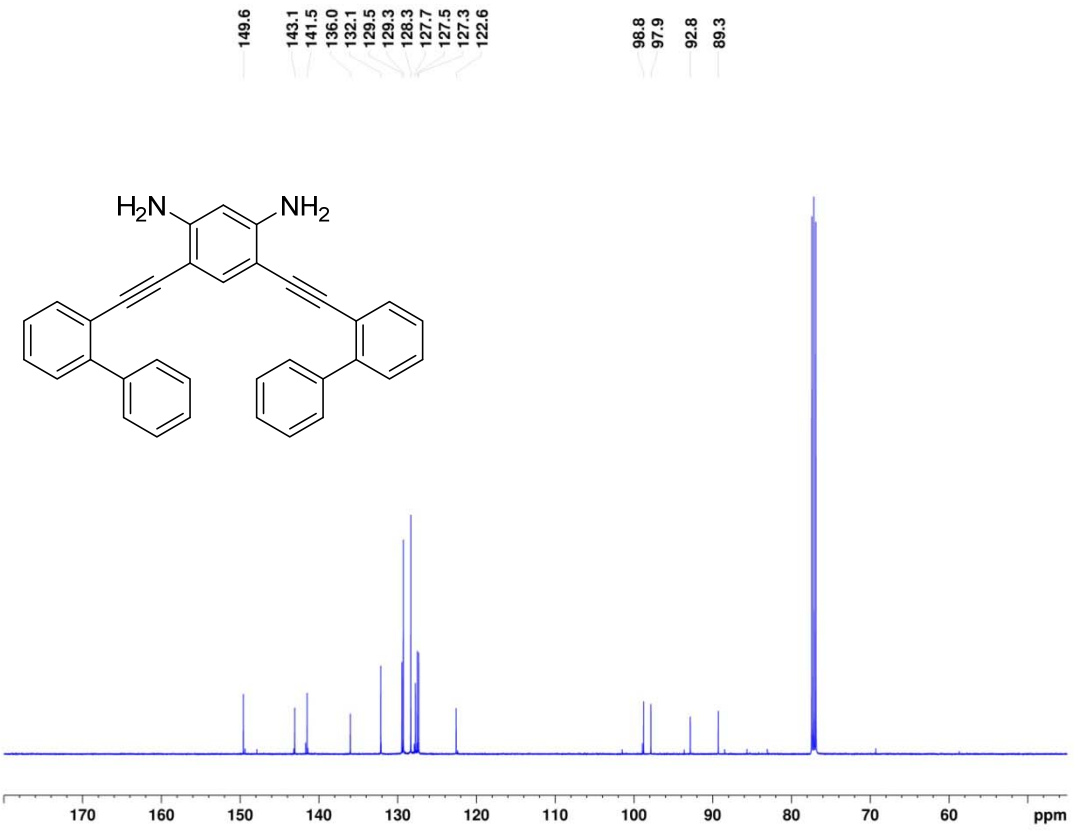

^{13}C NMR spectrum of **13b** in $CDCl_3$ at 125.8 MHz.

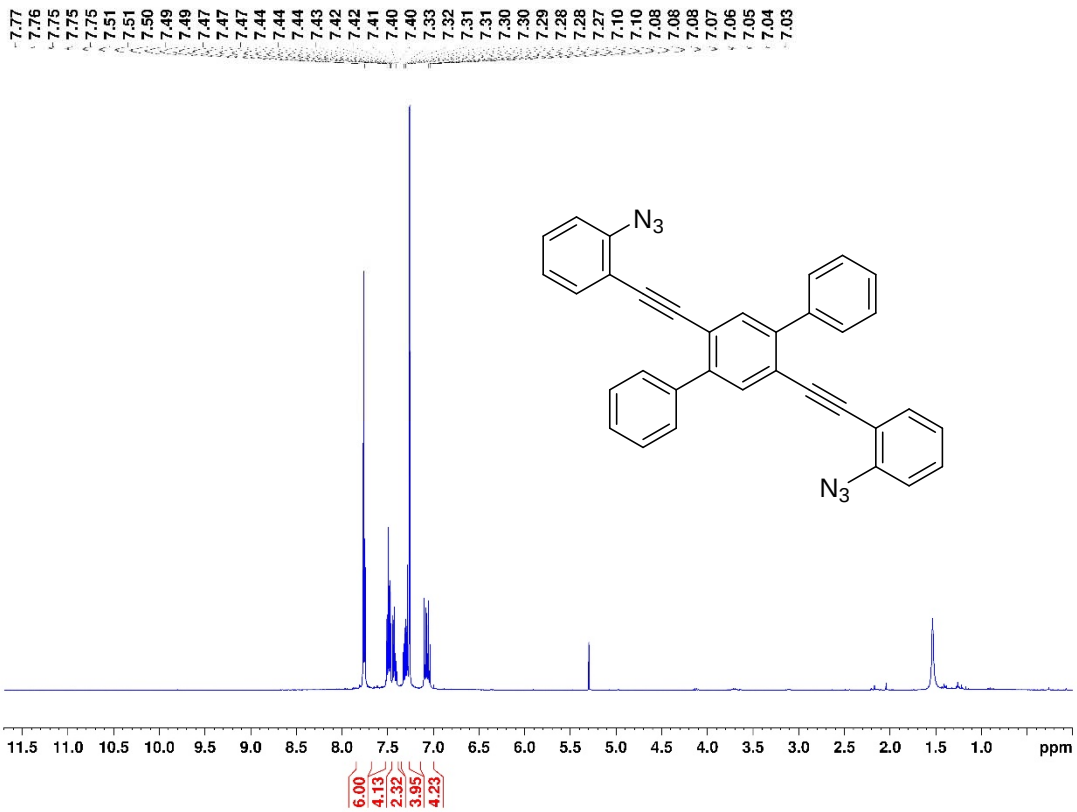

^{1}H NMR spectrum of **8a** in $CDCl_3$ at 400.3 MHz.

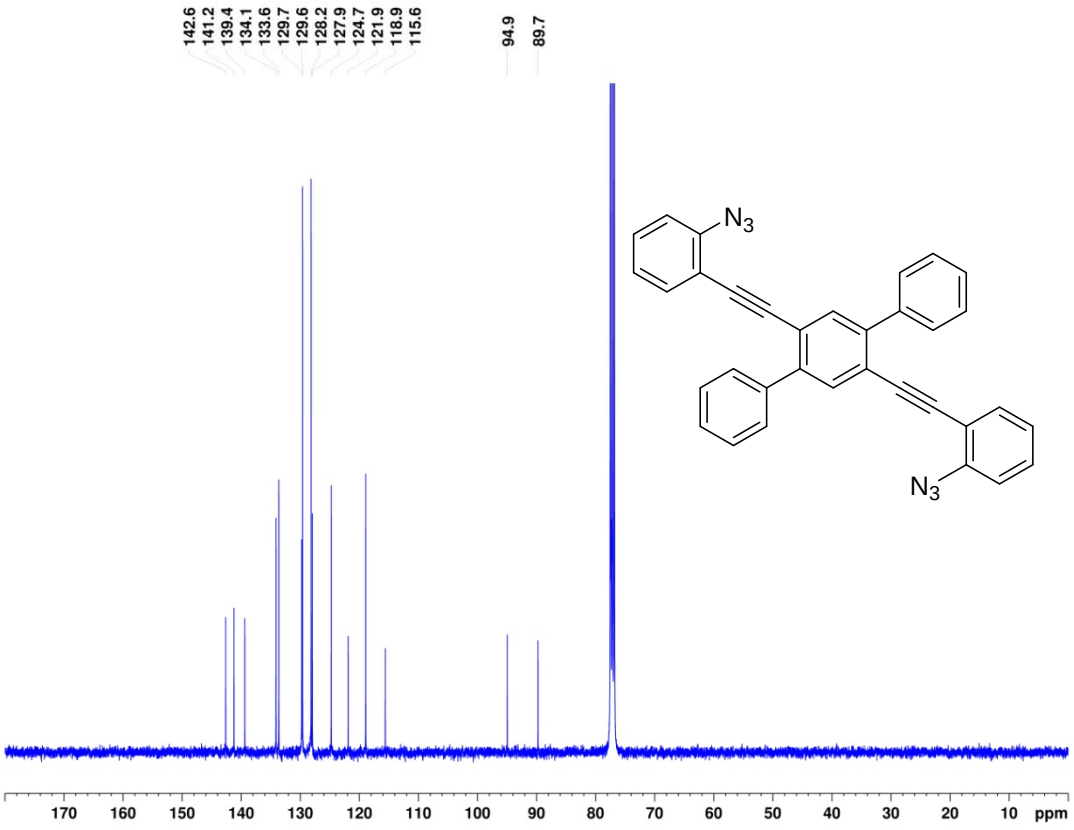

^{13}C NMR spectrum of **8a** in $CDCl_3$ at 100.7 MHz.

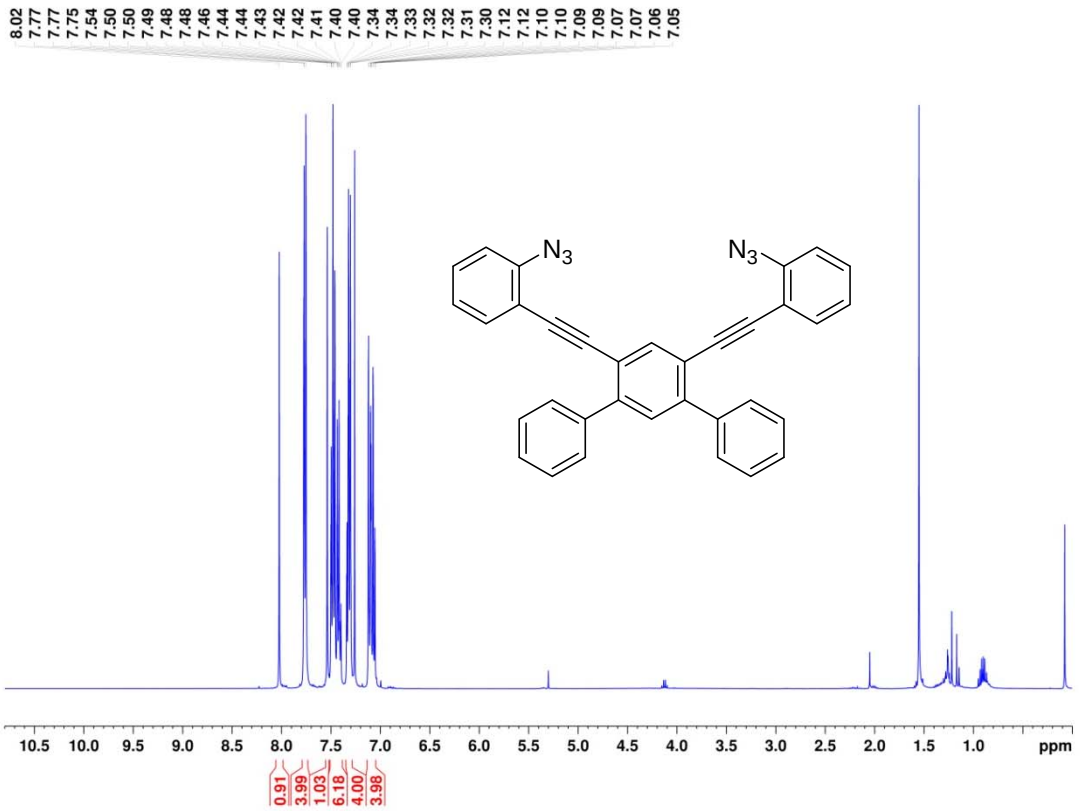

^{1}H NMR spectrum of **8b** in $CDCl_3$ at 400.3 MHz.

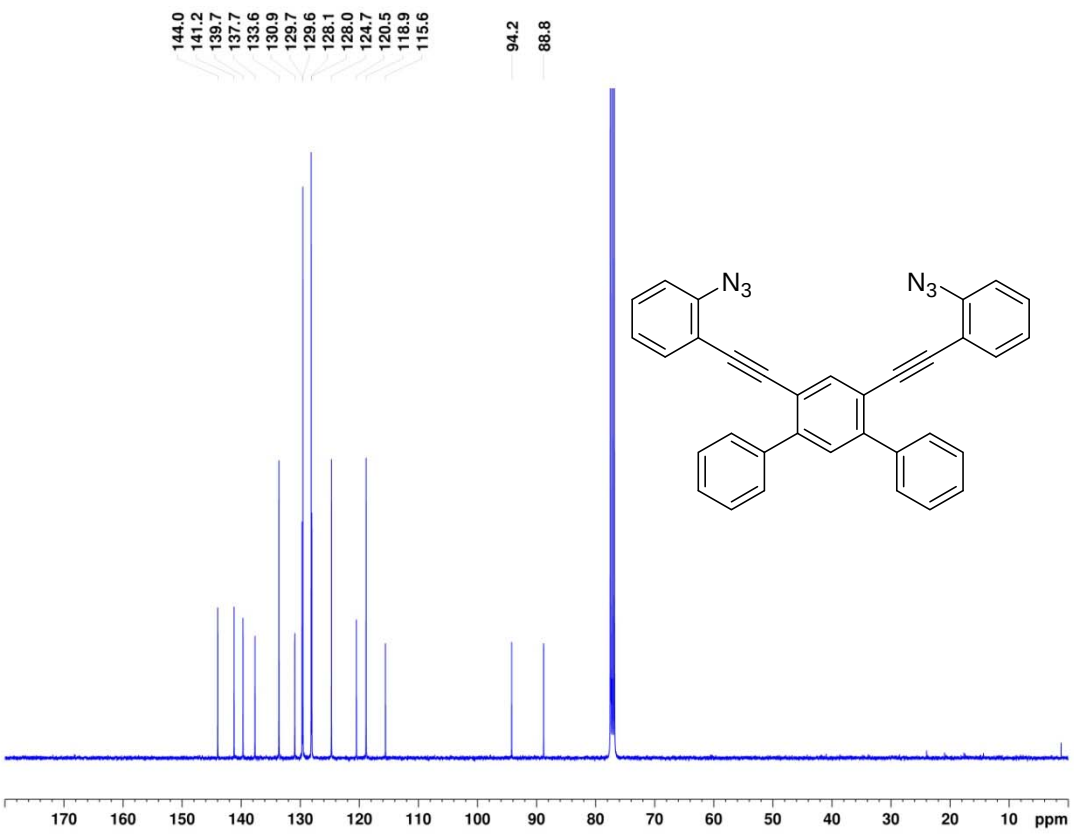

^{13}C NMR spectrum of **8b** in $CDCl_3$ at 100.7 MHz.

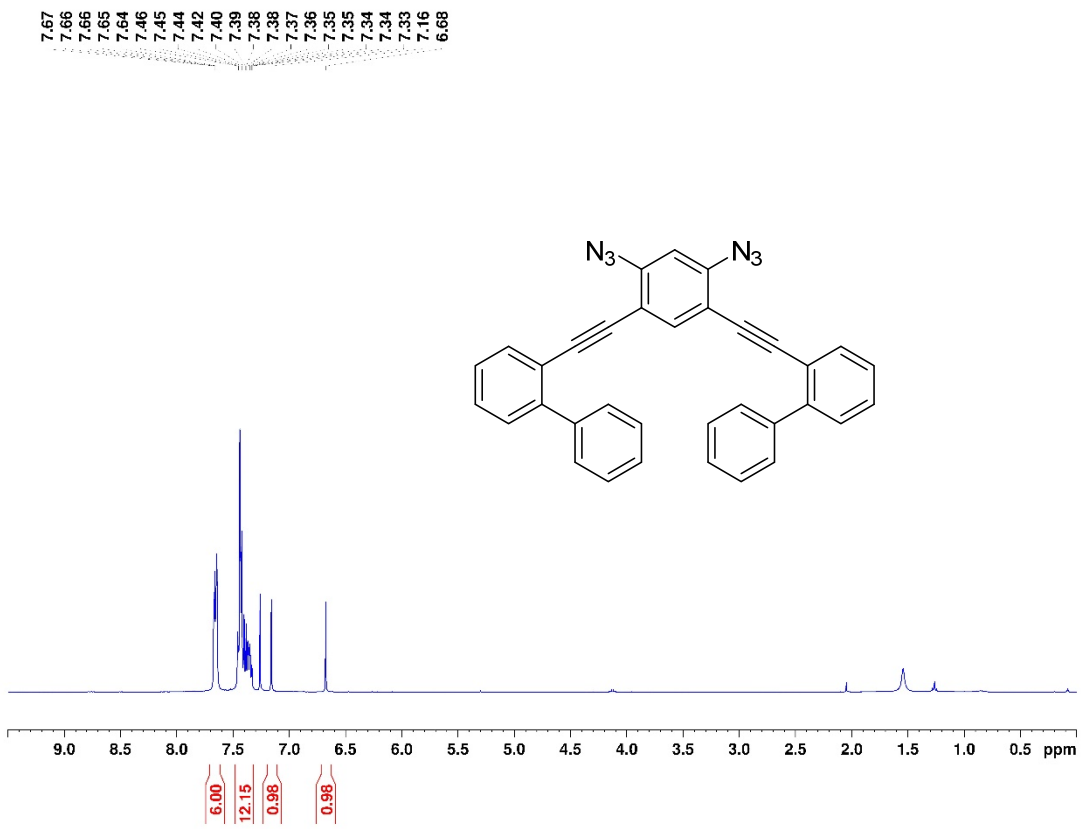

^{1}H NMR spectrum of **14b** in $CDCl_3$ at 600.2 MHz.

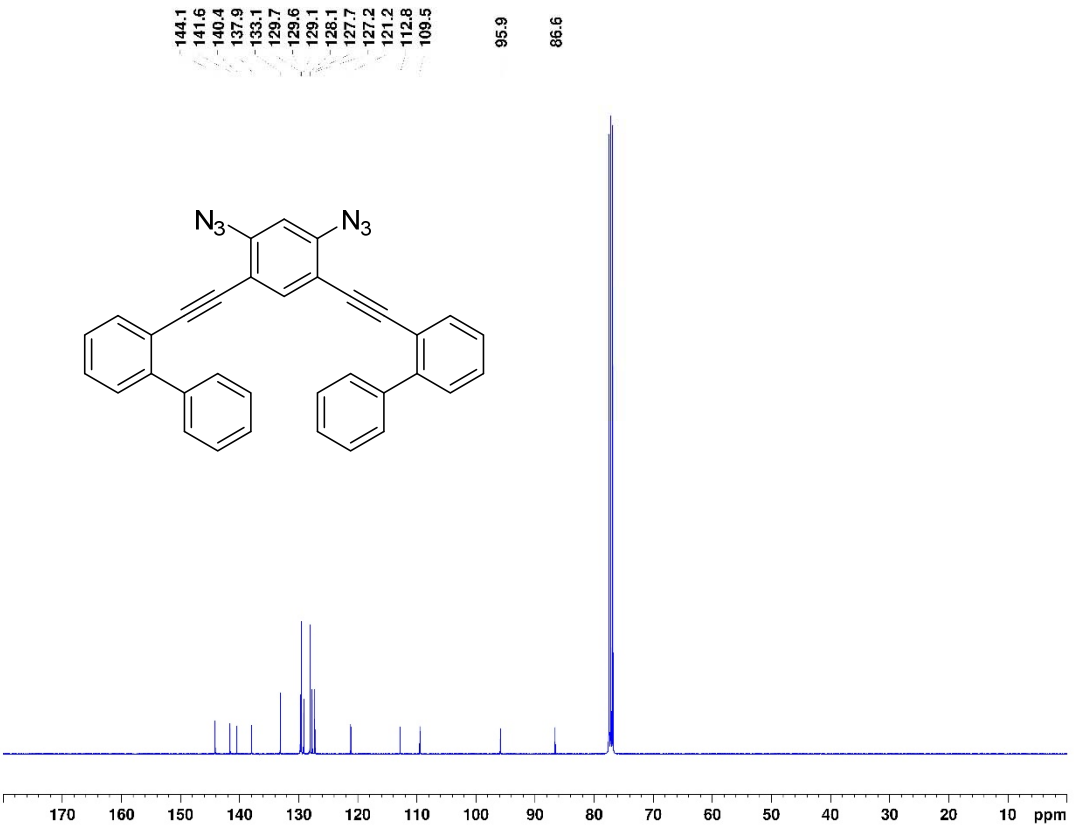

^{13}C NMR spectrum of **14b** in $CDCl_3$ at 150.9 MHz.

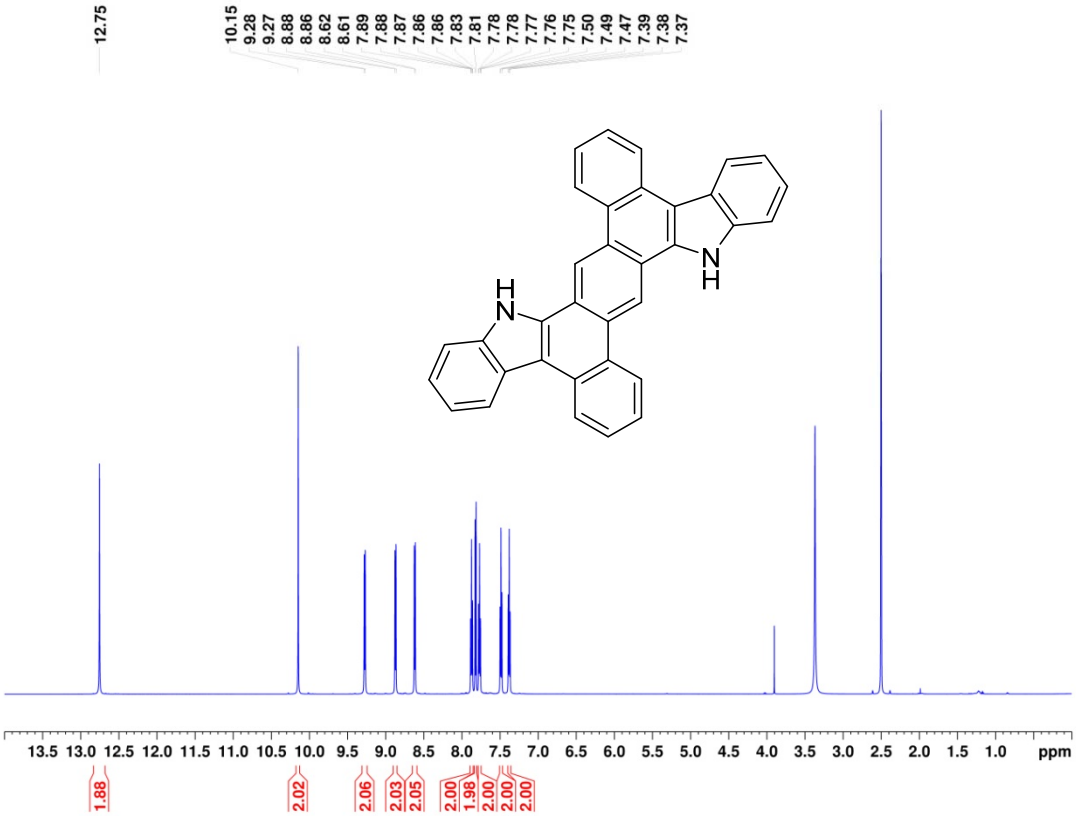

^{1}H NMR spectrum of **2a** in d_6-DMSO at 600.2 MHz.

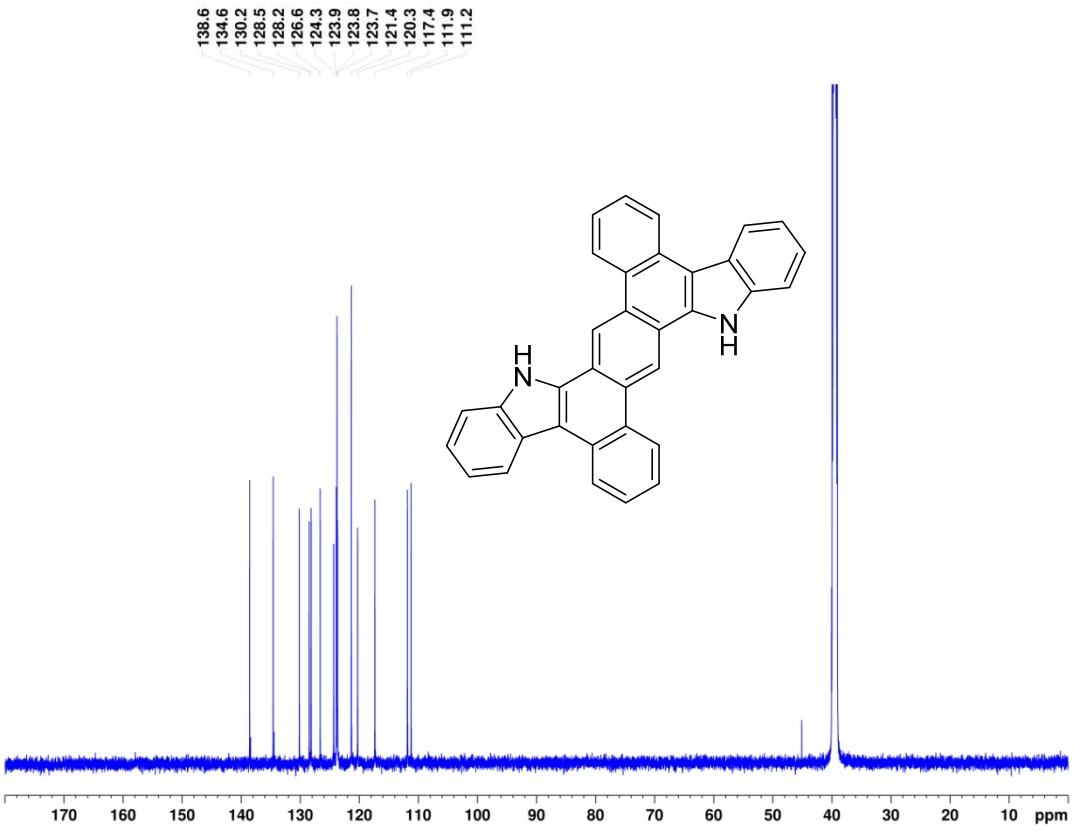

^{13}C NMR spectrum of **2a** in d_6-DMSO at 150.9 MHz.

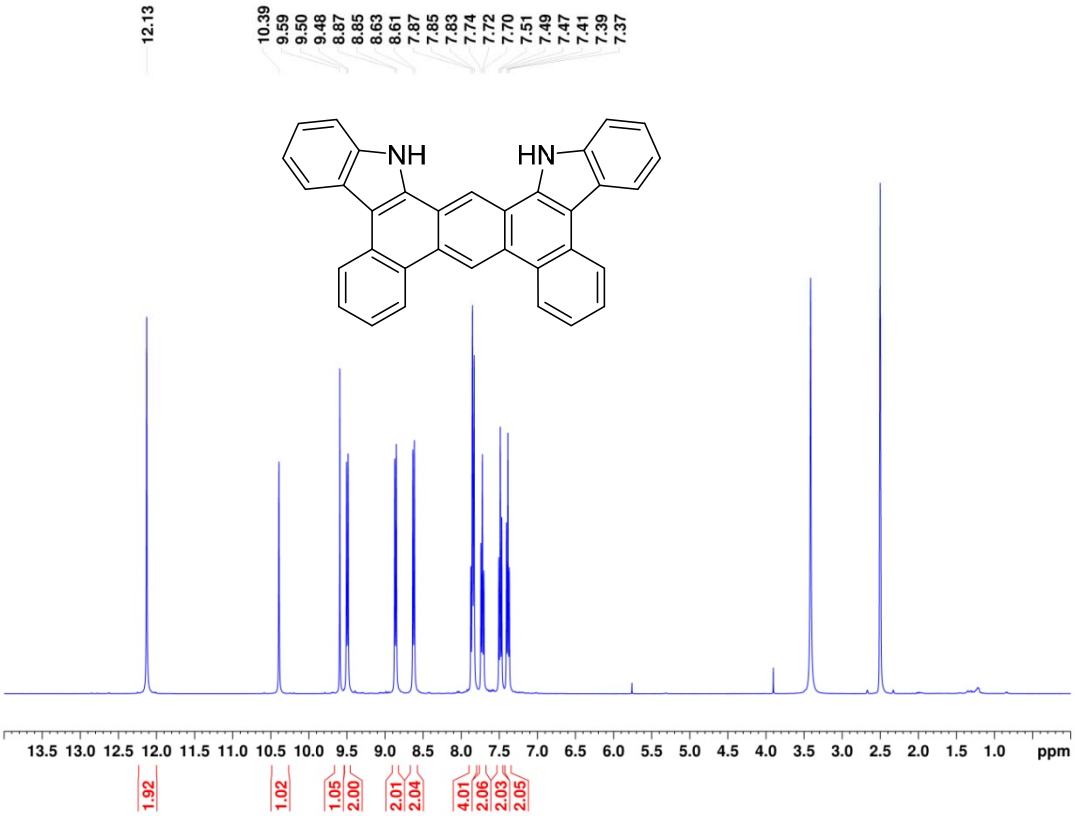

^{1}H NMR spectrum of **2b** in d_6-DMSO at 400.3 MHz.

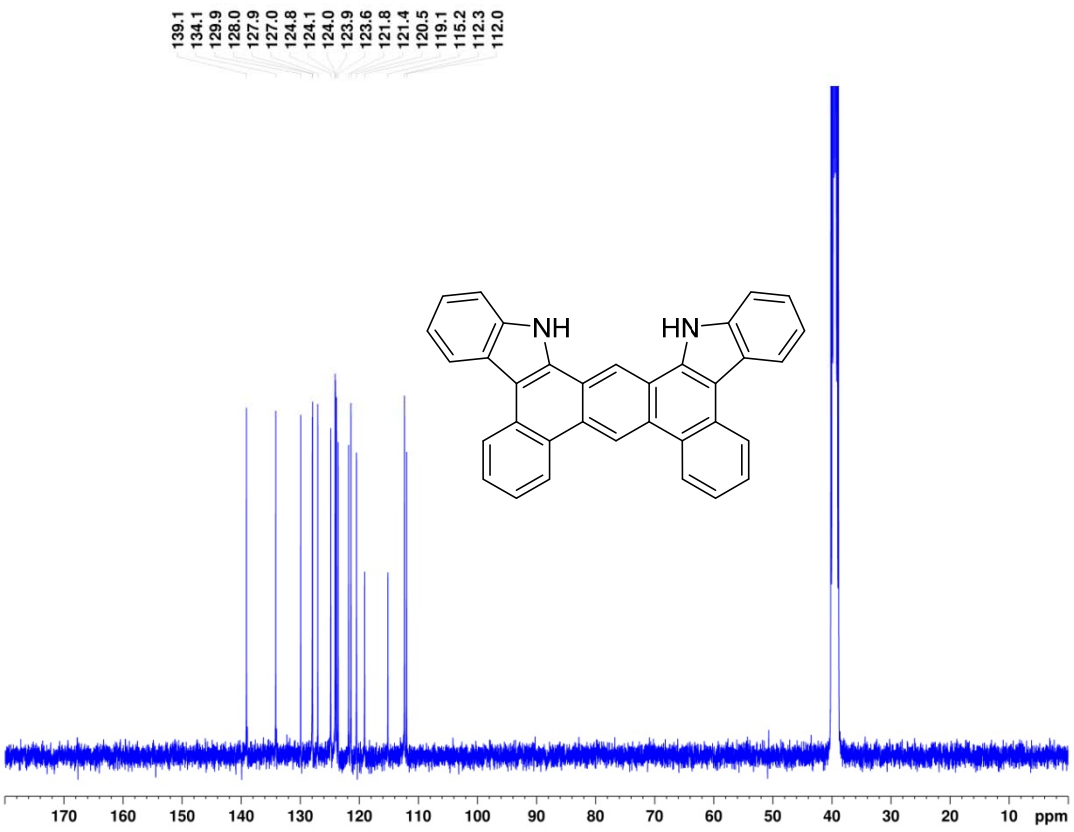

^{13}C NMR spectrum of **2b** in d_6-DMSO at 100.7 MHz.

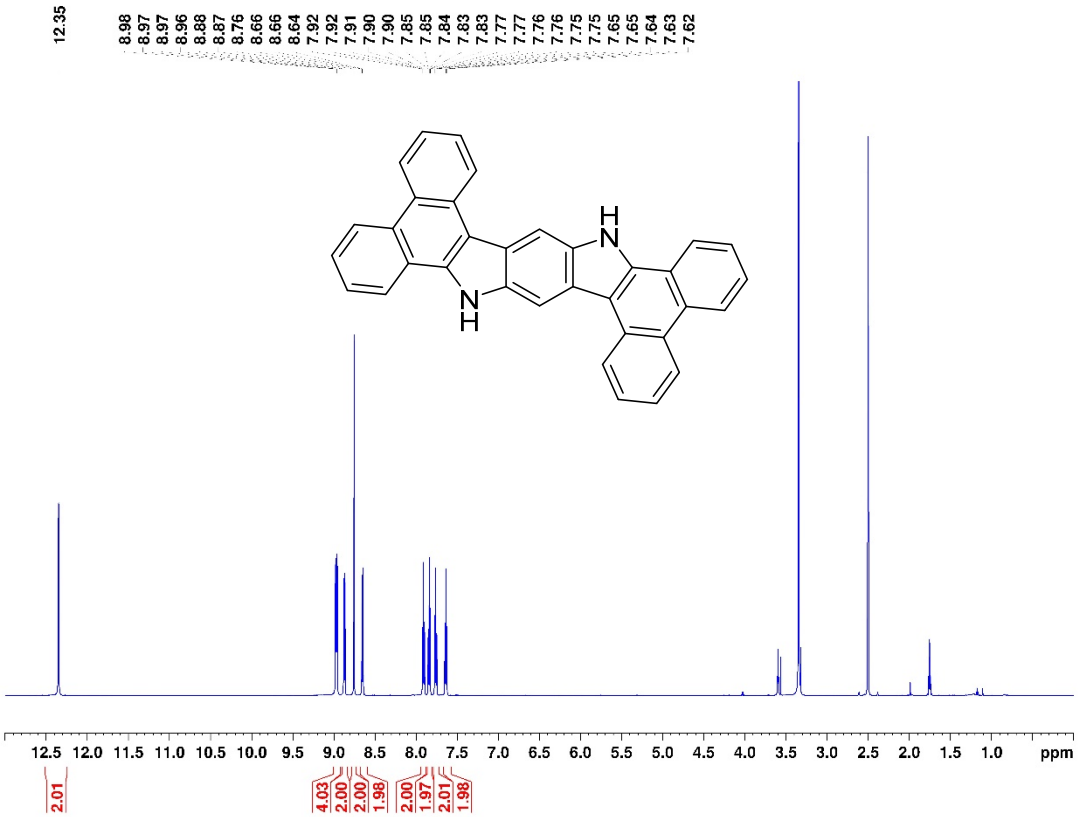

^{1}H NMR spectrum of **3a** in d_6-DMSO at 600.2 MHz.

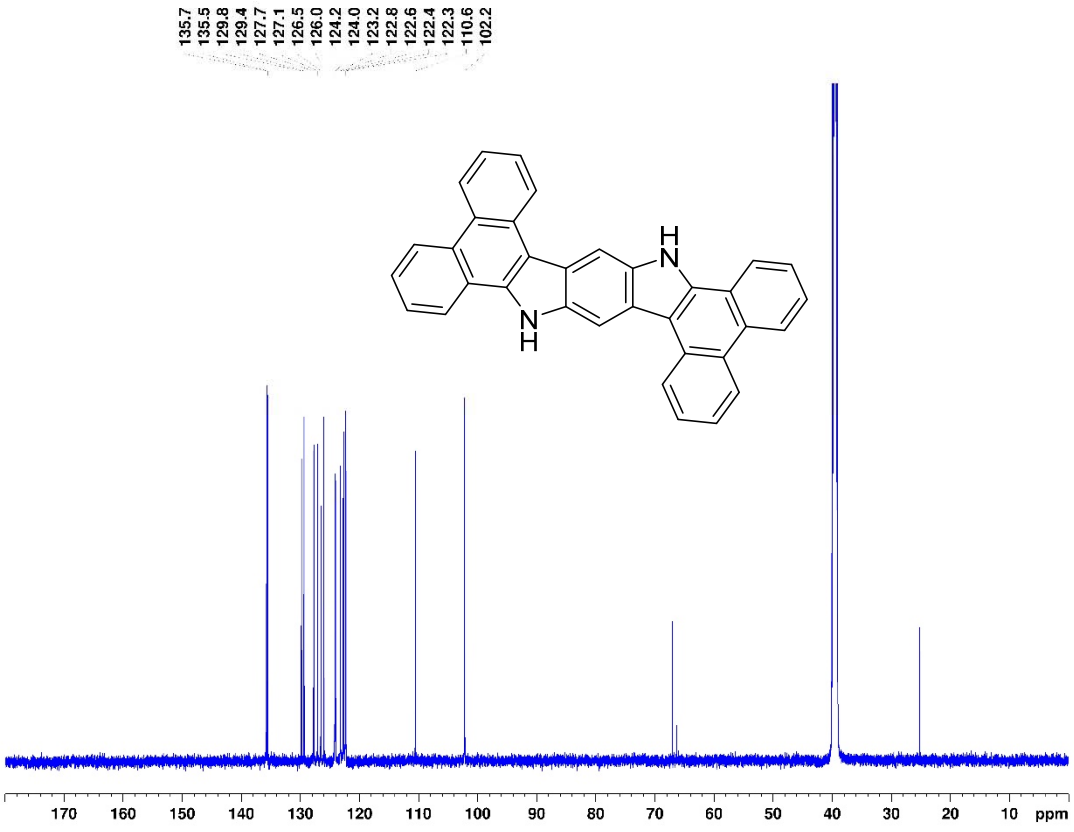

^{13}C NMR spectrum of **3a** in d_6-DMSO at 150.9 MHz.

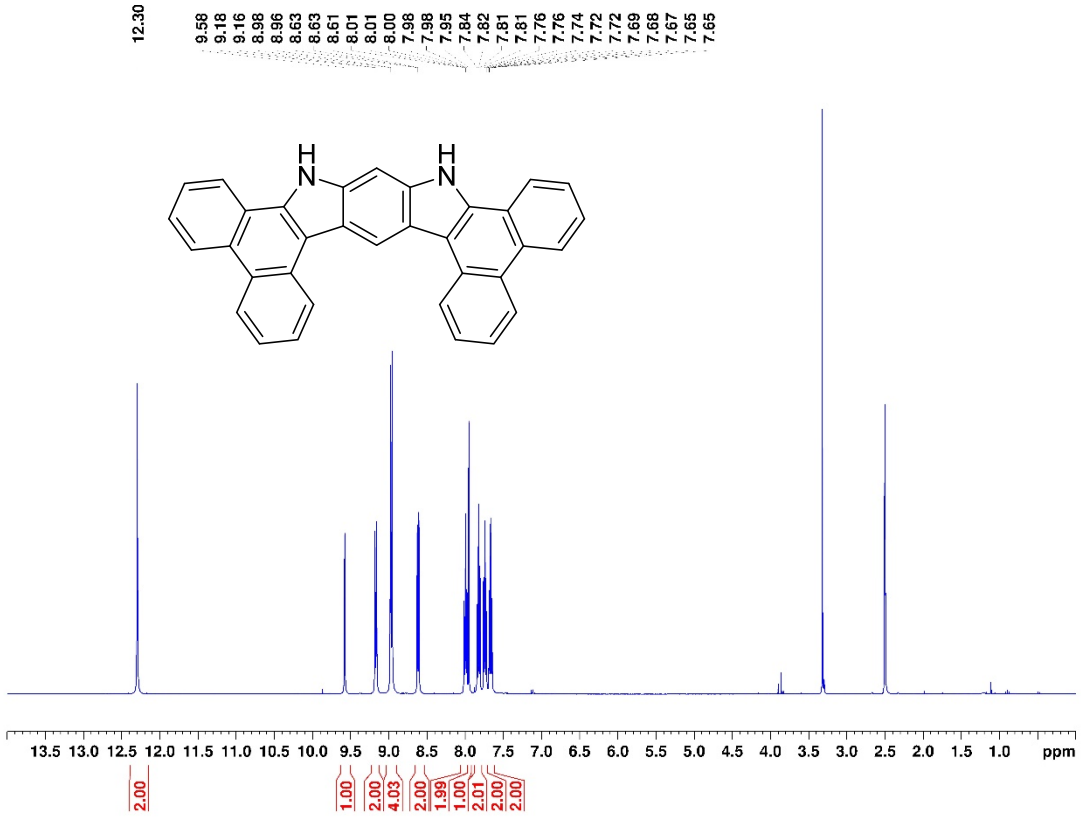

^{1}H NMR spectrum of **3b** in d_6-DMSO at 400.3 MHz.

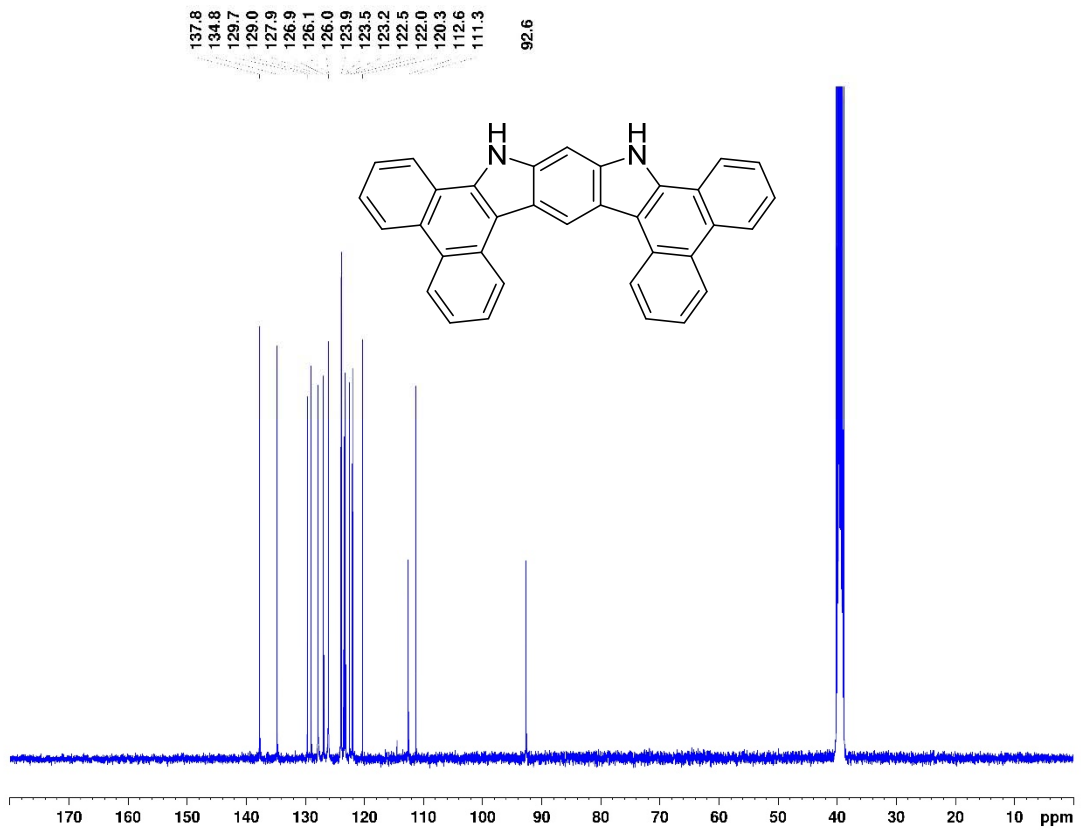

^{13}C NMR spectrum of **3b** in d_6-DMSO at 100.7 MHz.

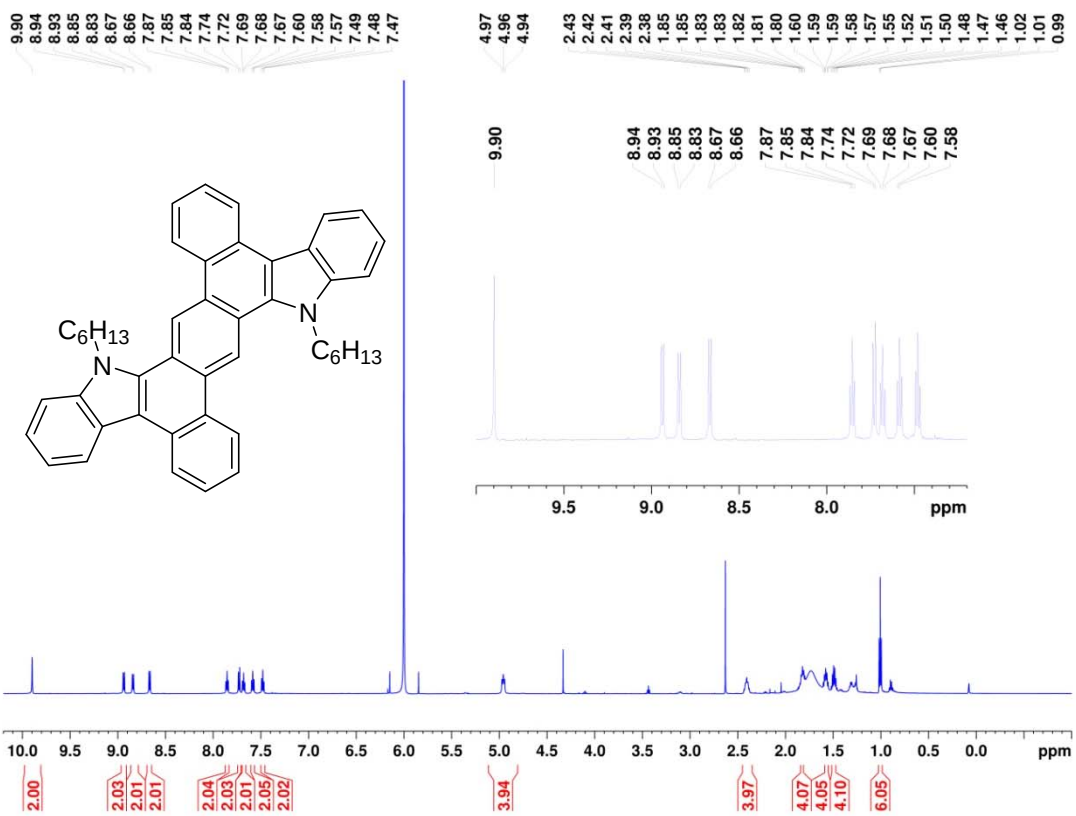

^{1}H NMR spectrum of **15a** in $C_2D_2Cl_4$ at 600.2 MHz (very low solubility).

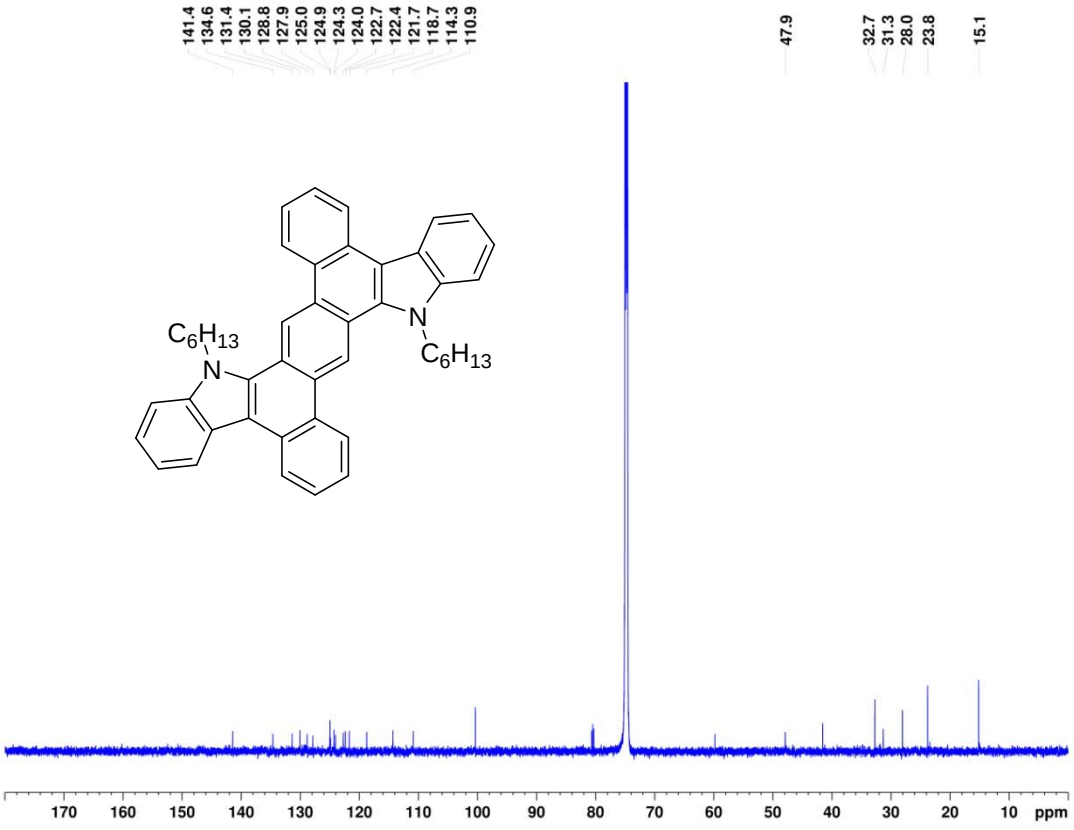

^{13}C NMR spectrum of **15a** in $C_2D_2Cl_4$ at 150.9 MHz (very low solubility).

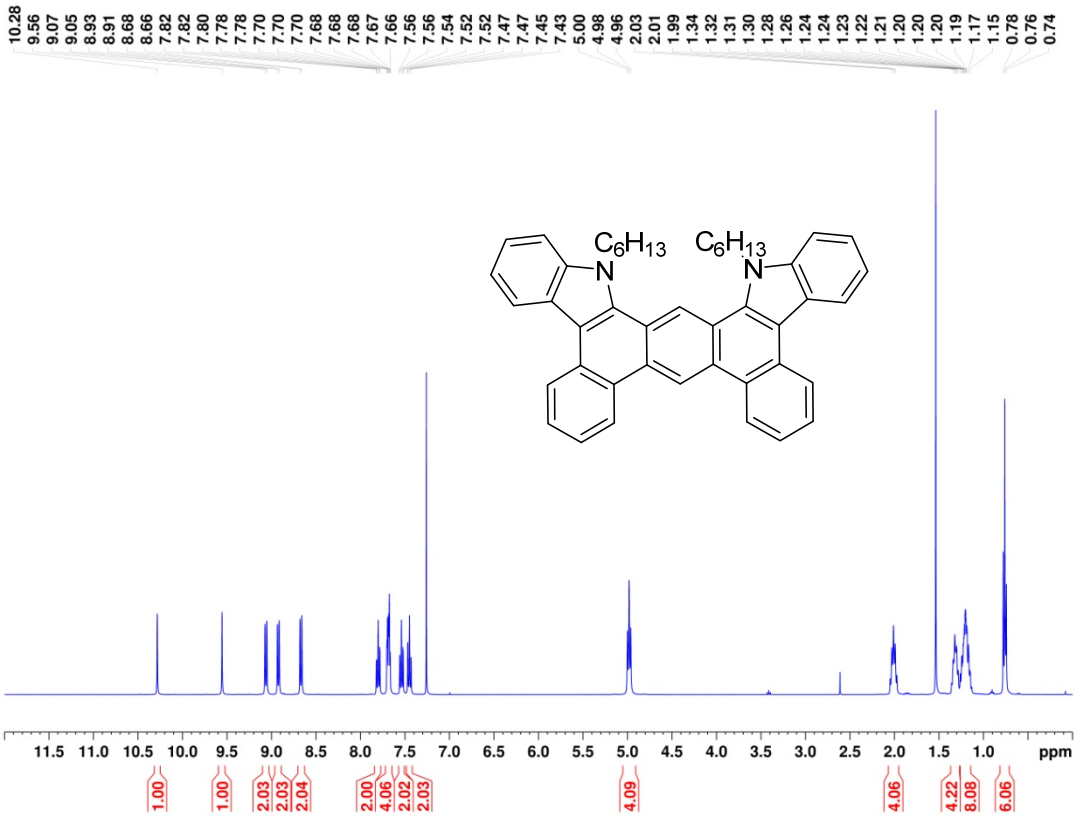

^{1}H NMR spectrum of **15b** in $CDCl_3$ at 400.3 MHz.

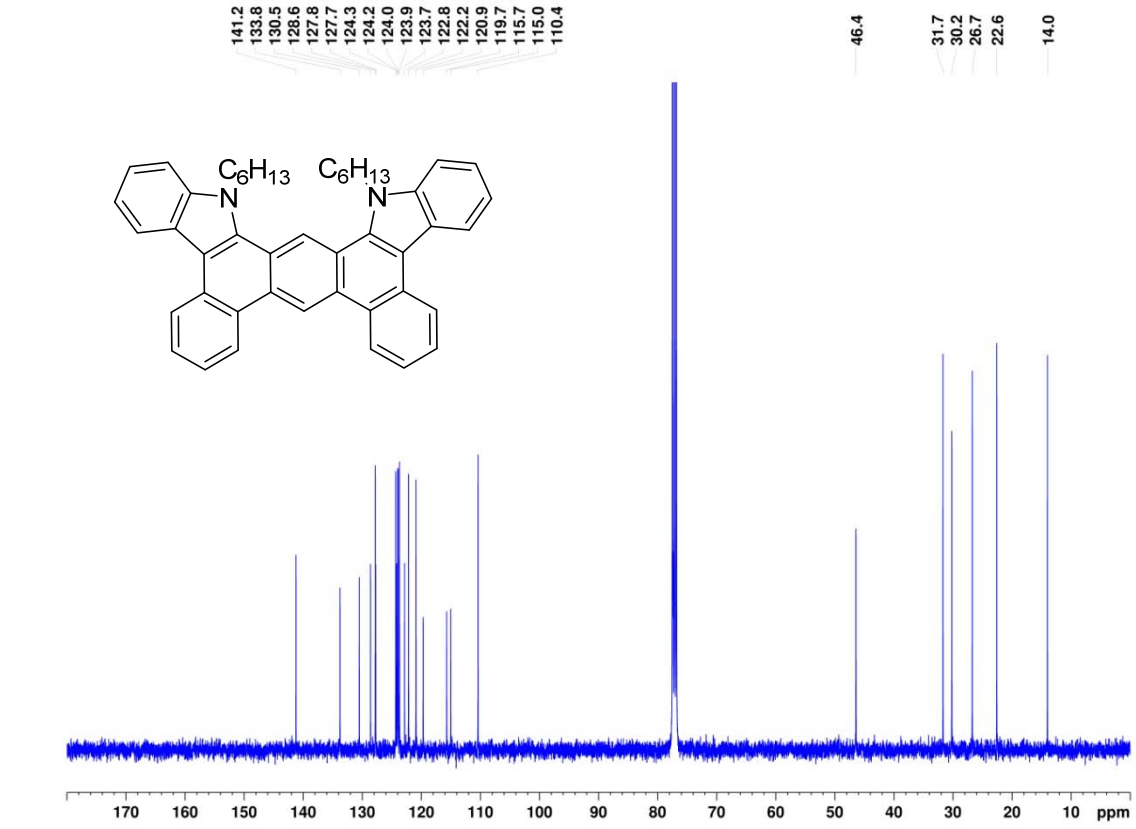

^{13}C NMR spectrum of **15b** in $CDCl_3$ at 100.7 MHz.

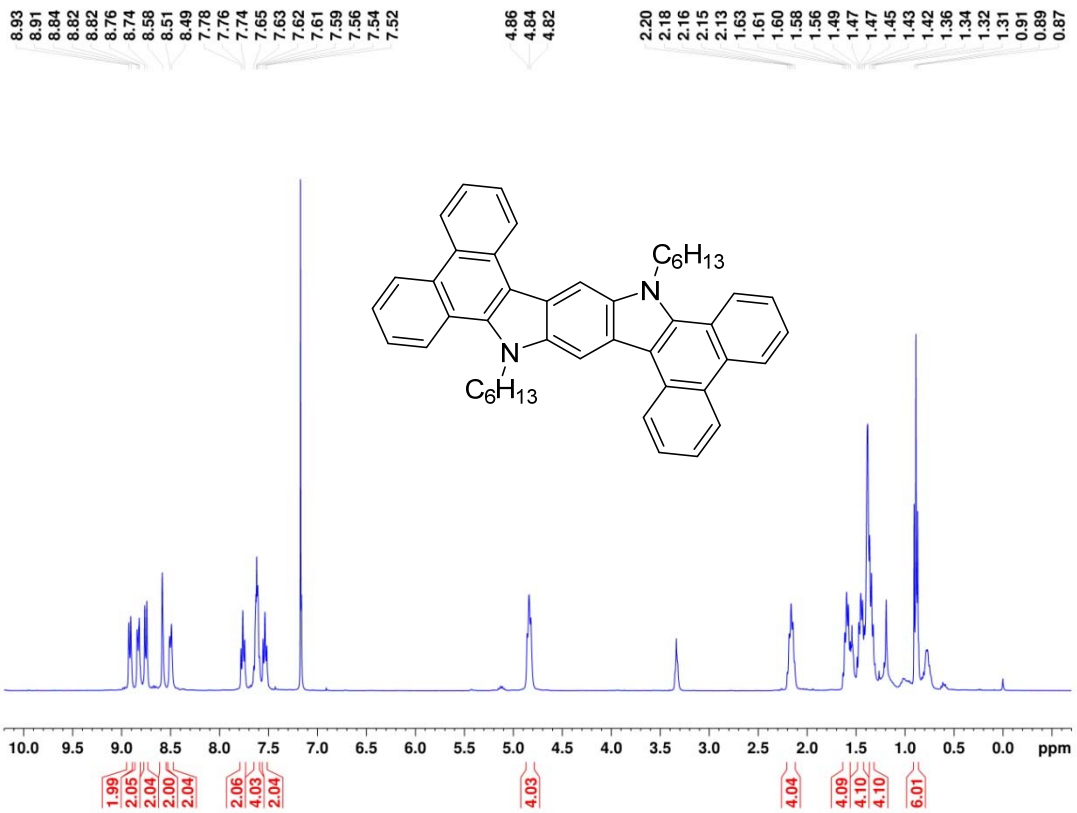

^{1}H NMR spectrum of **16a** in $CDCl_3$ at 400.3 MHz (323 K).

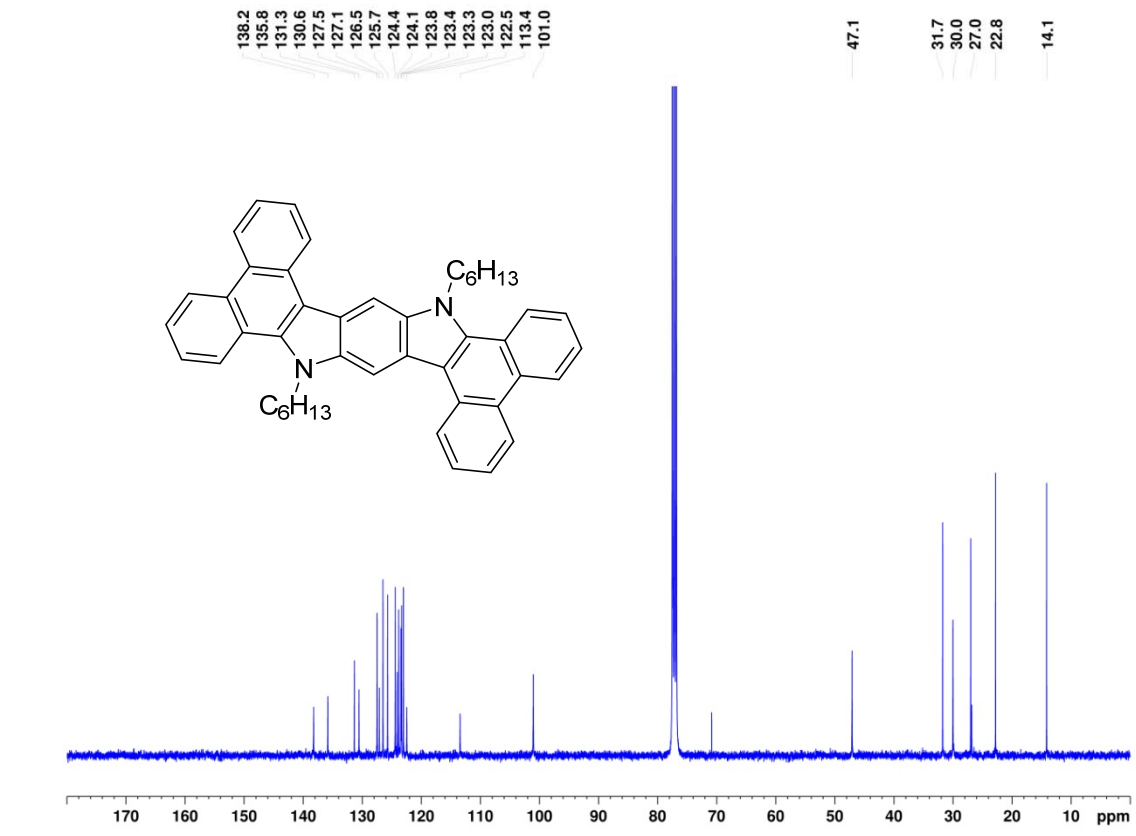

^{13}C NMR spectrum of **16a** in $CDCl_3$ at 100.7 MHz (323 K).

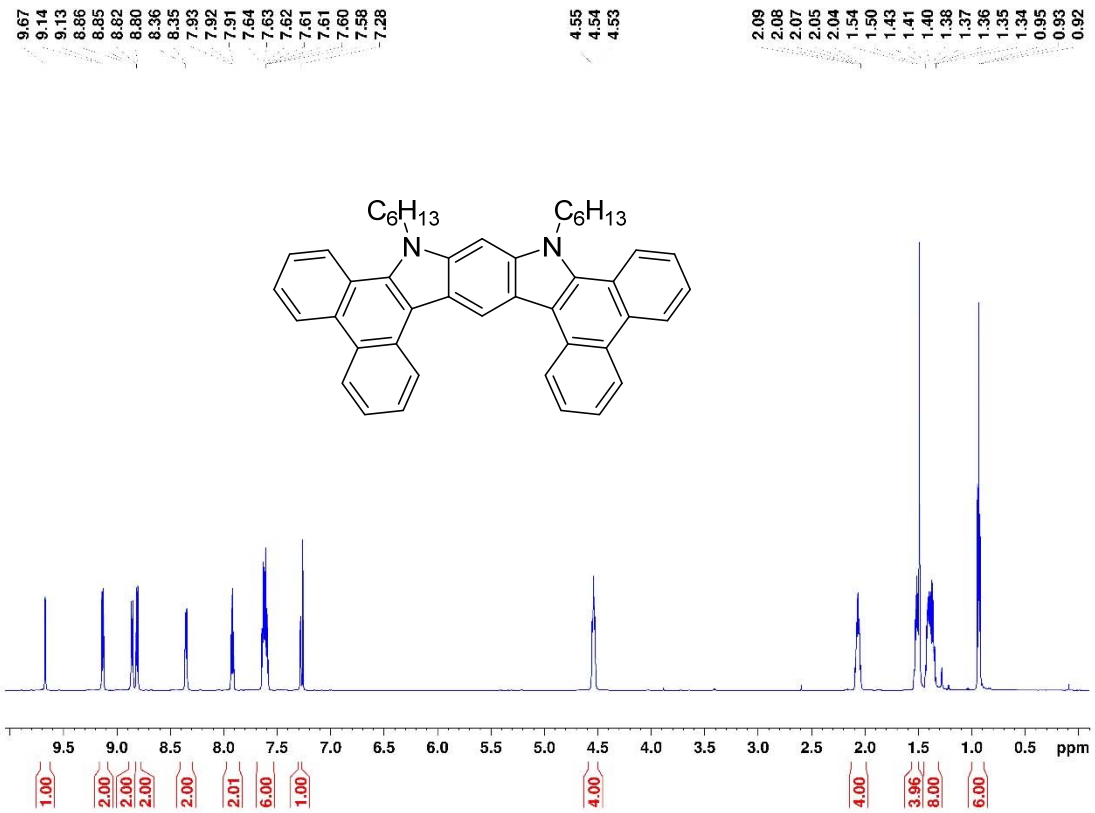

^{1}H NMR spectrum of **16b** in $CDCl_3$ at 600.2 MHz (323 K).

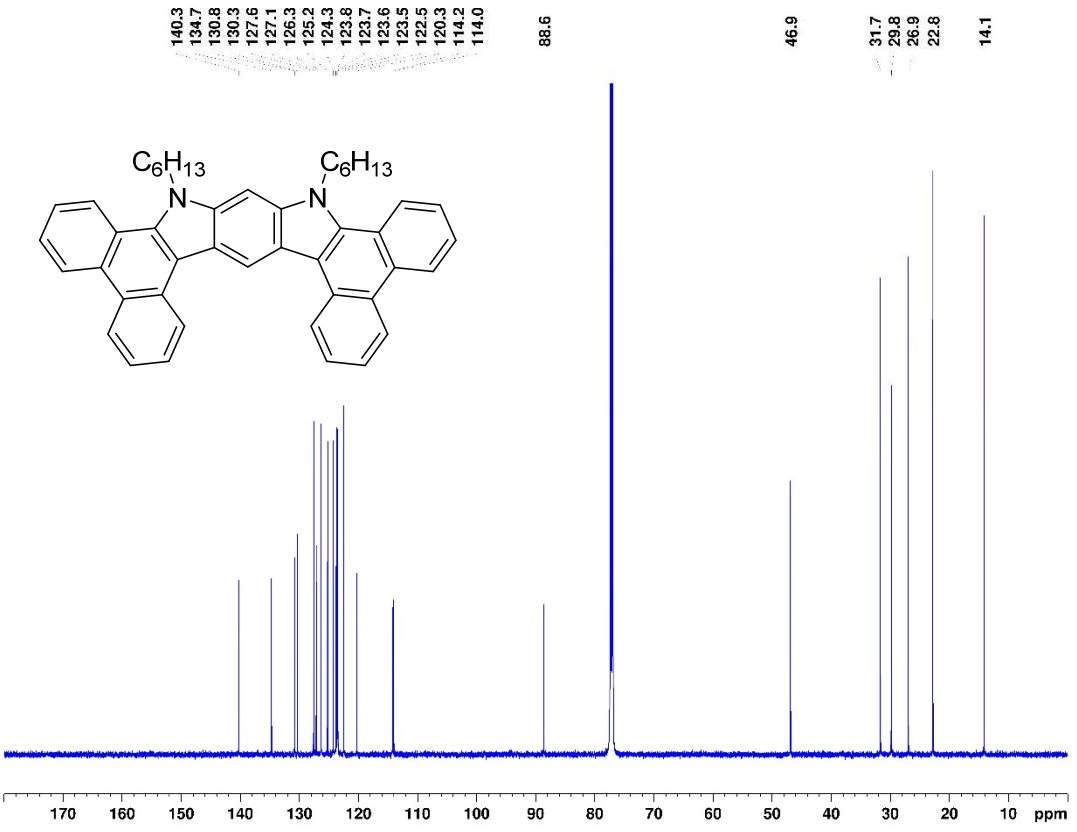

^{13}C NMR spectrum of **16b** in $CDCl_3$ at 150.9 MHz (323 K)**.**

5. UV/Vis and Fluorescence Data

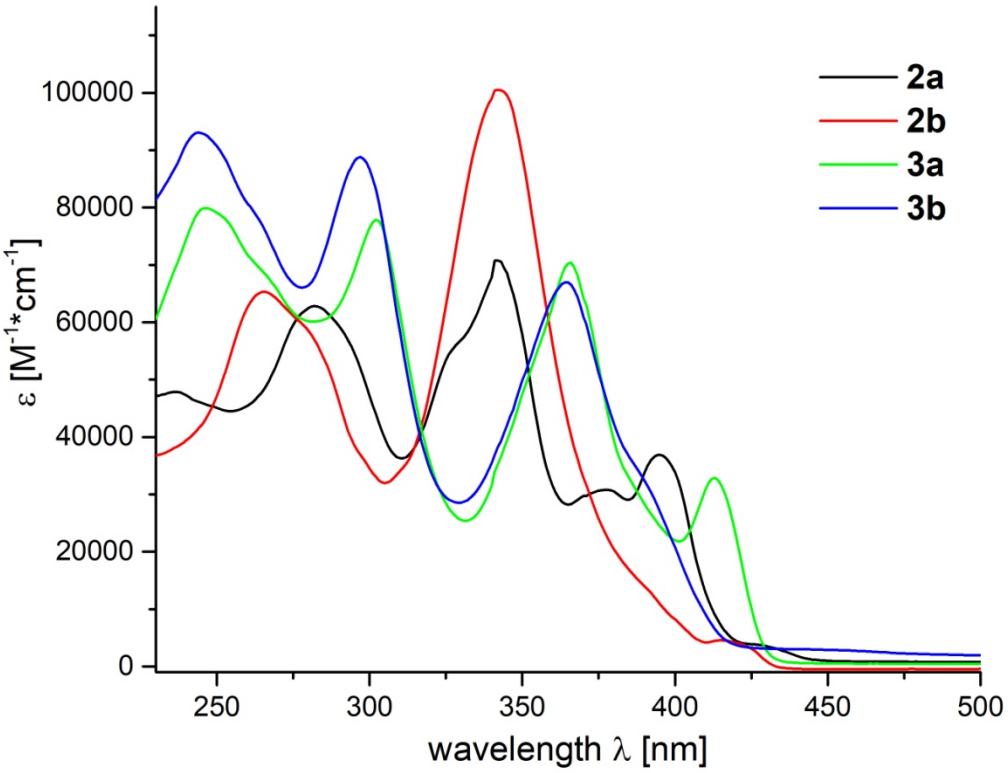

Figure SI1: Absorption spectra of **2a-b** and **3a-b** in THF.

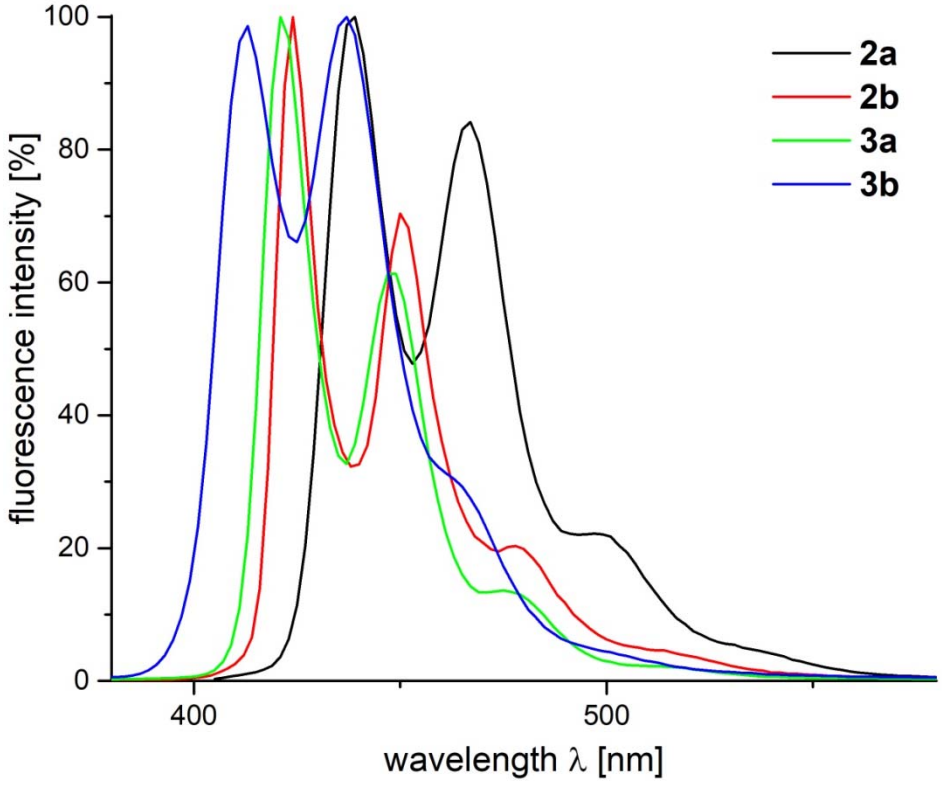

Figure SI2: Emission spectra of **2a-b** and **3a-b** in THF.

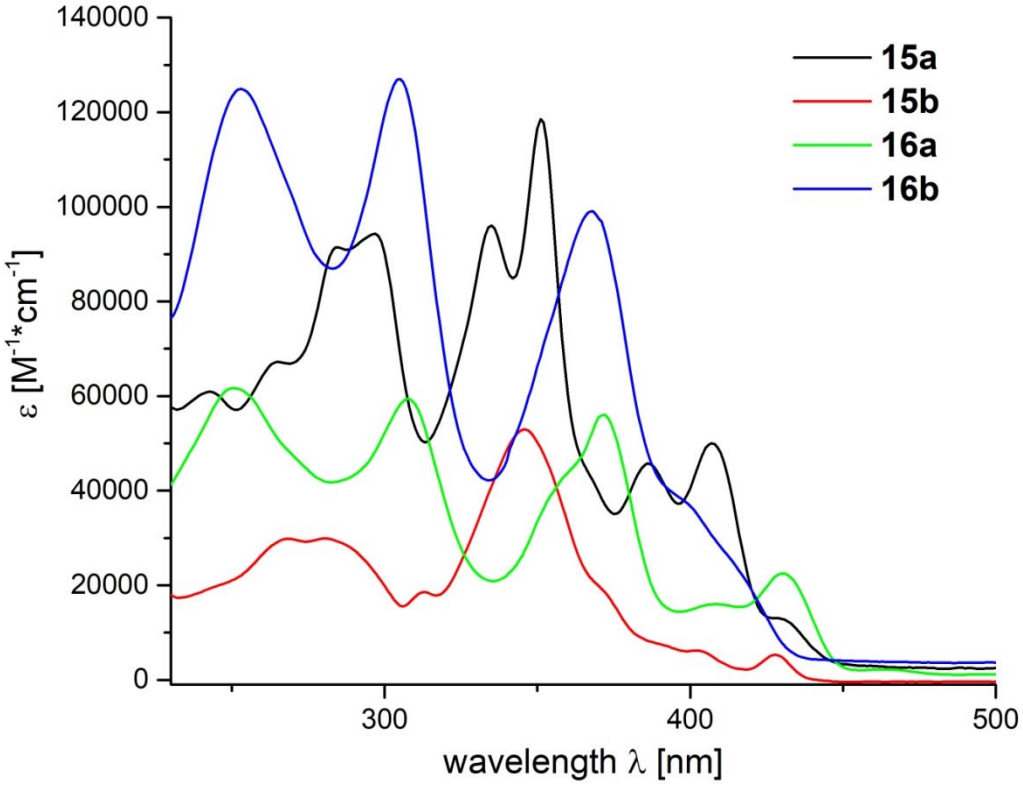

Figure SI3: Absorption spectra of **15a-b** and **16a-b** in DCM.

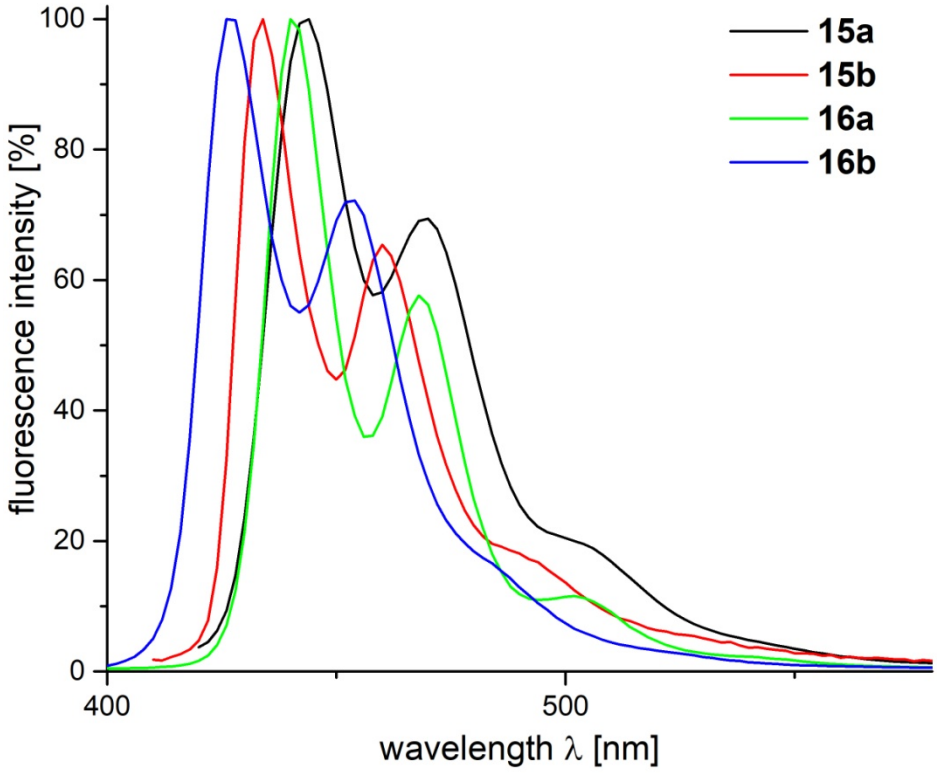

Figure SI4: Absorption spectra of **15a-b** and **16a-b** in DCM.

6. Crystallographic Data

Table 1: Crystal data and structure refinement for **2a** (CCDC 2043834).

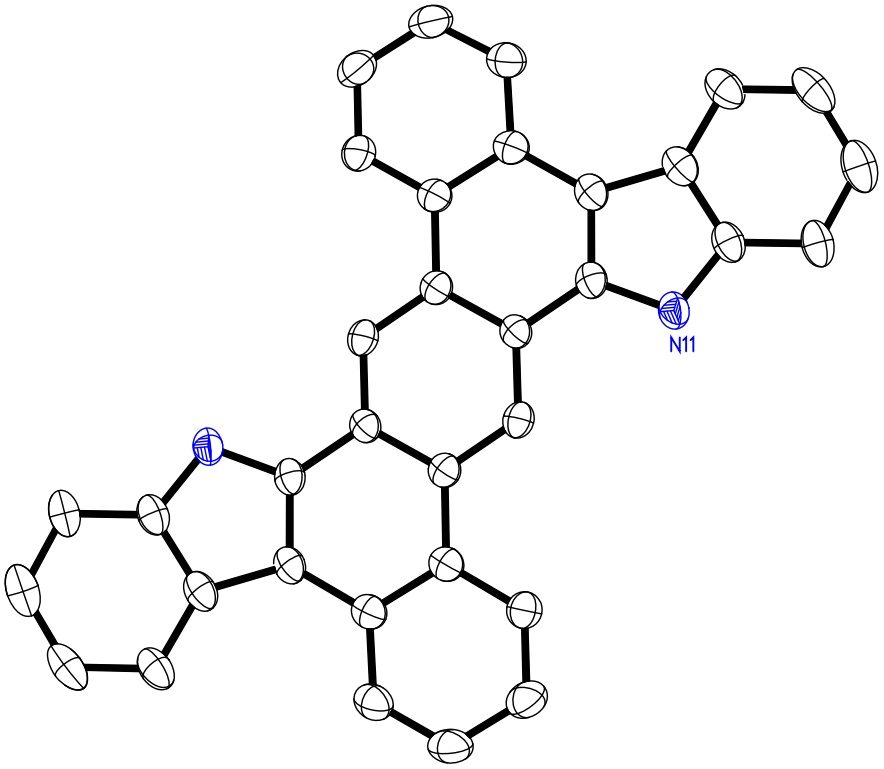

Empirical formula	$C_{42}H_{36}N_2O_2$	
Formula weight	600.73	
Temperature	200(2) K	
Wavelength	0.71073 Å	
Crystal system	triclinic	
Space group	P $\bar{1}$	
Z	1	
Unit cell dimensions	a =6.1683(15) Å	α =77.105(4) deg.
	b = 10.760(3) Å	β =81.593(4) deg.
	c = 12.079(3) Å	γ =82.231(4) deg.
Volume	768.7(3) $Å^3$	
Density (calculated)	1.30 g/cm^3	
Absorption coefficient	0.08 mm^{-1}	
Crystal shape	brick	
Crystal size	0.111 x 0.078 x 0.029 mm^3	
Crystal color	yellow	
Theta range for data collection	1.7 to 26.0 deg.	
Index ranges	-7≤h≤7, -13≤k≤13, -14≤l≤14	
Reflections collected	11898	
Independent reflections	3032 (R(int) = 0.0511)	
Observed reflections	2091 (I > 2σ(I))	
Absorption correction	Semi-empirical from equivalents	
Max. and min. transmission	0.96 and 0.77	
Refinement method	Full-matrix least-squares on F^2	
Data/restraints/parameters	3032 / 0 / 212	
Goodness-of-fit on F^2	1.03	
Final R indices (I>2sigma(I))	R1 = 0.060, wR2 = 0.161	
Largest diff. peak and hole	0.23 and -0.32 $eÅ^{-3}$	

Table 2: Crystal data and structure refinement for **2b** (CCDC 2043835).

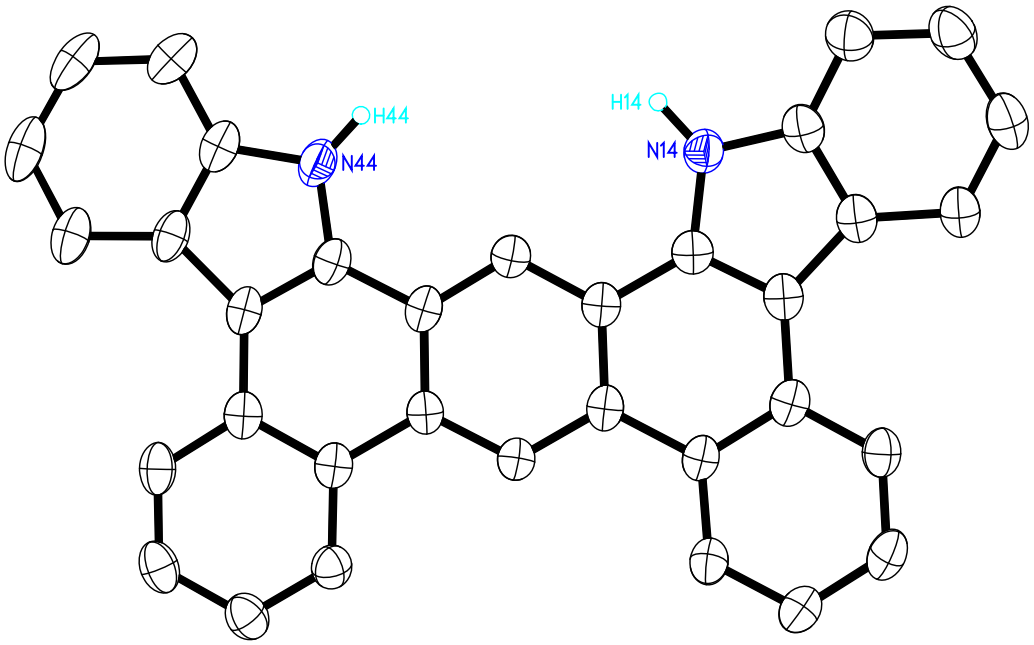

Empirical formula	$C_{35}H_{23}N_2O$	
Formula weight	487.55	
Temperature	200(2) K	
Wavelength	0.71073 Å	
Crystal system	orthorhombic	
Space group	$P2_12_12_1$	
Z	4	
Unit cell dimensions	a =5.0341(1) Å	α = 90 deg.
	b = 20.7818(3) Å	β = 90 deg.
	c = 23.1446(4) Å	γ = 90 deg.
Volume	2421.35(7) $Å^3$	
Density (calculated)	1.34 g/cm^3	
Absorption coefficient	0.08 mm^{-1}	
Crystal shape	brick	
Crystal size	0.234 x 0.073 x 0.069 mm^3	
Crystal color	brown	
Theta range for data collection	2.0 to 27.2 deg.	
Index ranges	-6≤h≤6, -26≤k≤26, -29≤l≤29	
Reflections collected	33281	
Independent reflections	5376 (R(int) = 0.0549)	
Observed reflections	4498 (I > 2σ(I))	
Absorption correction	Semi-empirical from equivalents	
Max. and min. transmission	0.96 and 0.92	
Refinement method	Full-matrix least-squares on F^2	
Data/restraints/parameters	5376 / 0 / 351	
Goodness-of-fit on F^2	1.05	
Final R indices (I>2sigma(I))	R1 = 0.052, wR2 = 0.138	
Absolute structure parameter	-0.3(10)	
Largest diff. peak and hole	0.44 and -0.28 $eÅ^{-3}$	

Table 3: Crystal data and structure refinement for **15b** (CCDC 2043836).

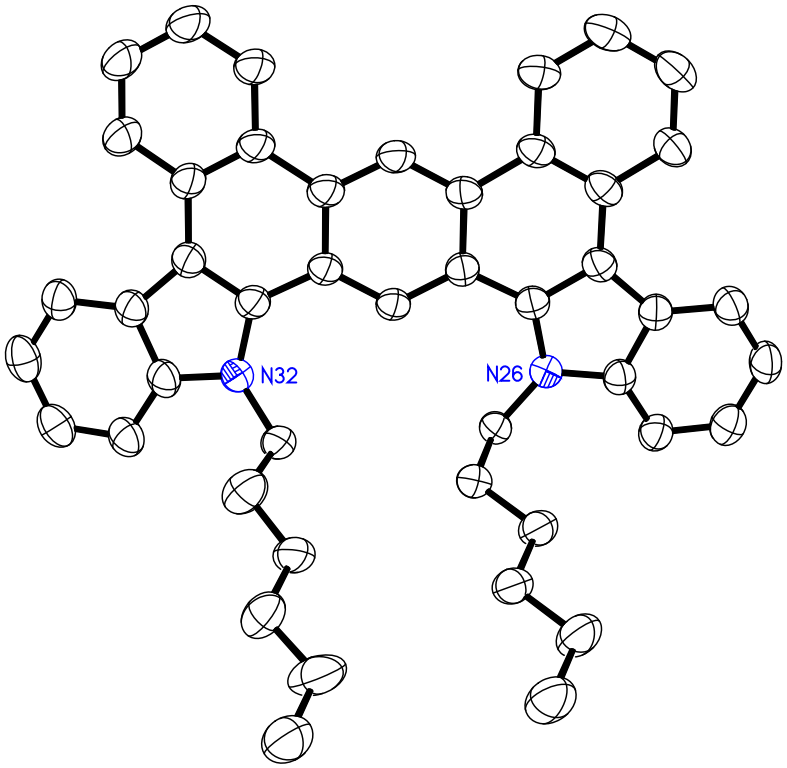

Empirical formula	$C_{47}H_{45}Cl_3N_2$	
Formula weight	744.20	
Temperature	200(2) K	
Wavelength	0.71073 Å	
Crystal system	monoclinic	
Space group	$P2_1/n$	
Z	4	
Unit cell dimensions	a = 16.1111(3) Å	α = 90 deg.
	b =8.5856(2) Å	β =104.1979(12) deg.
	c = 28.2125(5) Å	γ = 90 deg.
Volume	3783.25(13) $Å^3$	
Density (calculated)	1.31 g/cm^3	
Absorption coefficient	0.28 mm^{-1}	
Crystal shape	brick	
Crystal size	0.117 x 0.108 x 0.107 mm^3	
Crystal color	yellow	
Theta range for data collection	1.5 to 25.1 deg.	
Index ranges	-19≤h≤19, -10≤k≤10, -33≤l≤33	
Reflections collected	43703	
Independent reflections	6692 (R(int) = 0.0614)	
Observed reflections	4356 (I > 2σ(I))	
Absorption correction	Semi-empirical from equivalents	
Max. and min. transmission	0.94 and 0.90	
Refinement method	Full-matrix least-squares on F^2	
Data/restraints/parameters	6692 / 0 / 471	
Goodness-of-fit on F^2	1.04	
Final R indices (I>2sigma(I))	R1 = 0.076, wR2 = 0.191	
Largest diff. peak and hole	0.70 and -0.71 $eÅ^{-3}$	

Table 4: Crystal data and structure refinement for **3a** (CCDC 2043838).

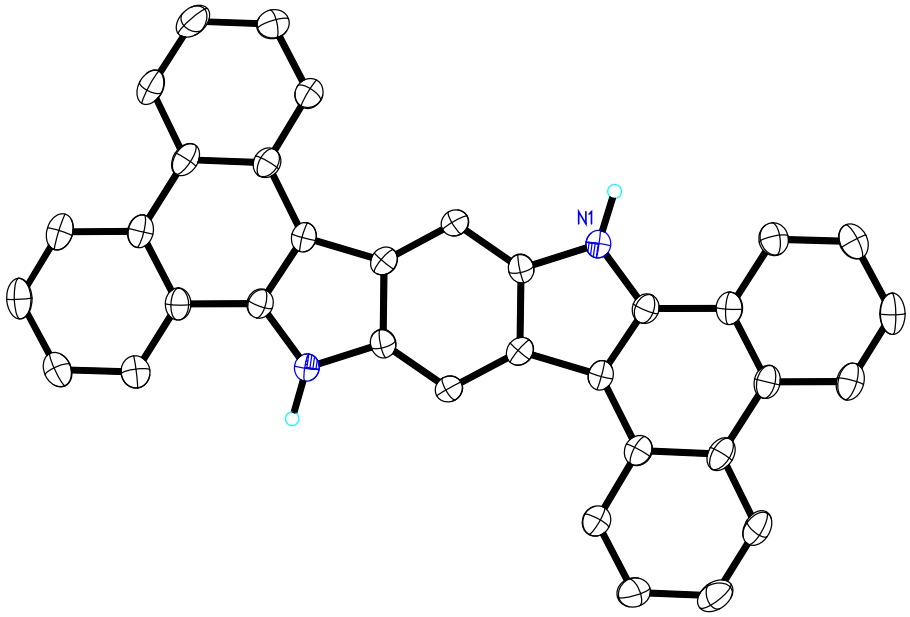

Empirical formula	$C_{34}H_{20}N_2$	
Formula weight	456.52	
Temperature	200(2) K	
Wavelength	0.71073 Å	
Crystal system	monoclinic	
Space group	$P2_1/c$	
Z	2	
Unit cell dimensions	a =8.1736(9) Å	α = 90 deg.
	b = 11.8554(12) Å	β = 107.819(3) deg.
	c = 11.4291(11) Å	γ = 90 deg.
Volume	1054.37(19) $Å^3$	
Density (calculated)	1.44 g/cm^3	
Absorption coefficient	0.08 mm^{-1}	
Crystal shape	brick	
Crystal size	0.097 x 0.070 x 0.033 mm^3	
Crystal color	brown	
Theta range for data collection	2.5 to 26.8 deg.	
Index ranges	$-10\leq h\leq 10$, $-15\leq k\leq 15$, $-14\leq l\leq 14$	
Reflections collected	10713	
Independent reflections	2243 (R(int) = 0.0333)	
Observed reflections	1766 ($I > 2\sigma(I)$)	
Absorption correction	Semi-empirical from equivalents	
Max. and min. transmission	0.96 and 0.90	
Refinement method	Full-matrix least-squares on F^2	
Data/restraints/parameters	2243 / 0 / 167	
Goodness-of-fit on F^2	1.07	
Final R indices (I>2sigma(I))	R1 = 0.049, wR2 = 0.124	
Largest diff. peak and hole	0.38 and -0.23 $eÅ^{-3}$	

Table 5: Crystal data and structure refinement for **3b** (CCDC 2043837).

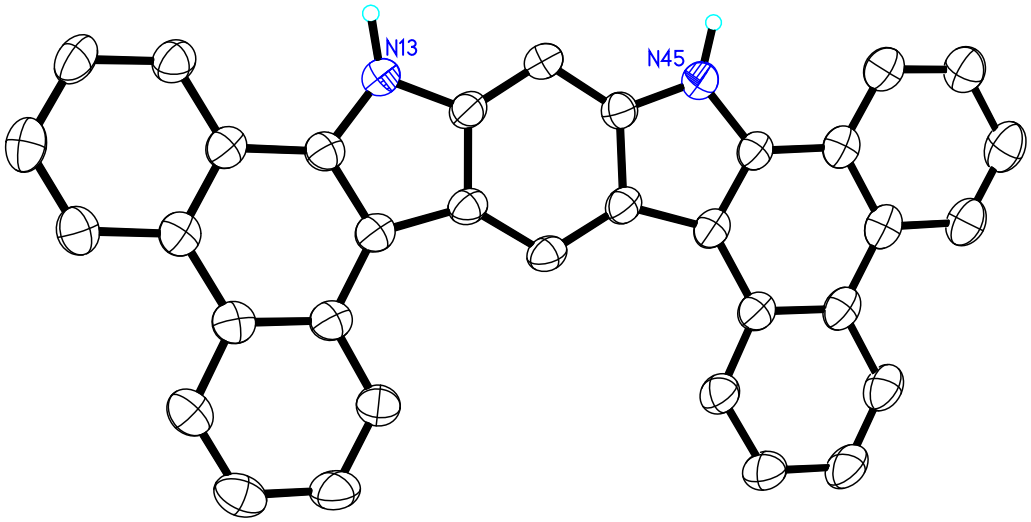

Empirical formula	$C_{42}H_{36}N_2O_2$	
Formula weight	600.73	
Temperature	200(2) K	
Wavelength	0.71073 Å	
Crystal system	orthorhombic	
Space group	Pbca	
Z	8	
Unit cell dimensions	a = 18.6216(8) Å	α = 90 deg.
	b = 14.4312(7) Å	β = 90 deg.
	c = 22.8204(10) Å	γ = 90 deg.
Volume	6132.6(5) $Å^3$	
Density (calculated)	1.30 g/cm^3	
Absorption coefficient	0.08 mm^{-1}	
Crystal shape	plate	
Crystal size	0.140 x 0.100 x 0.020 mm^3	
Crystal color	yellow	
Theta range for data collection	1.8 to 23.7 deg.	
Index ranges	$-20\leq h\leq 21$, $-16\leq k\leq 16$, $-25\leq l\leq 25$	
Reflections collected	32148	
Independent reflections	4675 (R(int) = 0.0790)	
Observed reflections	2958 ($I > 2\sigma(I)$)	
Absorption correction	Semi-empirical from equivalents	
Max. and min. transmission	0.96 and 0.88	
Refinement method	Full-matrix least-squares on F^2	
Data/restraints/parameters	4675 / 0 / 423	
Goodness-of-fit on F^2	1.04	
Final R indices (I>2sigma(I))	R1 = 0.058, wR2 = 0.128	
Largest diff. peak and hole	0.27 and -0.26 $eÅ^{-3}$	

7. Cyclic Voltammograms

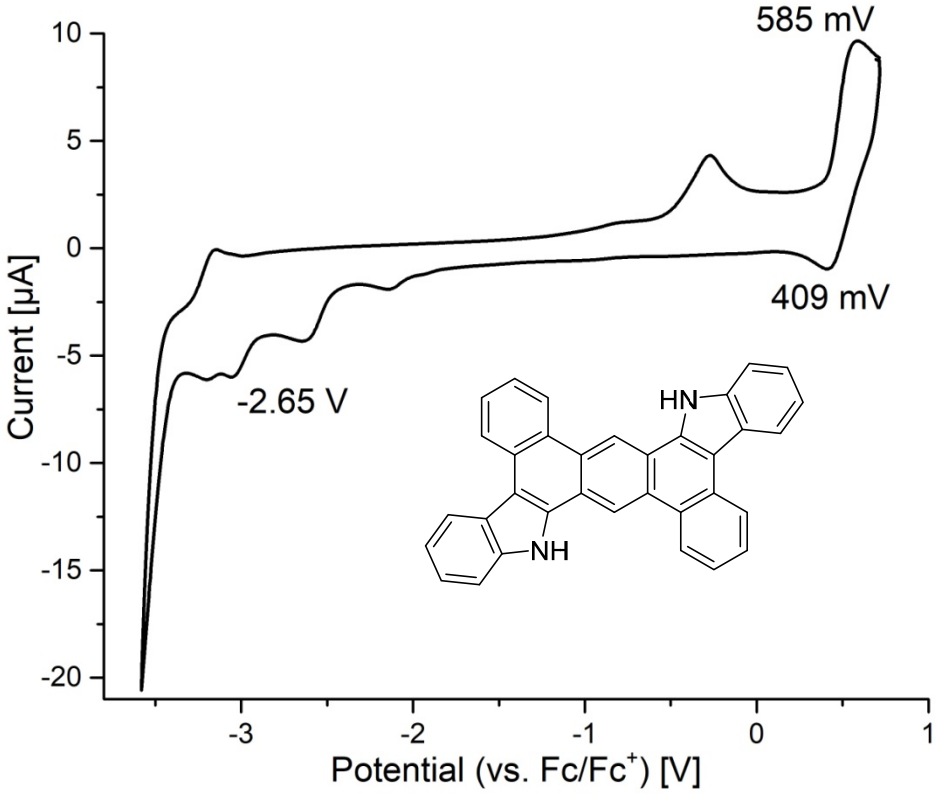

Figure SI5: Cyclic voltammogram of compound **2a** in DMSO against ferrocene/ferrocenium (Fc/Fc^+).

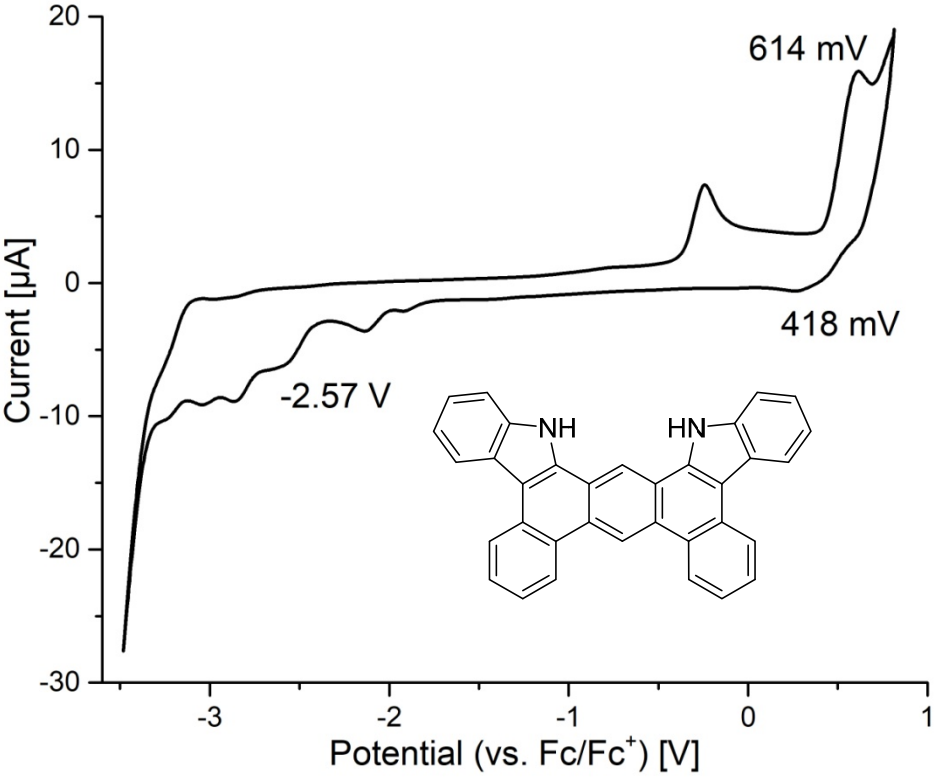

Figure SI6: Cyclic voltammogram of compound **2b** in DMSO against ferrocene/ferrocenium (Fc/Fc^+).

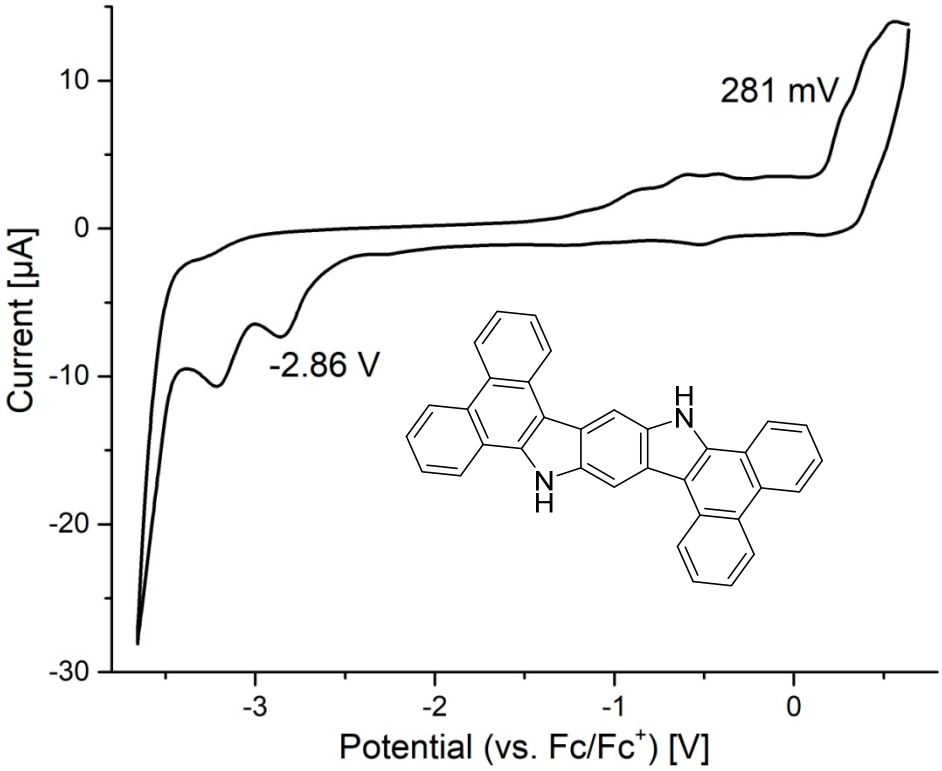

Figure SI7: Cyclic voltammogram of compound **3a** in DMSO against ferrocene/ferrocenium (Fc/Fc^+).

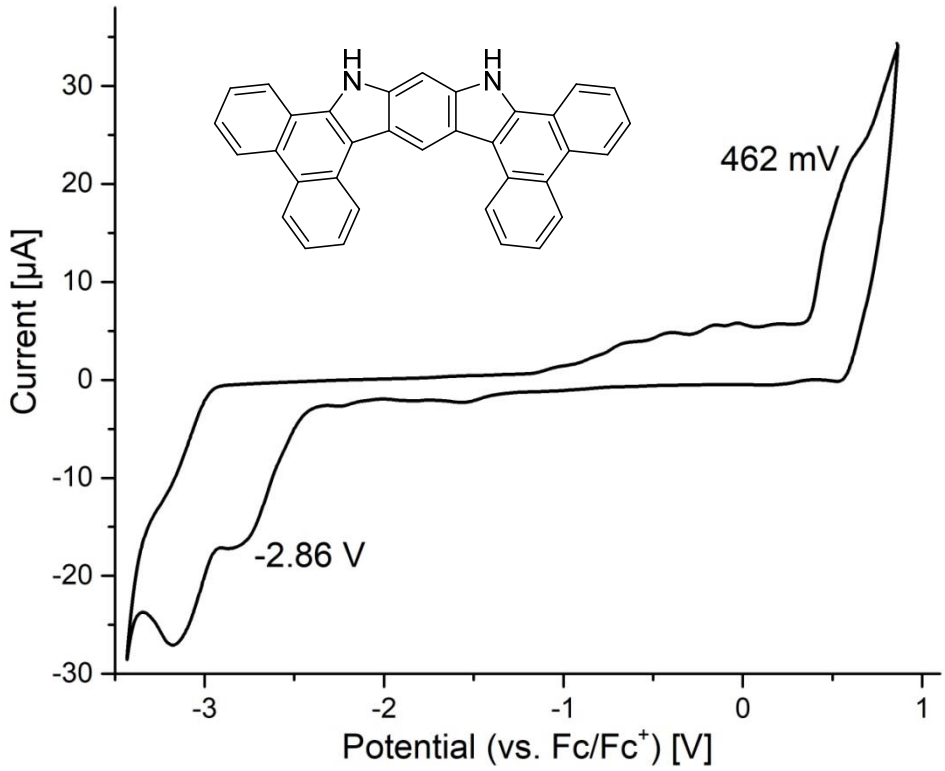

Figure SI8: Cyclic voltammogram of compound **3b** in DMSO against ferrocene/ferrocenium (Fc/Fc^+).

8. Computational Details

All calculations were performed using Orca 4.2.1.[10] The structures were optimized with PBEh-3c/def2-mSVP.[11] All optimized structures were checked to display no imaginary frequencies to ensure a true minimum. Subsequently B3LYP/G with 6-311+G** basis set was used to calculate the canonical HOMO/LUMO levels.

DBDCZ **2a**

N	4.774338000000	4.472301000000	5.559958000000	N	-1.553815000000	8.668585000000	6.128956000000
H	4.674241000000	4.195834000000	6.518487000000	H	-1.453724000000	8.945043000000	5.170424000000
C	3.929479000000	5.296840000000	4.873556000000	C	-0.708954000000	7.844047000000	6.815358000000
C	2.758769000000	5.933679000000	5.384017000000	C	0.461756000000	7.207209000000	6.304897000000
C	2.335467000000	5.777304000000	6.699366000000	C	0.885058000000	7.363584000000	4.989548000000
H	2.919140000000	5.146123000000	7.354826000000	H	0.301386000000	7.994766000000	4.334088000000
C	1.197150000000	6.392543000000	7.202883000000	C	2.023376000000	6.748346000000	4.486031000000
C	2.469807000000	6.912289000000	3.106510000000	C	0.750720000000	6.228601000000	8.582405000000
C	1.761878000000	7.710748000000	2.196635000000	C	1.458649000000	5.430143000000	9.492280000000
H	0.860179000000	8.219770000000	2.506434000000	H	2.360349000000	4.921121000000	9.182481000000
C	2.175340000000	7.874556000000	0.895631000000	C	1.045188000000	5.266336000000	10.793285000000
H	1.605907000000	8.500395000000	0.221989000000	H	1.614621000000	4.640498000000	11.466927000000
C	3.330628000000	7.232514000000	0.454775000000	C	-0.110100000000	5.908378000000	11.234141000000
H	3.665793000000	7.353271000000	-0.566797000000	H	-0.445264000000	5.787622000000	12.255713000000
C	4.045835000000	6.442441000000	1.322576000000	C	-0.825307000000	6.698450000000	10.366340000000
H	4.938071000000	5.953980000000	0.964270000000	H	-1.717544000000	7.186911000000	10.724645000000
C	3.642570000000	6.260475000000	2.654011000000	C	-0.422044000000	6.880414000000	9.034904000000
C	4.375217000000	5.435732000000	3.573817000000	C	-1.154692000000	7.705156000000	8.115097000000
C	5.571207000000	4.640192000000	3.462001000000	C	-2.350683000000	8.500695000000	8.226912000000
C	6.489348000000	4.344491000000	2.449255000000	C	-3.268824000000	8.796395000000	9.239659000000
H	6.388092000000	4.755083000000	1.455776000000	H	-3.167567000000	8.385805000000	10.233139000000
C	7.553442000000	3.506729000000	2.715800000000	C	-4.332920000000	9.634155000000	8.973113000000
H	8.260510000000	3.279157000000	1.929436000000	H	-5.039988000000	9.861726000000	9.759476000000
C	7.733542000000	2.945063000000	3.984079000000	C	-4.513021000000	10.195819000000	7.704833000000
H	8.577229000000	2.292456000000	4.164548000000	H	-5.356710000000	10.848424000000	7.524364000000
C	6.847830000000	3.212414000000	5.007711000000	C	-3.627309000000	9.928468000000	6.681201000000
H	6.982829000000	2.778518000000	5.990538000000	H	-3.762309000000	10.362363000000	5.698374000000
C	5.779284000000	4.056549000000	4.730693000000	C	-2.558762000000	9.084336000000	6.95822000000

DBDCZ **2b**

C	2.206382000000	9.696127000000	14.637175000000	C	-1.214391000000	8.277213000000	18.938810000000
H	2.105631000000	10.667956000000	14.167588000000	H	-1.957972000000	8.967781000000	19.304266000000
C	1.360967000000	9.365033000000	15.687816000000	C	-1.097299000000	7.050284000000	19.546982000000
C	0.353434000000	10.245146000000	16.183453000000	H	-1.748335000000	6.792253000000	20.371799000000
N	0.069922000000	11.502751000000	15.729989000000	C	-0.138268000000	6.145212000000	19.097760000000
H	0.548550000000	11.985567000000	14.993569000000	H	-0.039193000000	5.174861000000	19.565317000000
C	-0.965636000000	12.025330000000	16.454955000000	C	0.686930000000	6.490366000000	18.053425000000
C	-1.575351000000	13.268518000000	16.336433000000	H	1.419834000000	5.764811000000	17.730568000000
H	-1.247085000000	13.989676000000	15.598450000000	C	0.594673000000	7.735679000000	17.414028000000
C	-2.617115000000	13.554252000000	17.194868000000	C	1.480265000000	8.096531000000	16.310406000000
H	-3.113301000000	14.513438000000	17.131408000000	C	2.460118000000	7.234976000000	15.829591000000
C	-3.040188000000	12.618605000000	18.144611000000	H	2.554451000000	6.266802000000	16.292773000000
H	-3.863308000000	12.864086000000	18.802120000000	C	3.320209000000	7.545920000000	14.781621000000
C	-2.428074000000	11.386694000000	18.256537000000	C	4.340254000000	6.616697000000	14.304030000000
H	-2.791893000000	10.691039000000	18.998018000000	C	4.522630000000	5.357961000000	14.895846000000
C	-1.363849000000	11.063194000000	17.408191000000	H	3.905959000000	5.051460000000	15.728749000000
C	-0.499507000000	9.925738000000	17.220517000000	C	5.479808000000	4.476150000000	14.452254000000
C	-0.387796000000	8.648410000000	17.868396000000	H	5.590299000000	3.513186000000	14.932364000000

C	6.301757000000	4.830046000000	13.384749000000	H	7.850138000000	9.312347000000	8.960952000000
H	7.057786000000	4.144320000000	13.025917000000	C	6.426289000000	10.798060000000	9.572349000000
C	6.149312000000	6.057253000000	12.785007000000	H	6.739839000000	11.506154000000	8.817002000000
H	6.795917000000	6.315418000000	11.961402000000	C	5.409705000000	11.136105000000	10.441833000000
C	5.179426000000	6.972152000000	13.219879000000	H	4.919928000000	12.099764000000	10.380030000000
C	5.009954000000	8.259934000000	12.605717000000	C	5.041228000000	10.197030000000	11.397650000000
C	5.660970000000	8.933661000000	11.510744000000	N	4.074268000000	10.284333000000	12.360834000000
C	6.686285000000	8.626448000000	10.610187000000	H	3.481007000000	11.080107000000	12.500768000000
H	7.197399000000	7.675576000000	10.640291000000	C	4.049067000000	9.126417000000	13.086329000000
C	7.057198000000	9.552572000000	9.656393000000	C	3.175872000000	8.818029000000	14.171785000000

DDICZ **3a**

C	1.114177000000	-2.437940000000	0.115220000000	C	-4.636308000000	3.652477000000	-0.145121000000
C	2.530793000000	-2.471322000000	0.137107000000	C	-5.285999000000	4.861403000000	-0.192221000000
C	0.454386000000	-1.167125000000	0.068270000000	C	-6.679960000000	4.898675000000	-0.214158000000
C	1.205841000000	-0.007032000000	0.044117000000	C	-7.391378000000	3.723359000000	-0.187209000000
C	2.630689000000	0.012081000000	0.063677000000	C	0.409203000000	-3.652335000000	0.140639000000
C	3.296127000000	-1.232827000000	0.110261000000	C	1.058748000000	-4.861370000000	0.186574000000
C	-0.929330000000	-0.764180000000	0.037721000000	C	2.452697000000	-4.898783000000	0.209403000000
C	-0.929961000000	0.656213000000	-0.004445000000	C	3.164251000000	-3.723521000000	0.184782000000
N	0.377442000000	1.075801000000	0.001319000000	H	0.665396000000	2.035416000000	-0.029070000000
C	-2.152685000000	-1.429412000000	0.042211000000	H	-2.227682000000	-2.506734000000	0.072740000000
C	-3.296725000000	-0.655677000000	0.004919000000	H	-1.998591000000	2.507248000000	-0.071350000000
C	-3.297324000000	0.764632000000	-0.038599000000	H	-4.891633000000	-2.035375000000	0.019368000000
C	-2.073966000000	1.429910000000	-0.042042000000	H	-9.484855000000	2.136749000000	-0.155734000000
N	-4.604094000000	-1.075331000000	0.001421000000	H	-10.717420000000	0.060200000000	-0.107474000000
C	-5.432491000000	0.007230000000	-0.044672000000	H	-9.524116000000	-2.116229000000	-0.030593000000
C	-4.681128000000	1.167300000000	-0.070129000000	H	-7.083823000000	-2.161418000000	0.000253000000
C	-6.857277000000	-0.012020000000	-0.062891000000	H	5.257695000000	-2.137029000000	0.163685000000
C	-7.522959000000	1.232814000000	-0.108449000000	H	6.490743000000	-0.060561000000	0.117748000000
C	-6.757758000000	2.471345000000	-0.137706000000	H	5.297913000000	2.115907000000	0.036963000000
C	-5.341108000000	2.438055000000	-0.117177000000	H	2.857617000000	2.161405000000	0.001320000000
C	-8.927209000000	1.212194000000	-0.122879000000	H	-3.557974000000	3.643096000000	-0.129861000000
C	-9.636128000000	0.034674000000	-0.095726000000	H	-4.714706000000	5.780187000000	-0.213309000000
C	-8.966383000000	-1.189681000000	-0.052182000000	H	-7.202069000000	5.845293000000	-0.252843000000
C	-7.594261000000	-1.206696000000	-0.035739000000	H	-8.470173000000	3.785493000000	-0.205841000000
C	4.700346000000	-1.212382000000	0.128540000000	H	-0.669107000000	-3.642766000000	0.124101000000
C	5.409489000000	-0.034973000000	0.102988000000	H	0.487414000000	-5.780173000000	0.205658000000
C	4.739984000000	1.189454000000	0.057494000000	H	2.974680000000	-5.845530000000	0.246643000000
C	3.367913000000	1.206631000000	0.038085000000	H	4.243038000000	-3.785821000000	0.203199000000

DDICZ **3b**

C	6.330491000000	6.466016000000	11.531773000000	C	10.569759000000	7.447162000000	15.719384000000
H	5.326107000000	6.866868000000	11.477045000000	C	11.822854000000	7.334848000000	16.343235000000
C	7.195579000000	6.777423000000	12.565611000000	H	12.021878000000	7.867897000000	17.261914000000
N	6.975987000000	7.589330000000	13.643286000000	C	12.827698000000	6.555864000000	15.822968000000
H	6.125250000000	8.091113000000	13.815064000000	H	13.781425000000	6.495077000000	16.329768000000
C	8.100189000000	7.631555000000	14.424269000000	C	12.609742000000	5.847688000000	14.641355000000
C	8.264483000000	8.369049000000	15.630886000000	H	13.392618000000	5.228369000000	14.223934000000
C	7.242675000000	9.165085000000	16.173525000000	C	11.395725000000	5.936720000000	14.006672000000
H	6.282012000000	9.232400000000	15.677634000000	H	11.246724000000	5.380574000000	13.095150000000
C	7.436525000000	9.864699000000	17.337759000000	C	10.353233000000	6.728391000000	14.516420000000
H	6.642408000000	10.475557000000	17.745444000000	C	9.080726000000	6.837277000000	13.866672000000
C	8.667613000000	9.780777000000	17.991553000000	C	8.520014000000	6.270360000000	12.659978000000
H	8.830372000000	10.326751000000	18.911125000000	C	8.986161000000	5.410812000000	11.670737000000
C	9.676118000000	9.004230000000	17.472666000000	H	9.988167000000	5.020373000000	11.719889000000
H	10.612114000000	8.967058000000	18.011210000000	C	8.149409000000	5.066547000000	10.614296000000
C	9.513854000000	8.275325000000	16.282566000000	C	8.276894000000	4.233166000000	9.439020000000

C	9.329167000000	3.416458000000	8.910483000000
C	10.570380000000	3.274525000000	9.552891000000
H	10.752529000000	3.785446000000	10.484747000000
C	11.567671000000	2.489534000000	9.029389000000
H	12.513518000000	2.402407000000	9.547716000000
C	11.356795000000	1.807482000000	7.831207000000
H	12.135418000000	1.185580000000	7.410583000000
C	10.149816000000	1.925910000000	7.186235000000
H	10.014249000000	1.383445000000	6.261428000000
C	9.109306000000	2.720550000000	7.694710000000
C	7.833915000000	2.833275000000	7.002626000000
C	7.565501000000	2.164913000000	5.796591000000
H	8.318829000000	1.537087000000	5.344099000000
C	6.354865000000	2.280914000000	5.156155000000
H	6.185912000000	1.750593000000	4.228588000000
C	5.345816000000	3.080246000000	5.697876000000
H	4.392211000000	3.171343000000	5.195346000000
C	5.573917000000	3.748335000000	6.874366000000
H	4.786457000000	4.368448000000	7.285330000000
C	6.805259000000	3.637483000000	7.540543000000
C	7.077297000000	4.314822000000	8.762687000000
N	6.221124000000	5.137410000000	9.444656000000
H	5.281940000000	5.358868000000	9.173373000000
C	6.836533000000	5.609478000000	10.570355000000

9. Fabrication and Characterization of Organic Thin-Film Transistors

Organic thin-film transistors (TFTs) were fabricated in the inverted staggered (bottom-gate, top-contact) architecture on three different types of substrate: (1) heavily doped silicon wafers with a thick gate dielectric, (2) heavily doped silicon wafers with a thin gate dielectric, and (3) flexible polyethylene naphthalate (PEN) sheets with a thin gate dielectric.

(1) For the TFTs on silicon with a thick gate dielectric, the substrate also serves as the gate electrode, and the gate dielectric is a combination of a 100-nm-thick film of silicon dioxide (grown by thermal oxidation in dry oxygen), an 8-nm-thick film of aluminum oxide (deposited by atomic layer deposition), and a self-assembled monolayer of either *n*-tetradecylphosphonic acid (Alfa Aesar) or 12,12,13,13,14,14,15,15,16,16,17,17,18,18,18-pentadecafluorooctadecylphosphonic acid (provided by Matthias Schlörholz). The SAMs were formed by immersing the substrate into a dilute 2-propanol solution of the phosphonic acid, followed by rinsing with pure 2-propanol. These SiO_2/Al_2O_3/SAM gate dielectrics have a total thickness of about 110 nm and a unit-area capacitance of about 34 nF/cm^2.

(2) For the TFTs on silicon with a thin gate dielectric, an aluminum gate electrode with a thickness of 30 nm was deposited onto the silicon by thermal evaporation in vacuum. The surface of the aluminum was then briefly exposed to oxygen plasma to form an aluminum-oxide (AlO_x) film with a thickness of about 4 nm, followed by the formation of an *n*-tetradecyl- or pentadecafluorooctadecylphosphonic acid SAM on the aluminum-oxide surface from solution, as described above. These AlO_x/SAM gate dielectrics have a total thickness of about 6 nm and a unit-area capacitance of about 0.7 µF/cm^2.

(3) For the TFTs on flexible PEN with a thin gate dielectric, aluminum gate electrodes with a thickness of 30 nm were deposited onto the PEN by thermal evaporation in vacuum and patterned using a shadow mask. The surface of the aluminum was then briefly exposed to oxygen plasma to form an AlO_x film with a thickness of about 4 nm, followed by the formation of an *n*-tetradecyl- or pentadecafluorooctadecylphosphonic acid SAM on the aluminum-oxide surface from solution, as described above. These AlO_x/SAM gate dielectrics have a total thickness of about 6 nm and a unit-area capacitance of about 0.7 µF/cm^2.

For all TFTs, a 30-nm-thick film of the organic semiconductor was then deposited by thermal sublimation in vacuum (10^{-6} mbar). During the deposition of the organic semiconductor, the substrate was held at an elevated temperature (120 °C) to promote molecular ordering. Gold source and drain contacts were deposited onto the surface of the organic-semiconductor film by thermal evaporation in vacuum through a shadow mask. The TFTs have a channel length (L) of either 30 or 100 µm and a channel width (W) of either 100 or 200 µm. The current-voltage characteristics of the TFTs were measured in ambient air at room temperature.

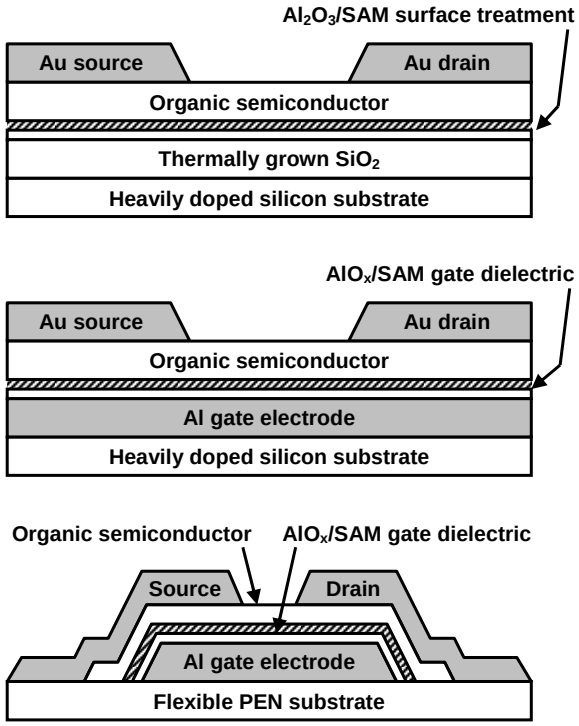

Figure SI9. Schematic TFT cross-sections.

Top: TFTs fabricated on silicon substrates with a thick gate dielectric.

Center: TFTs fabricated on silicon substrates with a thin gate dielectric.

Bottom: TFTs fabricated on flexible polyethylene naphthalate (PEN) substrates with a thin gate dielectric.

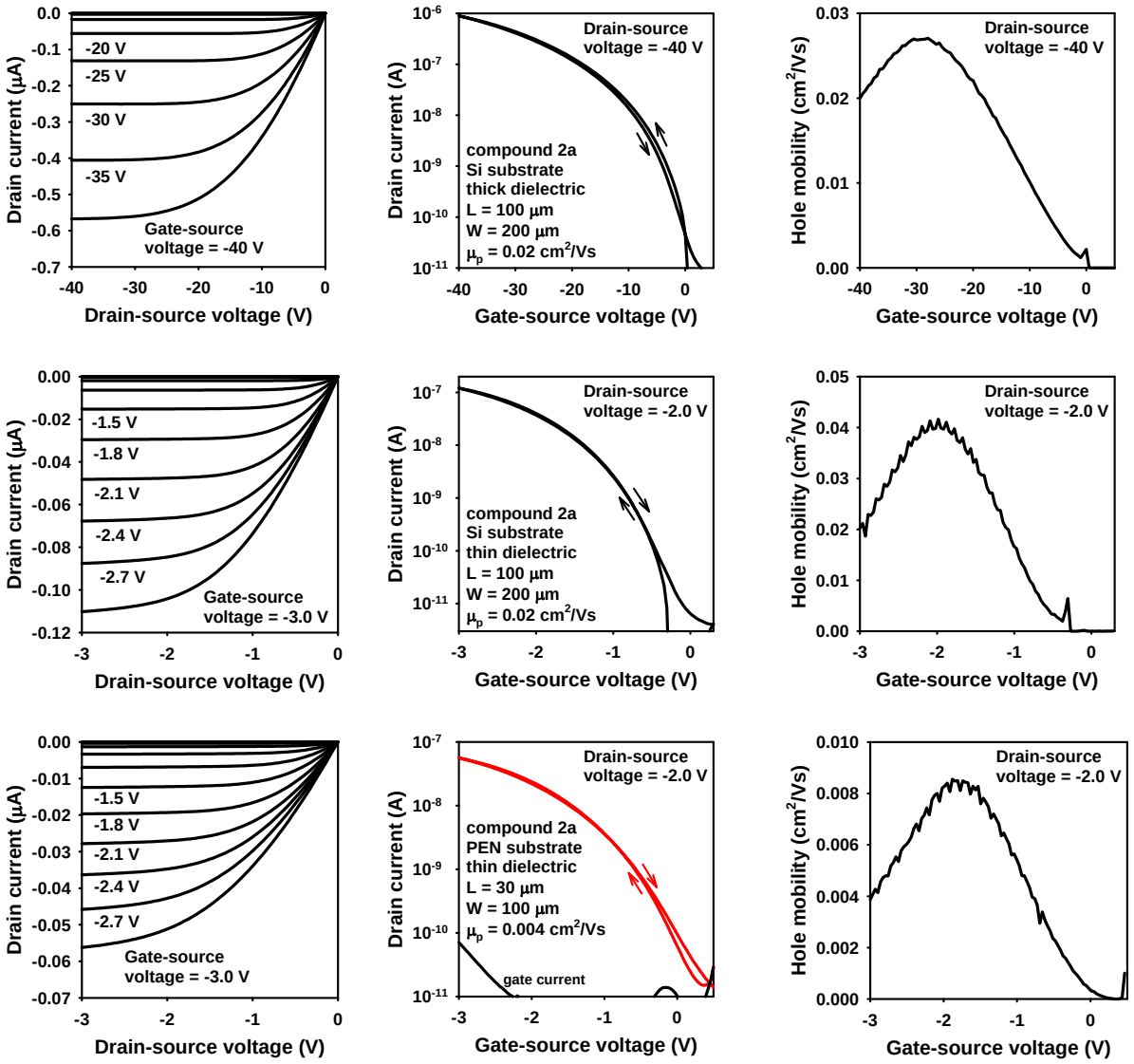

Figure SI10. Current-voltage characteristics of TFTs based on compound **2a**.

Top row: TFT fabricated on a silicon substrate with a 110-nm-thick SiO_2/Al_2O_3/SAM gate dielectric with a pentadecafluorooctadecylphosphonic acid SAM.

Center row: TFT fabricated on a silicon substrate with a 5.7-nm-thick AlO_x/SAM gate dielectric with a pentadecafluorooctadecylphosphonic acid SAM.

Bottom row: TFT fabricated on a PEN substrate with a 5.7-nm-thick AlO_x/SAM gate dielectric with a pentadecafluorooctadecylphosphonic SAM.

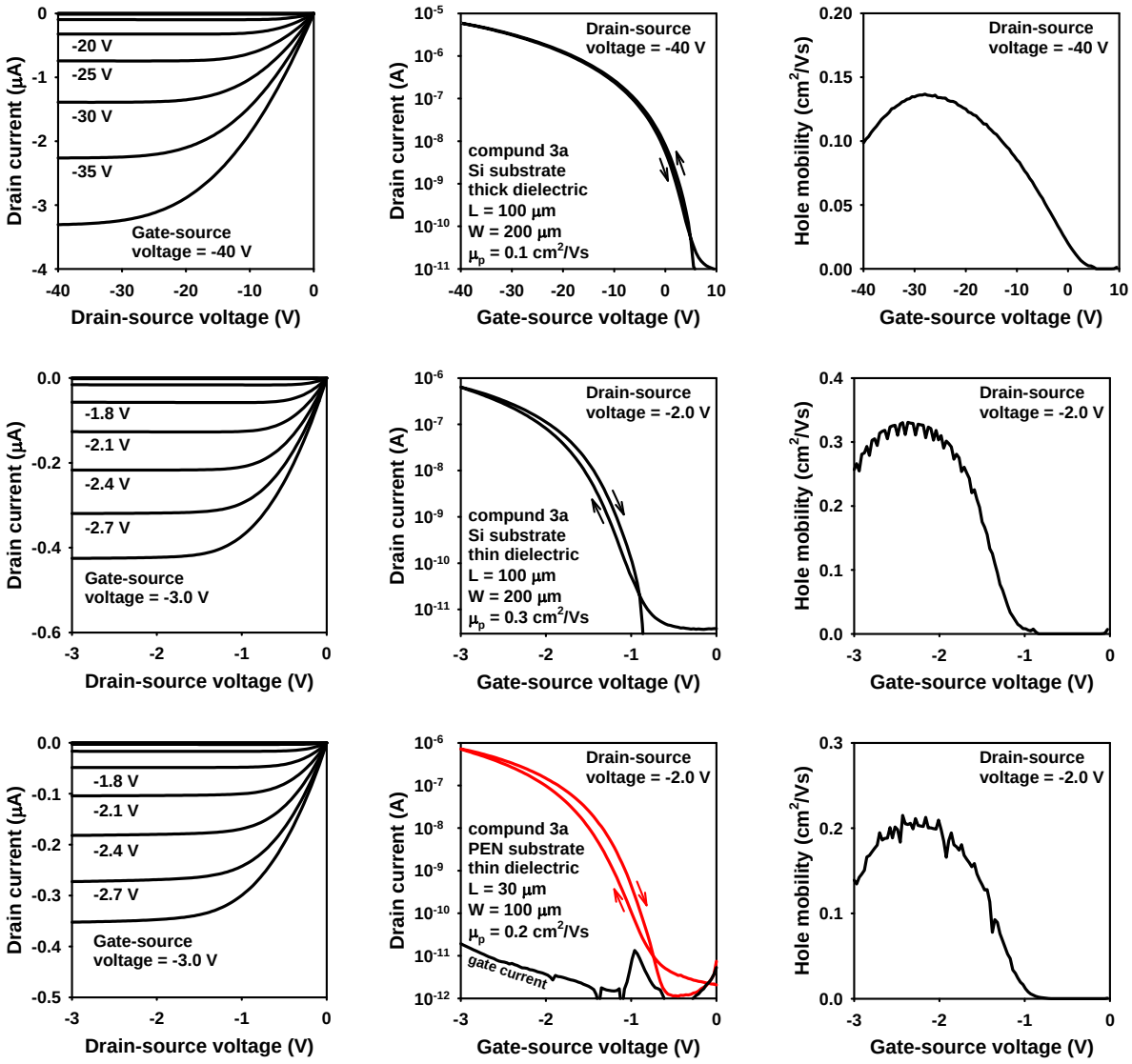

Figure SI11. Current-voltage characteristics of TFTs based on compound **3a**.

Top row: TFT fabricated on a silicon substrate with a 110-nm-thick SiO_2/Al_2O_3/SAM gate dielectric with an *n*-tetradecylphosphonic acid SAM.

Center row: TFT fabricated on a silicon substrate with a 5.7-nm-thick AlO_x/SAM gate dielectric with an *n*-tetradecylphosphonic acid SAM.

Bottom row: TFT fabricated on a PEN substrate with a 5.7-nm-thick AlO_x/SAM gate dielectric with a pentadecafluorooctadecylphosphonic SAM.

10. References

[1] G. R. Fulmer, A. J. M. Miller, N. H. Sherden, H. E. Gottlieb, A. Nudelman, B. M. Stoltz, J. E. Bercaw, K. I. Goldberg, *Organometallics* **2010**, *29*, 2176-2179.

[2] S. K. Mamidyala, M. A. Cooper, *Chem. Commun.* **2013**, *49*, 8407-8409.

[3] A. Isobe, J. Takagi, T. Katagiri, K. Uneyama, *Org. Lett.* **2008**, *10*, 2657-2659.

[4] M. Modjewski, S. V. Lindeman, R. Rathore, *Org. Lett.* **2009**, *11*, 4656-4659.

[5] K. Thakur, D. Wang, S. V. Lindeman, R. Rathore, *Chem. Eur. J.* **2018**, *24*, 13106-13109.

[6] J. Iskra, S. Stavber, M. Zupan, *Synthesis* **2004**, *2004*, 1869-1873.

[7] D. Lasanyi, G. L. Tolnai, *Org. Lett.* **2019**, *21*, 10057-10062.

[8] K. Naveen, S. A. Nikson, P. T. Perumal, *Adv. Synth. Catal.* **2017**, *359*, 2407-2413.

[9] C. Hendrich, L. M. Bongartz, M. Hoffmann, U. Zschieschang, J. W. Borchert, D. Sauter, P. Krämer, F. Rominger, F. F. Mulks, M. Rudolph, A. Dreuw, H. Klauk, A. S. K. Hashmi, *Adv. Synth. Catal.* **2020**, DOI: 10.1002/adsc.202001123.

[10] F. Neese, *WIREs Computational Molecular Science* **2011**, *2*, 73-78.

[11] a) S. Grimme, J. Antony, S. Ehrlich, H. Krieg, *J. Chem. Phys.* **2010**, *132*, 154104; b) S. Grimme, S. Ehrlich, L. Goerigk, *J. Comput. Chem.* **2011**, *32*, 1456-1465; c) H. Kruse, S. Grimme, *J. Chem. Phys.* **2012**, *136*, 154101; d) S. Grimme, J. G. Brandenburg, C. Bannwarth, A. Hansen, *J. Chem. Phys.* **2015**, *143*, 054107.